STUDY OF ELECTROMAGNETIC FIELD UNIFORMITY IN RADIO FREQUENCY HEATING APPLICATOR

By

JIAN WANG

A dissertation submitted in partial fulfillment of
the requirements for the degree of

DOCTOR OF PHILOSOPHY

WASHINGTON STATE UNIVERSITY
Department of Biological Systems Engineering

August 2007

To the Faculty of Washington State University:

The members of the Committee appointed to examine the dissertation of JIAN WANG find it satisfactory and recommend that it be accepted.

_____
Chair

_____

_____

_____

ACKNOWLEDGMENT

First of all, I thank my major advisor, Dr. Juming Tang, for his guidance, motivation and encouragement throughout the course of my study and research at Washington State University. I also express my sincere thanks to my doctoral committee members, Dr. Clary Carter, Dr. Robert Olsen, and Dr. Barry Swanson, for their support, advice and guidance during the course of my research and in the preparation of this dissertation.

I thank my former fellow graduate students Drs. Yifen Wang and Kunchalee Luechapattanaporn for support, assistance and encouragement, and the radio frequency sterilization project members, Drs. Zhongwei Tang and TVCT Chan for assistance to the final part of my dissertation. I am thankful to Mr. Frank Younce, Mr. Wayne Dewitt and Mr. Vincent Himsl for technical assistances.

The project was financially supported by the US Army Soldier and Biological Chemical Command, Natick, Massachusetts, with additional support from Kraft Foods, Glenview, Illinois, and Strayfield Fastran, Berkshire, England, and WSU IMPACT Center. Their supports have been essential and are greatly appreciated.

Finally, my most sincere thanks go to my parents and my friends for understanding, enduring, and support.

STUDY OF ELECTROMAGNETIC FIELD UNIFORMITY IN RADIO FREQUENCY HEATING APPLICATOR

ABSTRACT

by Jian Wang, Ph.D.

Washington State University

August 2007

Chair: Juming Tang

A 6kW 27MHz pilot scale radio frequency (RF) heating system was developed at Washington State University for processing 6-pound packaged foods to achieve shelf-stability. Although RF heating presents the possibility of improving food quality in a shorter processing time than the conventional retort heating method, it still confronts the heating non-uniformity caused by fringe effects. The objectives of this research were to gain a better understanding of the dielectric heating process, to study the factors that may influence the RF heating pattern and heating rate, and to investigate the possibility of achieving heating uniformity during the RF heating process.

To support this project, a dielectric properties measurement system was used to determine the complex permittivity of materials used in dielectric heating over a temperature range from 20 to 120 °C at radio frequencies (27 and 40 MHz) and microwave frequencies (915 and 1800 MHz). The dielectric properties of egg products

were measured with an open-end coaxial probe method. The dielectric property information was used to adjust the electric conductivity of the circulating water that immersed the packaged foods and mitigated fringing electric field and edge-heating effects during the RF heating process, and to support the implementation of the computer simulating on RF heating process.

Experiments and computer simulations using the finite element method were performed to study the influence of food dielectric properties and circulating water electric conductivity on RF heating rate and heating pattern. The results of this work indicated that with the increase of electric conductivity of circulating water or food loss factor, the heating rate decreased. Both the dielectric properties of food and electric conductivity of circulating water affected the electric field distribution inside the food.

Experiments and computer simulations were also conducted on RF heating of a heterogeneous food, meat balls in lasagna. The results demonstrated that RF heating had a potential to process pre-packaged heterogeneous food. Proper distribution and suitable size of each component, though with vastly different dielectric properties, are possible to ensure relatively uniform RF heating.

TABLE OF CONTENTS

Page

LIST OF FIGURES

Page

LIST OF TABLES

Page

Dedication

This dissertation is dedicated to my parents

who provided both emotional and financial supports

DISSERTATION OUTLINE

This dissertation is arranged into six chapters. The first chapter provides an introduction, problem statements, and justifications for radio frequency heating on foods and computer simulation. The second chapter is a literature review of fundamental principles, industrial applications, and academic researches of radio frequency heating. Chapter three describes equipments and methods to measure food dielectric properties. Chapter three also reports the dielectric properties of four egg products over the temperature range from 20 to 120°C at radio frequencies 27 and 40 MHz, and microwave frequencies 915 and 1800 MHz. Chapter four studies the influence of dielectric properties of food and electric conductivity of circulating water on the electric field distribution, heating rate, and heating pattern in packaged food during the radio frequency heating process. In this chapter, computer simulation is used to numerically simulate the experiment and to investigate the mechanism of effects. Chapter five describes radio frequency heating effect on heterogeneous foods. The experiment and computer simulation indicate that the fringing effects and local electromagnetic field concentration caused by various dielectric properties do not necessarily introduce overheating at certain parts of heterogeneous food. Finally, chapter six provides conclusions for the entire study and some recommendations for future work.

CHAPTER ONE

INTRODUCTION

The military field rations are normally stored in severe environment, therefore, they need more stringent criteria than commercial packaged foods on the market. Since it is demanded that an unopened military field ration must endure a 3-year-storage at 80ºF (27ºC) (Wig, 2001), shelf-stability is one of the most important characteristics of the field rations. The existence of pathogenic microorganisms in the rations can introduce health hazards and make food unstable and unsafe. In food processing plants, heating is usually used to inactive the microorganisms in foods.

Conventional thermal processing

Thermal processing has been used over the past two centuries in commercial production of low acid (pH > 4.6) shelf-stable foods in hermetically sealed containers (VanGarde and Woodburn, 1994). Conventional retort heating by steam or hot water is widely used in modern commercial food pasteurization and sterilization operations, in which thermal energy is supplied by condensing steam or pressurized hot water and transferred by conduction and/or convection from the surface to the interior of packaged foods. Thermal properties of the food such as specific heat, thermal conductivity, density, and geometry affect the heat transfer rate.

A typical thermal process to commercially sterilize food products can be divided into three phases, i.e. come-up, holding, and cooling phases (Guan, 2003). In the come-up phase, the cold spots in packaged foods are heated to a desired temperature. During the

holding phase, the temperature of foods is held at a selected temperature until the desired lethality or degree of sterilization value is obtained. Finally, in the cooling phase the heated foods are cooled to the temperature that the foods can be taken out at atmosphere pressure.

High temperature short time process

Commercial thermal processes not only inactive harmful microorganisms, but may also degrade the quality of food (Lund, 1988), such as color, texture and flavor, which are important for consumer acceptance of the food product. So the major goal in developing a thermal process is to determine the time-temperature history at the cold spots in packaged foods and to design a procedure to ensure the microbiological safety for the processed products with acceptable quality (Holdsworth, 1997).

The effects of thermal treatment on the food are commonly determined by two factors: sterilization value (F_0) and cooking value (C_{100}). F_0 is the cumulative thermal effect on the product during the thermal processing and can be expressed as (Stumbo, 1973):

$$F_0 = \int_0^t \left[10^{\left(\frac{T-121.1}{z} \right)} \right] dt \qquad (1.1)$$

where F_0 is process sterilizing value (minute), T is temperature (ºC), t is processing time (minute), and z is a temperature difference required for a tenfold change in the thermal death time (ºC).

C_{100}, called cooking value, is the relative thermal effect on food quality to reference temperature and defined as (Holdsworth, 1997):

$$C_{100} = \int_0^t \left[10^{\left(\frac{T-100}{z_c} \right)} \right] dt \qquad (1.2)$$

where C_{100} is cooking value refer to 100ºC (minute), and z_c is thermal destruction rate analogous to the z for microbial inactivation (ºC).

Since the commercial sterility has to be achieved throughout the processed foods, and at the same time a required quality standard has to be reached; both the sterilization value and the cooking value need to be considered in designing a heating sterilization process. The z values for microbial inactivation are normally 7-12 ºC, which is much smaller than the z_c value that is around 25 to 45 ºC for thermal degradation of foods (Lund, 1977). The smaller z value for sterilization compared to cooking z value indicates that the rate of destruction of nutrients is less temperature dependent than that of microbial spores (Lund, 1977; 1986). Therefore, a high temperature short time (HTST) process is the ideal food sterilization method.

Radio frequency heating

It is difficult to develop a HTST process for packaged foods by conventional retort methods, because it takes long time for the cold spots of packaged foods to achieve the temperature that is lethal to the target pathogens due to limited heat conduction and convection from steam or hot water to the surface and slow conduction and/or convection from the surface to the center of food. As a result, the surface of food is exposed to high temperature much longer than the inner part, leading to overcooking and degrading of quality at the surface of food.

Dielectric heating, which includes microwave and radio frequency (RF) heating, was introduced in the middle of the twentieth century (Cathcart et al., 1947; Kenyon et al., 1971) for its potential advantages of reducing processing times, achieving uniform product heating, and improving product quality.

Numerous studies have been conducted on dielectric heating. An advantage of dielectric heating over the conventional thermal processing is the rapid volumetric heating through direct interaction between electromagnetic wave and hermetically sealed packaged foods (Burfoot et al., 1988; Harlfinger, 1992).

Several frequency bands are reserved for dielectric heating according to international agreement. The Federal Communications Commission, the responsible regulatory agency in the United States, has adopted this frequency allocation scheme (FCC, 1988) with few additional requirements. The Industrial, Scientific, and Medical band assignments for dielectric heating in the United States of America are summarized in Table 1.1.

Microwave heating is limited to small food packages due to the relatively small penetration depth of microwaves in dielectric materials. This limitation can be overcome by using RF energy (Zhao et al., 2000). During RF heating, thermal energy is generated within dielectric materials when the electromagnetic field reverses the polarization of molecules and/or migrates of ions within the material as it alternates at high frequency (Barber, 1983). With a much longer wavelength than microwave as shown in Table 1.1, RF heating is particularly useful when processing the institutional size packaged food products, such as 6-pound capacity army rations.

RF dielectric heating is now widely used in industry to dry textile products and paper, to post-bake cookies and snack foods, and so on (Barber, 1983; Orfeuil, 1987; Rice, 1993; Mermelstein, 1998). However, a lack of knowledge about the dielectric properties of various foods as functions of composition, temperature, and frequency, the possible non-uniform temperature within products and the difficulty of applying overpressure during RF heating have restricted the optimum design of RF heating system in cooking and sterilizing food products (Zhao et al., 2000; Wang et al., 2003).

Problem Statements

Although RF heating has the potential to improve the heating uniformity, three major problems remain:

(1) Since the packaged food is heated through the conversion of electromagnetic energy into thermal energy in RF heating, the heating pattern of the food is affected by the distribution of the electromagnetic wave in the RF system. Due to the complexity of the RF heating equipment, several factors, such as food package geometry, initial food temperature distribution, surrounding medium properties, food dielectric properties, and cavity geometry may influence the distribution of the electromagnetic wave, and then influence the heating pattern and repeatability. The positions of the cold spots within the foods have to be determined and controlled to ensure the safety of packaged foods.

(2) During RF heating, fringing effects, which is caused by the distortion of electromagnetic field at the interface of foods and surrounding environment, can overheat the edge and surface of foods and damage the heating uniformity. It is desirable to determine the factors that influence the extent of fringing effects during RF heating.

(3) For heterogeneous food, electromagnetic wave distortion may also happen around the interfaces of different components of food, and introduce overheats at certain portions within the food. It is necessary to investigate the electromagnetic field distribution at the interfaces of different components and study the possible effects on the heating uniformity of packaged foods.

Objectives

In this research, the distribution of electric field inside a RF system was studied. The general goal was to validate and improve RF heating system as a sterilization method, with an aim to achieve better time-efficiency and better heating uniformity than conventional retort sterilization method, in selected foods.

In order to accomplish the general goal, several specific objectives were set for this research and discussed in the following sections.

Dielectric Properties of Eggs

It is essential to determine the dielectric properties of food materials in exploring the electric field and temperature distributions using the computer simulation. The knowledge of dielectric properties of foods provides general guidance to determining the effects of surrounding conditions on RF heating and determining the required thickness of the treated packages to ensure uniform RF treatments.

As a part of a larger project to thermally stabilize shelf-stable egg products with family prepared quality, we chose to use RF energy to reduce processing time. To obtain

the optimized RF heating result, it is necessary to gain knowledge of the dielectric properties for egg.

An objective of my study was to measure the dielectric properties of liquid whole eggs, pre-cooked whole eggs, liquid egg whites, and de-cooked egg whites at frequencies 27, 40, 915, and 1800 MHz over the temperature range from 20 to 121 ºC. The open-ended coaxial probe method, which commonly utilized to measuring liquid, semi-solid and solid materials, was used to test the dielectric properties of the egg products. A custom-made dielectric property measuring system built at Washington State University was used in this study.

Computer Simulation

In early studies, experiments were the major effective tools to determine electromagnetic wave distribution within dielectric heating equipment and heating pattern in food in RF systems. The approaches are time consuming at high operational costs. With rapid development of numerical simulation techniques, computer modeling provides great potential in predicting the wave distribution in RF systems. Several commercial electromagnetic modeling software packages are available nowadays. While many different electromagnetic modeling techniques exist, the Finite Element Method (FEM) and the Finite-Difference Time-Domain (FDTD) method are the most common (Sadiku, 2001).

The second objective of the study was to apply commercial software to analyze the electric field distribution inside a pilot-scale RF dielectric heating system, and compare with the simulation results with the experimental results.

Justification

If results show that the electromagnetic wave distribution inside the RF heating system can be simulated by computer models, we can utilize those models to assist the development of RF heating systems to improve heating uniformity and repeatability through proper design and adjustment of the equipment and by selecting appropriate process conditions. It is our intent to use RF dielectric heating technology in commercial applications to improve food product quality and safety. This overall goal of this study was to study the feasibility that RF heating can be used in commercial sterilized heterogeneous food processing.

Reference

Barber, H. 1983. Dielectric Heating. Chapter 8 in Electroheat. Grande Publishing Limited, London, UK. 226-276.

Burfoot, D., Griffin, W.J. and James, S.J.1988. Microwave pasteurization of prepared meals. Journal of Food Engineering 8: 145-156.

Cathcart, W.H., Parker, J.J., Beattie, H.G. 1947. The treatment of packaged bread with high frequency heat. Food Technology 1: 174 -177.

FCC. 2004. Title 47 CFR 18.301, Federal Communications Commission, Washington DC, USA.

Guan, D. 2003. Thermal processing of hermetically packaged low-acid foods using microwave-circulated water combination (MCWC) heating technology. Doctor of

philosophy dissertation. Department of Biological System Engineering. Washington State University, Pullman, WA, USA.

Harlfinger, L. 1992. Advances in microwave food processing. Food Technology 46(12): 57-60.

Holdsworth, S.D. 1997. Thermal processing of packaged foods. 1st edition. Blackie Academic and Professional, London, UK.

Kenyon, E.M., Westcott, D.E., Case, P.L., Gould, J.W. 1971. A system for continuous thermal processing of food pouches using microwave energy. Journal of Food Science 36: 289-293.

Lund, D.B. 1977. Maximizing nutrition retention. Food Technology. 30: 71-78.

Lund, D.B. 1986. Kinetics of physical changes in foods. In Physical and Chemical Properties of Food. Okos, M.R.(Ed.). American Society of Agricultural Engineers, Michigan, USA. 367-381.

Lund, D.B. 1988. Effects of heat processing on nutrients. In: Karmas E, Harris RS, editors. Nutritional evaluation of food processing. 3rd ed. Van Nostrand Reinhold Co. New York, NY, USA. 319-54.

Mermelstein, N.H. 1998. Microwave and radio frequency drying. Food Technology. 52(11): 84-86.

Orfeuil, M. 1987. Dielectric hystereris heating. Chapter 7 in Electric Process Heating: Battelle Memorial Institute, Columbus, Ohio, USA. 539-575.

Rice, J. 1993. RF technology sharpens bakery's competitive edge. Food Proc. 6: 18-24.

Sadiku, M.N.O. 2001. Numerical techniques in electromagnetics, 2nd edition. CRC Press LLC, Boca Raton, Florida, USA.

Stumbo, C.R. 1973. Thermobacteriology in food processing, 2nd edition. Academic Press, London, UK.

VanGarde, S.J. and Woodburn, M. 1994. Food preservation and safety – Principles and practice. Iowa State University Press, Ames, Iowa, USA.

Wang, Y., Wig, T., Tang, J., and Hallberg, L.M. (2003). Dielectric properties of food relevant to RF and microwave pasteurization and sterilization. Journal of Food Engineering. 57: 257-268.

Wig, T. 2001. Sterilization and pasteurization of foods using radio frequency heating. Doctor of philosophy dissertation. Department of Biological System Engineering. Washington State University, Pullman, WA, USA.

Zhao, Y., Flugstad, B., Kolbe, E., Park, J.W., Wells, J.H. 2000. Using capacitive (radio frequency) dielectric heating in food processing and preservation – a review. Journal of Food Process Engineering. 23: 25–55.

Tables

Table 1.1: FCC allocated frequency bands designated for ISM applications (FCC, 2004)

Dielectric Heating Range	Center Frequency (MHz)	Frequency Tolerance +/-	Free Space Wavelength (m)
RF	13.56	0.052%	22.1
	27.12	0.6%	11.1
	40.68	0.005%	7.4
MW	915	13MHz	0.328
	2450	50MHz	0.122

CHAPTER TWO

LITERATURE REVIEW

Introduction

Heating is one of the most common methods for food preservation. Conventional heating methods use external heat sources, such as steam and boiling water. With those methods, heat is transferred by conduction, convection, and radiation. Poor thermal conducting ability of food, especially solid food, introduces the non-uniform and inefficient heating (Barber, 1983; Zhao et al., 2000).

To solve the problem of slow energy transfer and to provide even distribution of temperature, electric resistance heating was introduced (Barber, 1983; Jun and Sastry, 2005). The electric resistance heating uses Ohm's law by applying voltages through electrodes in close contact with food to produce heat. Electrical resistance heating, commonly referred as Ohmic heating, can heat food more thoroughly and rapidly than conventional heating method, except for dielectric materials. Dielectric materials are characterized by the presence of relatively few charge carriers so that the application of a voltage gradient to the material will result in only a very small current, therefore, the electrical resistance heating is not anymore effective (Barber, 1983).

Since most foods are dielectric materials, an alternative heating method, dielectric heating method, was introduced in the middle of the twentieth century for its potential advantages of reducing processing times, uniform product heating, and improving product quality. Dielectric heating is broadly used nowadays. It is regarded as one of the best methods to heat food efficiently and quickly (Cathcart et al., 1947; Kenyon et al.,

1971). Dielectric heating includes Radio Frequency (RF) heating technology and microwave heating technology (Zhao et al., 2000).

The effectiveness of dielectric heating is determined by two factors. First, the knowledge of dielectric properties of the food is necessary. Second, the mechanism of producing and applying electromagnetic wave on food has to be understood.

Dielectric Properties of Food

Dielectric Properties theory

The dielectric properties of foods are of engineering interest because they describe the ability of food to store and dissipate electrical energy in response to an alternating electromagnetic field (Mudgett, 1986).

Dielectric properties are normally described by complex permittivity, ε_c:

$$\varepsilon_c = \varepsilon' - j\varepsilon'' \tag{2.1}$$

where $j = \sqrt{-1}$. The real part, ε', known as the dielectric constant, is a measure of how much energy from an external field is stored in a material. The imaginary part, ε'', referred as the loss factor, describes the ability of a material to dissipate energy, which typically results in heat generation, in response to an applied electric field (Nyfors and Vainikainen, 1989; Lorrain et al., 1988). Complex relative permittivity, ε_r, is a relative value, with respect to that of the free space:

$$\varepsilon_c = \varepsilon_r \varepsilon_0 = \varepsilon_0 (\varepsilon_r' - j\varepsilon_r'') \tag{2.2}$$

where $\varepsilon_0 = 8.854 \times 10^{-12}$ Farads/meter (Sadiku, 2001b) is permittivity of free space.

The ability of the electric wave to penetrate a dielectric material is described by microwave power penetration depth, d_p. Microwave power penetration depth is associated with the frequency of the electromagnetic field and the electric properties of material, and can be calculated according to (Von Hippel, 1954):

$$d_p = \frac{c}{2\sqrt{2}\pi f\left[\varepsilon'\left(\sqrt{1+\left(\frac{\varepsilon''}{\varepsilon'}\right)^2}-1\right)\right]^{\frac{1}{2}}} \tag{2.3}$$

where c is speed of light in free space; f is frequency of the applying electromagnetic wave.

Measurement of Dielectric Properties

The determination of the heating rate and microwave power penetration depth depends on the dielectric properties of food. Dielectric constant and loss factor are important factors for dielectric heating. However, a lack of knowledge about the dielectric properties of various foods as functions of food composition, food temperature, and frequency of processing electromagnetic wave restricted our ability to design optimum dielectric heating systems (Zhao et al., 2000). Measurement of dielectric properties is necessary for the successful application of dielectric heating.

The dielectric properties can be measured by several methods, including open-ended coaxial probe methods, transmission line methods, and resonance cavity methods.

1) Open-Ended Coaxial Probe Methods

The open-ended coaxial probe method uses a coaxial probe with the open end in contact with the sample. During the measurement, a signal is sent by a vector network

analyzer or an impedance analyzer, and reflected back by the material. The magnitude and phase change of the reflected wave are used to calculate the dielectric properties of the sample (Agilent, 2006a; Athey et al., 1982; Tang et al., 2002).

The open-ended coaxial probe is easy to use and suitable for all kinds of material, especially for liquid and semi-solid food material. It allows a large frequency range for measurement from 10 to 20,000 MHz, and requires little sample preparation (Agilent, 2006b; Engelder and Buffler, 1991).

Open-ended coaxial probe method has some restrictions. The method has limited accuracy in dielectric constant and low loss factor resolution. For the accuracy of measurement, the sample thickness should typically greater than 1 cm. The solid samples must have a flat surface. The method is not suitable for high dielectric constant and low loss factor materials (Agilent, 2006b; Ryynanen, 1995; Tang et al., 2002).

Three major error sources for measurement are the cable stability, air gaps, and sample thickness (Agilent, 2006b). First of all it is better to minimize the cable flexing. Because the instability and flexing of cable may distort the detective signal sent by network analyzer or impedance analyzer, then cause inaccuracy during measurement. Secondly, the existence of air gap can distort the detective signal and influence accuracy of measurement. So the sample surface, which contacts the coaxial probe, should be made as flat and smooth as possible. Thirdly, the detective signal can penetrate sample and introduce the insufficient reflection, thus reduce the accuracy of measurement. So the thickness of the sample should be greater than the recommended minimum sample thickness, t_{min} (Hewlett-Packard Company, 1993), which is expressed as:

$t_{\min} = 20/\sqrt{\varepsilon_r}$ (mm).

Although open-ended coaxial probe method has limitations, it is an ideal method for measuring the dielectric properties of liquids or semisolids, and it is one of the most widely and commonly used methods in food research community (Seaman and Seals, 1991; Herve et al., 1998). Most of the time, the accuracy of measured dielectric properties is adequate for dielectric heating research (Tang et al., 2002).

2) Transmission Line Method

This method needs the cross-section of a transmission line to be filled by a sample. The transmission line may be either rectangular or coaxial (Engelder and Buffler, 1991). During the measurement, a vector network analyzer is used to detect the change of the impedance and propagation characteristics due to the filling of dielectric material. The dielectric properties of the sample are calculated by software (Agilent, 2006b).

Both the accuracy and sensitivity of transmission line method are higher than that of the open-ended coaxial probe method. However, the precise fixture limits the measuring frequencies of transmission line method to narrow bands of frequencies, such as S-Band: 2.6 to 3.95 GHz etc. So the measuring frequency range is narrower than the open-ended coaxial probe method. Samples need to be carefully prepared to fit to the cross-section of the transmission line. It is difficult for the transmission line method to handle liquid and semisolid sample material (Engelder and Buffler, 1991; Ryynanen, 1995; Tang et al., 2002).

3) Resonance Cavity Method

With the resonance cavity method, a sample is placed in a cavity with high quality resonance. Upon inserting the sample, both the center resonance frequency f_c and quality factor Q change (ASTM, 1971). Two changes of the parameter are measured by a vector

network analyzer, and special software calculated the dielectric properties of the sample material (Agilent, 2006b; Engelder and Buffler, 1991).

Resonance cavity method can be very accurate and give an overall accuracy of ±2 to 3% (Ohlsson, 1989). It is sensitive to very low values of loss factor. However, the method provides the dielectric properties of only one frequency for a specific resonance cavity and the cavities are difficult to design and use.

Theory of dielectric heating

The presence of electric field can polarize the dielectric materials by forcing the displacement and rotation of electron, molecular, dipolar, and free charge inside the material. An alternating electromagnetic field can successively reverse the displacement and the energy absorbed by the material in carrying out these displacements is dissipated as heat (Orfeuil, 1987).

There are four types of polarization: electronic, atomic, dipolar, and interfacial polarization. Only dipolar polarization, which is the rotation of dipoles, and migration of free charge carriers can produce significant heat that be used in industrial heating, at radio and microwave frequencies (Barber, 1983).

RF Heating System

RF power generator

RF power generator can generally be divided in two classes: the conventional power oscillator design and relatively new 50 Ω power amplifier design (Barber, 1983; Marchand and Meunier, 1990).

The conventional power oscillator RF heating system consists of a main power, a high voltage transformer, a self excited oscillator with one or more triodes, a high voltage rectifier, a tank circuit, and a work circuit, as shown schematically in Figure 2.1. The RF applicator and foods are part of the power generator circuit; a change in the capacitance or inductance of the work circuit affects the power coupled from the tank circuit to the load (Wig, 2001). The RF power is typically coupled from the tank circuit to the work circuit by changing the space interval between the electrodes and/or by adjusting the length of variable inductor in the work circuit. The power oscillator design is able to reach high overall efficiency because the load is part of the circuit (Orfeuil, 1987). The conventional design is also simple to construct and is relatively inexpensive.

However during a heating process, variations in the gap between electrodes, food product dielectric properties, and other factors may change the capacitance and quality factor of the applicator in the circuit, which in turn shifts the intrinsic frequency of the applicator. It is intolerable in regions where strict operating frequency limitations are enforced, so power amplifier generators were introduced to solve the problem.

Power amplifier generators, also known as 50 Ω generators, use a different approach for the generation of RF power. The system, demonstrated in Figure 2.2, consists of an oscillator, a power amplifier, a 50 Ω transmission line, an impedance

matching circuit, and a work circuit (Roussy and Pearce, 1995; Jones and Rowley, 1996). In this type of system, a stable, fixed frequency oscillator supplies a radio frequency signal to a power amplifier that supplies power to the load. The output of the power is transferred to a load through the transmission line and impedance matching circuit that is used to match the impedance of amplifier and load to avoid the power reflection (Wig, 2001).

The power amplifier system has the advantage of stringently controlled operating frequency that meet the requirement of International Electromagnetic Compatibility. It also physically separates the matching circuit from generator. Finally it provides flexibility for improving the working circuit, the process control system, and the efficiency of generator. However, the much higher cost and limitation of power output hinder the wide spreading of power amplifier system.

RF Applicator

Several configurations of RF applicators are used in research and industry applications, such as simple parallel plate, Garland, and stray-field applicators.

1) Simple Parallel Plate Applicator

Simple parallel plate applicator, illustrated in Figure 2.3, is the simplest form of arrangement for dielectric heating at radio frequency. Plate electrodes structure is used for heating small objects, or small areas of large pieces. Plate electrodes structure is more suitable for research or small-scale industrial production (Barber, 1983). But since the applicator directs energy uniformly through the bulk of a product, it is suitable for RF sterilization process.

2) Garland and Strayfield applicator

To heat large size material, the plate is replaced by a series of rods. A simple illustration of Garland and Strayfield applicators are shown in Figure 2.4 and 2.5, respectively. The rod applicator simplifies the mechanical and makes the evaporation of vapor possible.

By altering the distribution of the rods, the heating equipment can be used by different applications, such as welding, curing, drying, heating, blanching, thawing, pasteurization, sterilization, and so on.

Computer Simulation

Techniques for solving electromagnetic problem

Several techniques can be used to provide insight into electromagnetic heating phenomena. Those techniques can be classified as experimental, analytical, or numerical. Experimental techniques are expensive, time consuming, and usually do not allow adequate flexibility for parameter variation. Analytical techniques can provide exact electromagnetic field distribution; however, the technique can only solve the problem with very limited and extremely simple configurations. Numerical techniques are used for problems associated with complicated constructions. The finite difference time domain method and finite element method are among the most commonly used in electromagnetic (Sadiku, 2001a).

Analytical and numerical methods solve the dominant equations, Maxwell Equations, for all the electromagnetic problems. Maxwell Equations describe electromagnetic fields are written as (Sadiku, 2001b):

$$\nabla \times \mathbf{H} = \mathbf{J} + \frac{\partial \mathbf{D}}{\partial t} \tag{2.4}$$

$$\nabla \times \mathbf{E} = -\frac{\partial \mathbf{B}}{\partial t} \tag{2.5}$$

$$\nabla \bullet \mathbf{D} = \rho_e \tag{2.6}$$

$$\nabla \bullet \mathbf{B} = 0 \tag{2.7}$$

where **E** is electric field, **H** is magnetic field, **D** is electric flux density, **B** is magnetic field density, **J** is electric current density, and ρ_e is electric charge density.

E, **H, D**, **B,** and **J** represent the instantaneous field vectors as the function of spatial position and time. However in many practical systems, the time variations are of cosinusoidal form and are referred to as time-harmonic situation. Under time-harmonic condition, the Maxwell's equation can be modified to (Balanis, 1989):

$$\nabla \times \mathbf{H} = \mathbf{J} + j\omega\mathbf{D} = \mathbf{J} + j\omega\varepsilon\mathbf{E} \tag{2.8}$$

$$\nabla \times \mathbf{E} = -j\omega\mathbf{B} = -j\omega\mu\mathbf{H} \tag{2.9}$$

$$\nabla \cdot \mathbf{D} = \nabla \cdot \varepsilon\mathbf{E} = \rho_e \tag{2.10}$$

$$\nabla \cdot \mathbf{B} = \nabla \cdot \mu\mathbf{H} = 0 \tag{2.11}$$

where **E**, **H**, **D**, **B**, and **J** represent the corresponding complex spatial forms which are only a function of position.

Finite-difference time domain method

The finite-difference time-domain (FDTD) method is a convenient, easy-to-use, and efficient method for solving electromagnetic scattering problems. It was firstly introduced in 1966 by Yee (1966) and was developed by Taflove (Taflove and Brodwin,

1975; Taflove, 1980; Umashankar and Taflove, 1982) to solve Maxwell's time-dependent curl equations.

Several key attributes combine to make the FDTD method a useful and powerful tool. First is the method's simplicity; Maxwell's equations in differential form are discretized in space and time in a straightforward manner. Second, since the method tracks the time-varying fields throughout a volume of space, FDTD results lend themselves well to scientific visualization methods. These, in turn, provide the user with excellent physical insights into the behavior of electromagnetic fields. Finally, the geometric flexibility of the method permits the solution of a wide variety of radiation, scattering, and coupling problems (Sadiku, 2001a).

The fundamental scheme for finding the finite difference solution of Maxwell's equations is the numerical approximation of the derivative of a function *f(x)*. The central-difference formula is (Sadiku, 2001a):

$$f'(x_0) = \frac{f(x_0 + \Delta x/2) - f(x_0 - \Delta x/2)}{\Delta x} + O(\Delta x^2) \qquad (2.12)$$

where Δx is a sufficiently small interval.

A grid point in a solution region as shown in Figure 2.6 can be defined as (Sadiku, 2001a):

$$(i, j, k) \equiv (i\Delta x, j\Delta y, k\Delta z) \qquad (2.13)$$

And any function of space and time in the solution region can be presented as:

$$F(i, j, k) = F(i\delta, j\delta, k\delta, n\Delta t) \qquad (2.14)$$

where $\delta = \Delta x = \Delta y = \Delta z$ is the space increment, Δt is the time increment, and i, j, k, n are integers.

In applying Eq. (2.12) and with using notation in Eq. (2.13) and (2.14), Eq. (2.4) and (2.5) can be approximated to (Sadiku, 2001a):

$$H_x^{n+1/2}(i,j+1/2,k+1/2) = H_x^{n-1/2}(i,j+1/2,k+1/2) + \frac{\delta t}{\mu(i,j+1/2,k+1/2)\delta}\begin{bmatrix} E_y^n(i,j+1/2,k+1) - E_y^n(i,j+1/2,k) \\ + E_z^n(i,j,k+1/2) - E_z^n(i,j+1,k+1/2) \end{bmatrix} \quad (2.15a)$$

$$H_y^{n+1/2}(i+1/2,j,k+1/2) = H_y^{n-1/2}(i+1/2,j,k+1/2) + \frac{\delta t}{\mu(i+1/2,j,k+1/2)\delta}\begin{bmatrix} E_z^n(i+1,j,k+1/2) - E_z^n(i,j,k+1/2) \\ + E_x^n(i+1/2,j,k) - E_x^n(i+1/2,j,k+1) \end{bmatrix} \quad (2.15b)$$

$$H_z^{n+1/2}(i+1/2,j+1/2,k) = H_z^{n-1/2}(i+1/2,j+1/2,k) + \frac{\delta t}{\mu(i+1/2,j+1/2,k)\delta}\begin{bmatrix} E_x^n(i+1/2,j+1,k) - E_x^n(i+1/2,j,k) \\ + E_y^n(i,j+1/2,k) - E_y^n(i+1,j+1/2,k) \end{bmatrix} \quad (2.15c)$$

$$E_x^{n+1}(i+1/2,j,k) = \left(1 - \frac{\sigma(i+1/2,j,k)\delta t}{\varepsilon(i+1/2,j,k)}\right)E_x^n(i+1/2,j,k) + \frac{\delta t}{\varepsilon(i+1/2,j,k)\delta}\begin{bmatrix} H_z^{n+1/2}(i+1/2,j+1/2,k) - H_z^{n+1/2}(i+1/2,j-1/2,k) \\ + H_y^{n+1/2}(i+1/2,j,k-1/2) - H_y^{n+1/2}(i+1/2,j,k+1/2) \end{bmatrix} \quad (2.15d)$$

$$E_y^{n+1}(i,j+1/2,k) = \left(1 - \frac{\sigma(i,j+1/2,k)\delta t}{\varepsilon(i,j+1/2,k)}\right)E_y^n(i,j+1/2,k) + \frac{\delta t}{\varepsilon(i,j+1/2,k)\delta}\begin{bmatrix} H_x^{n+1/2}(i,j+1/2,k+1/2) - H_x^{n+1/2}(i,j+1/2,k-1/2) \\ + H_z^{n+1/2}(i-1/2,j+1/2,k) - H_z^{n+1/2}(i+1/2,j+1/2,k) \end{bmatrix} \quad (2.15e)$$

$$E_z^{n+1}(i,j,k+1/2) = \left(1 - \frac{\sigma(i,j,k+1/2)\delta t}{\varepsilon(i,j,k+1/2)}\right)E_z^n(i,j,k+1/2) + \frac{\delta t}{\varepsilon(i,j,k+1/2)\delta}\begin{bmatrix} H_y^{n+1/2}(i+1/2,j,k+1/2) - H_y^{n+1/2}(i-1/2,j,k+1/2) \\ + H_x^{n+1/2}(i,j-1/2,k+1/2) - H_x^{n+1/2}(i,j+1/2,k+1/2) \end{bmatrix} \quad (2.15f)$$

To ensure the accuracy of the computed results, the spatial increment must be small compared to the wavelength (usually $\leq \lambda/10$) or minimum dimension of the scatterer. To ensure the stability of the finite difference scheme of equations, the time

increment Δt must satisfy the following stability condition (Sheen et al., 1990; Sadiku, 2001a):

$$u_{\max}\Delta t \le \left(\frac{1}{\Delta x^2}+\frac{1}{\Delta y^2}+\frac{1}{\Delta z^2}\right)^{-\frac{1}{2}} \tag{2.16}$$

where u_{max} is the maximum wave phase velocity within the model.

The principle of the FDTD method makes it more effective in finding the dynamic electromagnetic solutions when the size of the structure is comparable with the wavelength, so the method is normally applied to the structures of the size between 0.1 and 20 wavelengths (QWED, 2005). For the structures whose physical size is smaller than 0.1 of wavelength, the field distribution is close to quasi-static and in general the methods of quasi-static field solutions are advised to be used.

Finite element method

Originally finite element method (FEM) was developed and applied in the field of structural analysis (Cook et al., 2001). In 1968 the method was applied to electromagnetic problems. Although the concept and programming of FEM is not as simple and easy as finite difference method and method of moment, it is a more powerful and versatile numerical technique for handling problems involving complex geometries and inhomogeneous media (Sadiku, 2001a).

Basically a four-step scheme is applied to solve problem by FEM (Sadiku, 1989):

1. discretizing the solution region into a finite number of sub-regions or elements;
2. deriving governing equations for a typical element;
3. assembling of all elements in the solution region;

4. solving the system of equations obtained.

Coupling problem

The traditional electromagnetic simulation softwares concentrate on the applications such as microwave circuits designing, where thermal effects are normally neglected. To simulate a RF heating process, however, thermal effect analysis, besides electromagnetic field investigation, becomes an essential part of the simulation process. During the RF heating two physical factors, temperature and electromagnetic field intensity, will interrelate with each other, because the dissipated energy produced by electromagnetic field heats the materials while their dielectric properties change with temperature. The changes in dielectric properties in turn influence the electromagnetic field distribution. The coupling of two physical phenomena is one of the most critical factors for the successful simulation of RF heating processes.

Previous simulation works

Several previous works have been conducted to numerically simulate the RF drying and heating processes. Neophytou and Metaxas (1998; 1999) demonstrated the capability of finite element method to model the RF heating system. Chan et al. (2004) studied RF heating patterns in foods due to electromagnetic field distribution. Baginski et al. (1990) and Marshall and Metaxas (1998) showed the potential of computer simulation to model RF drying processes, and to couple the electromagnetic and thermodynamic phenomenon during the simulation. However, there has been little systematic research on

the specific application of RF energy in food sterilization processes, and on the influences of the variation in dielectric properties of foods and electric conductivity of circulating water, which is used to mitigate the edge heating effect, on the electromagnetic field distribution, heating rate, and heating pattern in packaged food immersed in circulating water during RF heating process.

Conclusions

Although prior works demonstrated the capability of finite element method in modeling the RF heating system and predicting heating patterns in foods, there has been little systematic research on the influences caused by the variation of dielectric properties of food and circulating water to the electromagnetic field distribution, heating rate, heating pattern. In order to improve RF heating uniformity, it is necessary to study the effects of dielectric properties on electromagnetic field distribution pattern, which is also helpful for the study of RF thermal treatment to heterogeneous foods.

Reference

American Society for Testing and Materials (ASTM). 1971. Standard test methods for complex permittivity. Designation D 2520-86. Method B. West Conshohocken, PA, USA.

Agilent Technologies Co. Ltd. 2006a. The Impedance Measurement Handbook: A Guide to Measurement Technology and Techniques. Agilent Technologies Co. Ltd. Santa Clara, CA, USA.

Agilent Technologies Co. Ltd. 2006b. Agilent Basics of Measuring the Dielectric Properties of Materials Application Note. Agilent Technologies Co. Ltd. Santa Clara, CA, USA.

Athey, T.W., Stuchly, M.A., Stuchly, S.S. 1982. Measurement of radio frequency permittivity of biological tissues with an open-ended coaxial line: Part I. IEEE Transactions on Microwave Theory and Techniques. 30(1): 82-86.

Balanis, C.A. 1989. Advanced engineering electromagnetics. John Wiley & Sons, New York, NY, USA.

Barber, H. 1983. Electroheat. Grande Publishing Limited, London, UK.

Baginski, B., Broughton, R., Hall, D., Christman, L. 1990. Experimental and numerical characterization of the radio-frequency drying of textile materials (II). Journal of Microwave Power and Electromagnetic Energy. 25(2): 104-113.

Cathcart, W.H., Parker, J.J., Beattie, H.G. 1947. The treatment of packaged bread with high frequency heat. Food Technology. 1: 174 -177.

Chan, T.V.C.T., Tang, J.M., Younce, F. 2004. Three-dimensional numerical modeling of an industrial radio frequency heating system using finite elements. Journal of Microwave Power and Electromagnetic Energy. 39(2): 87-106.

Cook, R.D., Malkus, D.S., Plesha, M.E., and Witt, R.J. 2001. Concepts and applications of finite element analysis (fourth edition). John Wiley & Sons Inc, New York, NY, USA.

Engelder, D.S. and Buffler, C.R. 1991. Measuring dielectric properties of food products at microwave frequencies. Microwave World. 12(2): 6-15.

Herve, A. G., Tang, J. Luedecke, L. and Feng, H. 1998. Dielectric properties of cottage cheese and surface treatment using microwaves. Journal of Food Engineering. 37(4): 389-410.

Hewlett-Packard Company.1993. HP 85070M Dielectric probe measurement system, HP 85070B high-temperature dielectric probe kit. Hewlett-Packard Company: 5091-6247E. Palo Alto, CA, USA.

Jones, P.L. and Rowley, A.T. 1996. Dielectric drying. Drying Technology. 14(5): 1063-1098.

Jun, S. and Sastry, S. 2005. Modeling and optimization of ohmic heating of foods inside a flexible package. Journal of Food Process Engineering. 28: 417-436.

Kenyon, E.M., Westcott, D.E., Case, P.L., Gould, J.W. 1971. A system for continuous thermal processing of food pouches using microwave energy. Journal of Food Science. 36: 289-293.

Lorrain, P., Corson, D.R., and Lorrain, F. 1988. Electromagnetic Fields and Waves, 3rd edition. W.H. Freeman and Company, New York, NY, USA.

Marchand, C. and Meunier, T. 1990. Recent developments in industrial radio-frequency technology. Journal of Microwave Power and Electromagnetic Energy. 25(1): 39-46.

Marshall, M.G. and Metaxas, A.C. 1998. Modeling of the radio frequency electric field strength developed during the RF assisted heat pump drying of particulates. Journal of Microwave Power and Electromagnetic Energy. 33(3): 167-177.

Mudgett, R.E. 1986. Electrical properties of foods. In: Mao A, Rizvi SSH, editors. Engineering properties of foods. Marcel Dekker, Inc., New York, NY, USA.

Neophytou, R.I. and Metaxas, A.C. 1998. Combined 3D FE and circuit modeling of radio frequency heating systems. Journal of Microwave Power and Electromagnetic Energy. 33(4): 243-262.

Neophytou, R.I. and Metaxas, A.C. 1999. Combined Tank and Applicator Design of Radio Frequency Heating Systems. IEE Proceedings. – Microwaves, antennas, and propagation. 146(5): 311-318.

Nyfors, E. and Vainikainen, P. 1989. Industrial Microwave Sensors. Artech House, Norwood, MA, USA.

Ohlsson, T. 1989. Dielectric properties and microwave processing. In Food Properties and Computer-Aided Engineering of Food Processing Systems (ed.) R.P. Single and A.G. Medina. Kluwer Academic Publisher, Dordrecht, Netherlands.

Orfeuil, M. 1987. Dielectric hystereris heating. Chapter 7 in Electric Process Heating: 539-575. Battelle Memorial Institute, Columbus, Ohio, USA.

QWED. 2005. Quick Wave User Guide, version 5.0. Warsaw, Poland.

Roussy, G. and Pearce, J.A. 1995. Foundations and industrial applications of microwaves and radio frequency fields. Physical and Chemical Process. John Wiley & Sons, New York, NY, USA.

Ryynanen. S. 1995. The electromagnetic properties of food materials: A review of the basic principles. Journal of Food Engineering. 26(4): 409-429.

Sadiku, M.N.O. 1989. A simple introduction to finite element analysis of electromagnetic problems. IEEE Transaction on Education. 32(2): 85-93.

Sadiku, M.N.O. 2001a. Numerical techniques in electromagnetics, 2nd edition. CRC Press LLC, Boca Raton, Florida, USA.

Sadiku, M.N.O. 2001b. Elements of Electromagnetics, 3rd edition. Oxford University Press Inc., New York, NY, USA.

Seaman, R., Seals, J. 1991. Fruit pulp and skin dielectric properties for 150 MHz to 6400 MHz. Journal of Microwave Power Electromagnetic Energy. 26: 72-81.

Sheen, D.M., Ali, S.M., Abouzahra, M.D., and Kong, J.A. 1990. Application of the three-dimensional finite-difference time-domain method to the analysis of planar microstrip circuits. IEEE Transaction on Microwave Theory and Techniques. 38(7):849-857.

Taflove, A., and Brodwin, M.E. 1975. Numerical solution of steady-state electromagnetic scattering problems using the time-dependent Maxwell's equations. IEEE Microwave Theory Technology. 23(8): 623-630.

Taflove, A.1980. Application of the finite-difference time-domain method to sinusoidal steady-state electromagnetic-penetration problems. IEEE Transaction on Electromagnetic Compatibility. 22(3): 191-202.

Tang, J., Hao, F., Lau, M.2002. Microwave heating in food processing. Chapter 1 in Advances in Bioprocessing Engineering. World Scientific, New York, NY, USA.

Umashankar, K., and Taflove, A. 1982. A novel method to analyze electromagnetic scattering of complex objects. IEEE Trans. EM Comp. 24(4): 397-405.

Von Hippel, A.R. 1954. Dielectric properties and waves. John Wiley & Sons, New York, NY, USA.

Wig, T. 2001. Sterilization and pasteurization of foods using radio frequency heating. Doctor of philosophy dissertation. Department of Biological System Engineering. Washington State University, Pullman, WA, USA.

Yee, K.S. 1966. Numerical solution of initial boundary-value problems involving Maxwell's equations in isotropic media. IEEE Transaction on Antennas and Propagation. 14: 302-307.

Zhao, Y., Flugstad, B., Kolbe, E., Park, J.W., Wells, J.H. 2000. Using capacitive (radio frequency) dielectric heating in food processing and preservation – a review. Journal of Food Process Engineering. 23: 25-55.

Figures

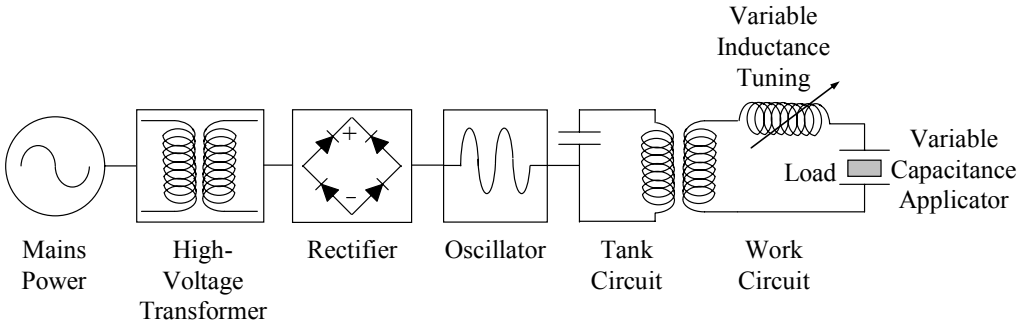

Figure 2.1: Diagram of power oscillator circuit (Wig, 2001)

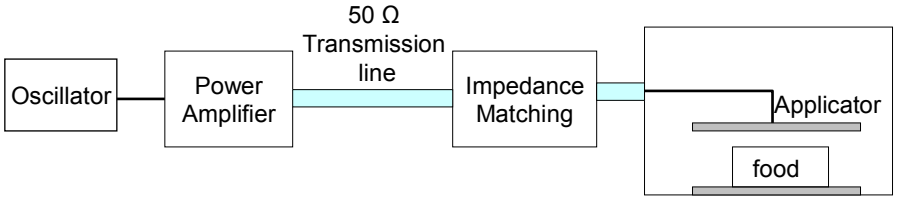

Figure 2.2: Diagram of power amplifier circuit or 50 Ω generator (Pearce, 1996)

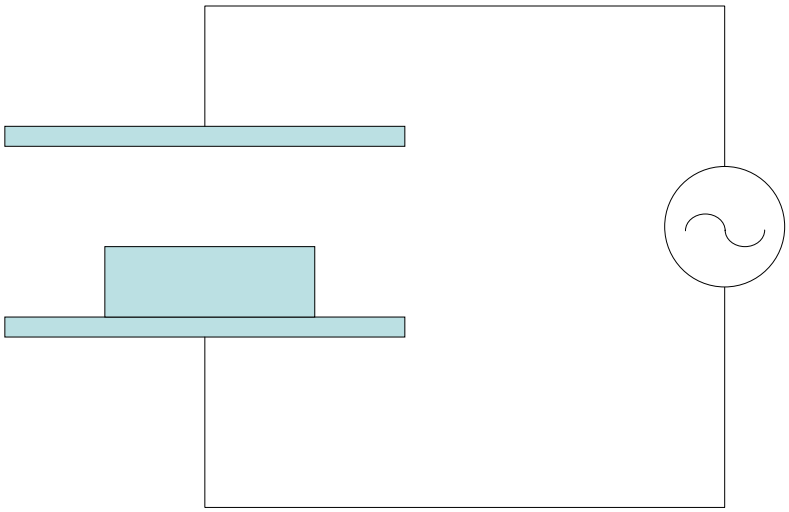

Figure 2.3: Diagram of simple parallel plate applicator

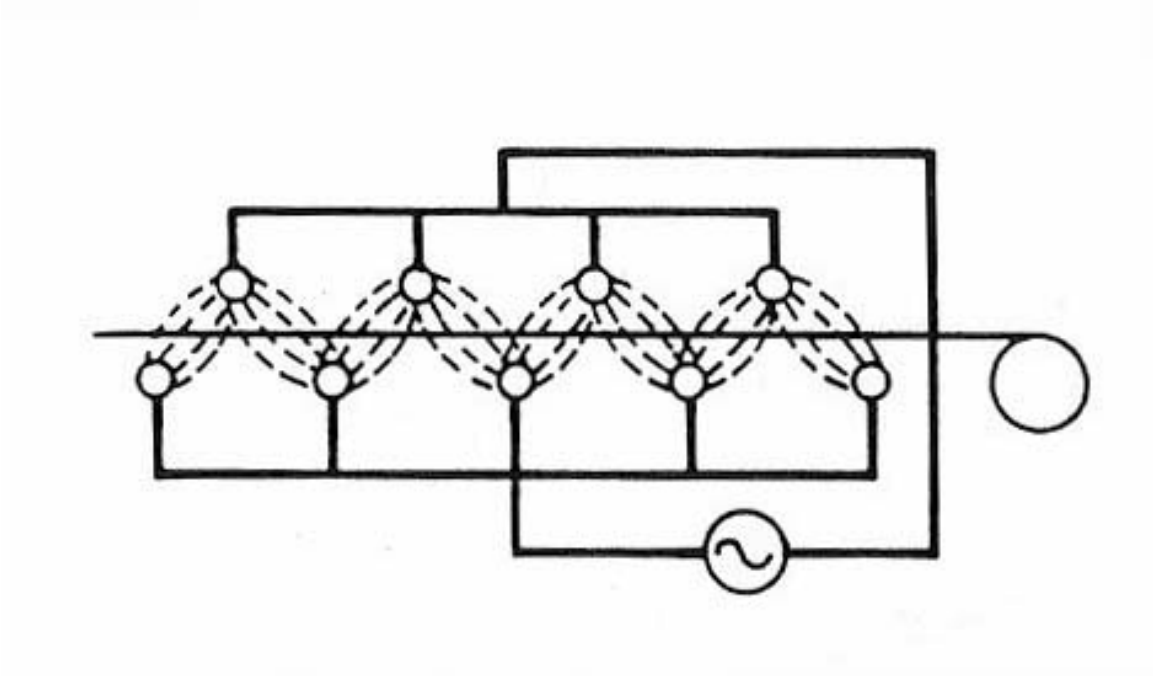

Figure 2.4: Diagram of Garland applicators (Orfeuil, 1987)

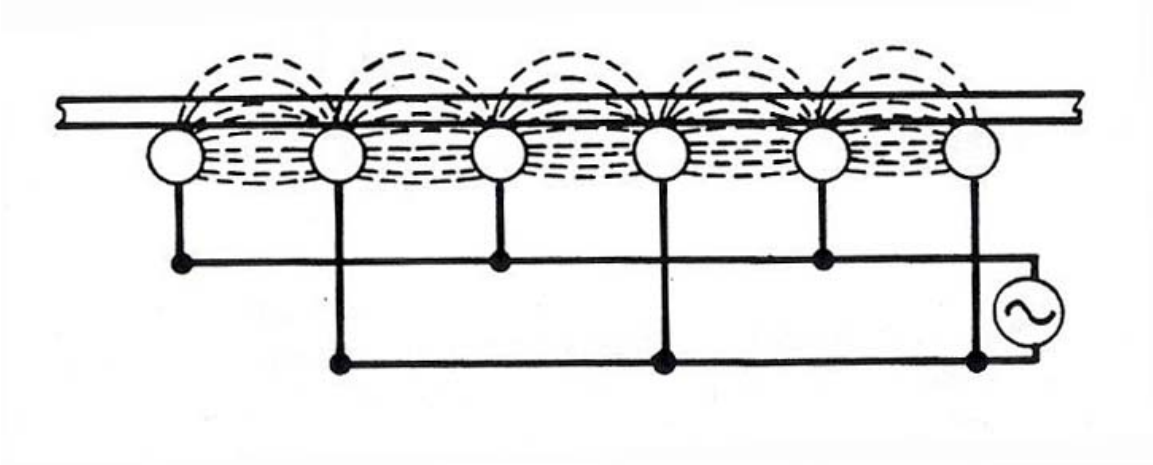

Figure 2.5: Diagram of Strayfield applicators (Orfeuil, 1987)

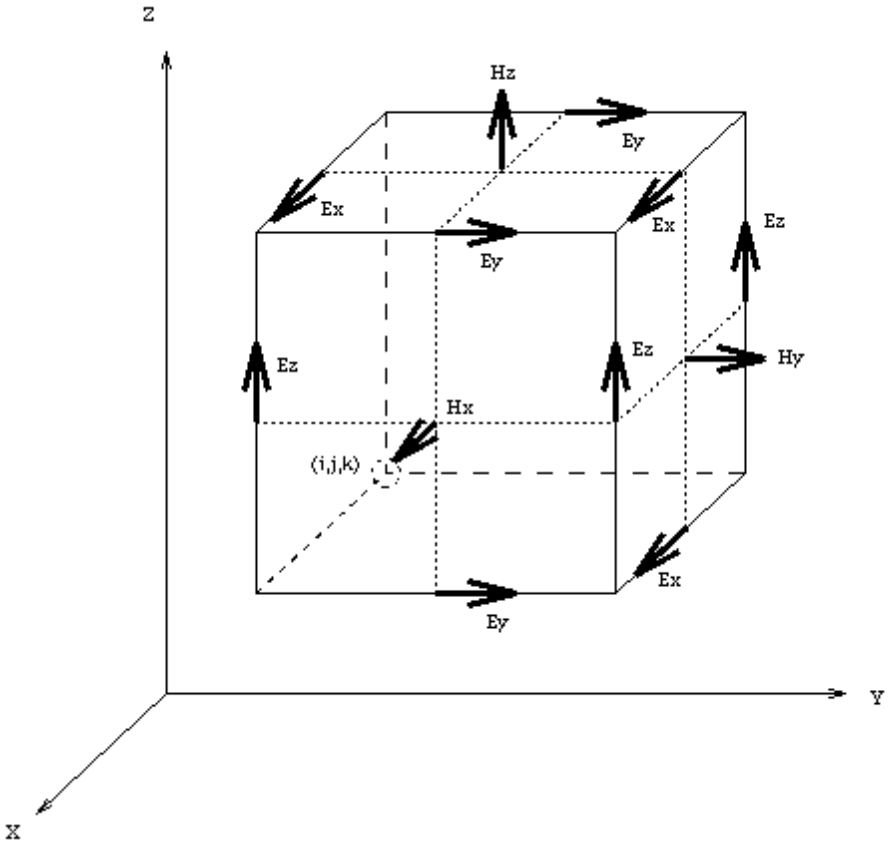

Figure 2.6: Positions of field components in a unit cell (Sadiku, 2001a)

CHAPTER THREE

DIELECTRIC PROPERTIES OF EGG WHITES AND WHOLE EGGS

Abstract

The dielectric properties of liquid whole eggs, pre-cooked whole eggs, liquid egg whites, and pre-cooked egg whites were determined with an open-ended coaxial probe method. The dielectric properties were measured over the temperature range between 20 and 120 °C at radio frequencies 27 and 40 MHz, and microwave frequencies 915 and 1800 MHz. The loss factors exhibited a quadratic relationship with temperature within the measured temperature range. Statistically, the denaturation of liquid egg whites and whole eggs showed significant influences on the dielectric constants and dipole loss component of egg products. Without the influence of denaturation, the dielectric constants of pre-cooked egg whites and whole eggs represented a quadratic relationship with temperature at the selected radio frequencies and microwave frequencies.

Introduction

Shelf stability is one of the most important quality parameters of combat rations, and thermal processing is a common preservation method to produce shelf-stable foods. To achieve commercial sterility, foods are hermetically packed in containers and thermally processed at high temperatures (up to 121 °C) to inactivate spores of toxin-producing organisms (Mudgett, 1986). For foods, especially solid and semisolid foods, conventional retort processes are time-consuming due to the slow heat transfer within

containers. During a conventional sterilization process, the surface of the packaged food is exposed to high temperature much longer than the inner part, and therefore cooked more. Dielectric heating, including radio frequency (RF) and microwave heating, has the potential to reduce processing time and improve heating uniformity because the heat is volumetrically generated inside the food by conversion of alternating electromagnetic (EM) energy to thermal energy (Cathcart et al., 1947; Kinn, 1947; Kenyon et al., 1971). Therefore, dielectric heating can be a more effective alternative to conventional food sterilization processes. However, the optimum design of dielectric heating is hindered by a lack of knowledge about the dielectric properties of selected foods as functions of food composition, temperature, and EM wave frequencies (Zhao et al., 2000).

The dielectric properties of a food describe its ability to store and dissipate electrical energy in response to an alternating EM field (Mudgett, 1986). Dielectric properties are normally described by complex permittivity, ε_c:

$$\varepsilon_c = \varepsilon' - \varepsilon'' = \varepsilon_0(\varepsilon_r' - j\varepsilon_r'') \tag{3.1}$$

where $j = \sqrt{-1}$. ε_0 is permittivity of free space, and ε_r', the relative dielectric constant, is a measure of how much energy from a selected EM field is stored in a material. The relative loss factor, ε_r'', describes the property of a food material to dissipate energy, which typically results in the generation of heat in an applied EM field (Nyfors and Vainikainen, 1989; Lorrain et al., 1998).

The dielectric constant of a polar material can be expressed as (Debye, 1929):

$$\varepsilon' = \varepsilon_\infty + \frac{\varepsilon_s - \varepsilon_\infty}{1 + \omega^2\tau^2} \tag{3.2}$$

where ε_∞ represents the dielectric constant when the molecules do not have adequate time to follow the alternating of external electric field to polarize, ε_s represents the static dielectric constant, and τ is relaxation time, a measure of time taken by the molecules to reach random orientation after the external electric field is switched off (Gabriel et al., 1998). At low and high frequencies, the dielectric constant change is small and close to the value of ε_s and ε_∞, respectively. At intermediate frequencies, the dielectric constant decreases dramatically with the increased frequency and the frequency region is designated as the region of dispersion or relaxation.

Many studies determine the dielectric properties of food materials in RF and MW frequency ranges, including vegetables, fruits, meat, pasta, and others (Tinga and Nelson, 1973; Nelson, 1992; Tran and Stuchly, 1987; Tong and Lentz, 1993; Bircan and Barringer, 2002; Sipahioglu and Barringer, 2003; Wang et al., 2003b; Guan et al., 2004). However, there is a lack of complete documentation of the dielectric properties of whole eggs and egg whites at RF from 27 – 1,800 MHz over temperatures from 20 – 120 ºC. Knowledge of these properties is important to the research of RF and microwave heating, in particular pasteurization and sterilization of egg products

The objectives of this study presented in this chapter were to: 1) measure the dielectric properties of liquid and pre-cooked egg whites and whole eggs at 27, 40, 915, and 1,800 MHz and selected temperatures from 20 to 120 ºC; 2) investigate the influence of temperature and frequency on the dielectric properties of the egg products; and 3) determine the influence of protein denaturation on the dielectric properties of the egg products.

Materials and Methods

Dielectric properties measuring equipment

The open-ended coaxial probe method is an effective broadband measuring technique that keeps sample disturbance to a minimum and does not require a particular sample shape or container (Sheen and Woodhead, 1999). Because the open-ended coaxial probe method is ideal for measuring the dielectric properties of liquids or semisolids, it is the most commonly used method by the food research community (Seaman and Seals, 1991; Herve et al., 1998) and chosen for this study to determine the dielectric properties of egg products.

The dielectric property measurement system (Figure 3.1) consisted of an Agilent 4291B impedance analyzer (Agilent Technologies, Palo Alto, CA), a custom-built test cell (Figure 3.2), a VWR Model 1157 programmable temperature control circulation system (VWR Science Products, West Chester, PA), a high-temperature coaxial cable, and a dielectric probe included in the Hewlett Packard 85070B dielectric probe kit. The custom-built test cell was made with two coaxial stainless steel tubes with 11 and 19 mm radii, respectively. Two tubes were welded to two ferrules with 22 mm radii at both ends. The dielectric probe was fixed by an end-cap and sealed with an o-ring to the ferrule by a clamp. A thermocouple was mounted through the bottom cap to monitor the sample temperature inside the cell. A stainless steel spring and piston provided constant pressure to maintain tight contact between the sample and dielectric probe. A temperature-controlled liquid (90% ethylene glycol and 10% water by volume) was pumped through the space between the two stainless steel tubes of the test cell to control the temperature (from 10 – 130 ºC) of the sample inside the inner stainless steel tube. The impedance

analyzer was connected through an IEEE-488 (GPIB) bus to a computer equipped with custom-designed software DMS 85070 (Innovative Measurement Solutions) to control the impedance analyzer and log the recorded data. The system was used to measure the dielectric properties of samples over frequencies from 1 – 1,800 MHz and temperatures from 10 – 120 ºC. Wang et al. (2003b) provides a detailed description of the dielectric property measurement system.

Materials

Commercially available frozen pasteurized liquid whole eggs for food services were purchased from M.G. Waldbaum Company (Wakefield, NE). The frozen whole eggs were stored below -18 ºC and placed at room temperature for at least 24 h before measurement. The pasteurized egg whites were obtained from Beatrice Foods (Downers Grove, IL) and stored in a refrigerator at 4 ºC.

Liquid whole eggs contain about 73.7% water, 12.9% protein, 11.5% fat, and 1.9% other components such as carbohydrate and ash. Liquid egg whites consist of more than 85% water, around 10% protein, and 5% other components such as lipid, carbohydrate, and ash (Stadelman and Cotterill, 1977). The protein compositions in egg whites are approximately 54% ovalbumin, 13% conalbumin, 11% ovomucoid, and 22% others (Parkinson, 1966).

To prepare pre-cooked whole eggs and egg whites, liquid egg products were poured in beakers. The beakers were then covered with plastic film and heated in an 80 ºC water bath for 10 min. The pre-cooked solid whole eggs and egg whites were then cut

to the shape of a cylinder (radius = 11 mm, height = 70 mm) and placed into the test cell for measurement.

Experiment procedures

Before the measurements, the impedance analyzer was turned on and allowed to warm up for at least 30 min. According to the manufacturer's recommendations, a 4219 B kit that included four calibration standards (an open circuit, a short circuit, a 50 Ω load, and a low-loss capacitor) was used to calibrate the impedance analyzer. The testing probe was connected to the impedance analyzer and further calibrated using an 85070B dielectric probe kit that included a short circuit, an open circuit, and a selected standard load (deionized water at room temperature) (Wang et al., 2003a).

After the calibration, the selected egg sample was placed and sealed in the custom-built test cell. The dielectric properties of the sample were then determined with the impedance analyzer over a 1 – 1,800 MHz frequency range at selected temperatures. The liquid and pre-cooked whole eggs were measured from 20 – 120 °C in steps of 10 °C, and the liquid and pre-cooked egg whites were determined at 20, 40, 60, 70, 80, 100, and 120 °C. Ten to fifteen minute intervals were required to increase egg sample temperatures by 10 and 20 °C, respectively, and achieve a uniform temperature distribution inside the egg samples. All the measurements were conducted in at least four replicates.

Electric conductivity was measured for liquid egg whites and whole eggs at room temperature for four replicates using a conductivity meter (CON-500, Cole-Parmer

Instrument Co., Vernon 124 Hills, IL, USA) equipped with a platinum/epoxy conductivity probe and a built-in temperature sensor.

The Federal Communications Commission allocates 13.56, 27.12, and 40.68 MHz to the RF range, and 915 and 2,450 MHz to the microwave frequency range for industrial, scientific, and medical applications. In this study, the dielectric properties of the selected egg products were measured at 27 and 40 MHz RF frequencies and 915 and 1,800 MHz microwave frequencies. The 1800 MHz was the upper limit of the measurement system and the closest frequency to 2,450 MHz. The measured dielectric property data at selected frequencies and temperatures are listed in Appendices 3.1 to 3.4.

Results and Discussion

Dielectric properties of egg whites

The dielectric properties of egg whites are primarily dependent on water, electrolytes, and proteins such as ovalbumin and conalbumin (Bircan and Barringer, 2002; Ragni et al., 2007). Previous researches reported that the protein denaturation temperature in liquid egg whites is in the range of 58–62 °C, ovalbumin at around 84 °C, and conalbumin in the range of 65–70 °C (Payawal et al., 1946; Donovan et al., 1975; Bircan and Barringer, 2002).

Dielectric constant of pre-cooked egg whites and liquid egg whites

Figure 3.3 shows that the dielectric constants of pre-cooked egg whites as influenced by increasing temperatures decreased in the microwave range but increased in

the RF range. Dielectric constants of pre-cooked and liquid egg whites at 10–1,800 MHz are presented in Figure 3.4 (A) and (B), respectively. For both preheated and liquid egg whites, the observed trend in changes of dielectric constants with temperature was reversed at frequencies around 90 MHz. That is, above 90 MHz, for a given temperature the dielectric constants of egg whites decreased slightly with the increase of frequency, and for a given frequency they decreased with the increase in temperature. But within frequencies from 10–90 MHz, the dielectric constant decreased sharply with the increase in frequency and increased with increasing temperatures

The dielectric constants of liquid egg whites at four selected frequencies as influenced by temperature are presented in Figure 3.5. Egg white dielectric property values at room temperature agree with those reported by Ragni et al. (2007). At 915 and 1,800 MHz microwave frequencies, the dielectric constant of egg whites decreased with increasing temperature until about 60 – 65 ºC, then increased slightly from 65 – 100 ºC, and decreased slightly from 100 – 120 ºC (Figure 3.5A). The initial reduction in the dielectric constants at microwave frequencies when temperature increased from 20 – 60 ºC was mainly caused by influence of water solution. Similar trends were reported by Wang et al. (2003b) for whey protein gels, liquid whey protein mixture, macaroni noodles, and cheese sauce at 915 and 1,800 MHz; by Guan et al. (2004) for mashed potatoes at 915 and 1,800 MHz; and by Bircan et al. (2001) for whey protein solution at microwave frequencies (300 – 2450 MHz).

Egg while solidification at gelation temperatures changed the trend. At 60 – 100 ºC, the dielectric constants increased with increasing temperature, which was similar to that reported by Bircan and Barringer (2002) for water structure stabilization and

relaxation frequency shifting. The smallest dielectric constants were observed at 60 – 65 ºC in this study, whereas the minimum dielectric constant was reported at 70 ºC in Bircan and Barringer (2002). The difference was most probably a result of the triethyl citrate added in our samples by the supplier to improve the foamability of egg whites as a whipping agent. Triethyl citrate served as a denaturing agent (Nakamura, 1964; Meyer and Potter, 1975), which reduced the denaturation temperature. From 100 – 120 ºC, the dielectric properties decreased. The 915 and 1,800 MHz MW frequencies are out of the region of dispersion or relaxation where the molecules do not have sufficient time to follow the alternating of external electric field to polarize. We propose that although the increase of temperature increases the mobility of molecules and ions, so does the chance of collision among them. Because only a few molecules can follow an alternating of electric field, collision may neutralize the possibility of an increased dielectric constant caused by increased temperature. It may even decrease the number of molecules that can successfully rotate with the external electric field, and therefore decrease the dielectric constant.

At 27 and 40 MHz RF, the dielectric constant of liquid egg whites decreased slightly from 20 – 65 ºC, and then increased from 65 – 120 ºC (Figure 3.5B). From 20 – 65 ºC, the dielectric constants of liquid egg whites were close to those of the water solutions reported by Ohlsson et al. (1974); Barber (1983); and Mudgett (1986), indicating that the dielectric constants of liquid egg whites had a corollary dependence on those of water solutions.

Changes in dielectric constant of liquid egg while at microwave and RF frequencies as influenced by temperature differs from that of the pre-cooked solidified

egg whites observed in Figure 3.3. At temperatures greater than 60 ºC, protein begins to denature, protein, water and other components are bound to form a continuous three-dimensional network by intermolecular interactions (Shimada and Matsushita, 1980; Goldsmith and Toledo, 1985). The protein network constrains the movement of water molecular and ions to suppress the electrostatic forces, reduce the net free charge, and decrease the dielectric constants (Shimada and Matsushita, 1980; Bircan and Barringer, 2002). In order to form a homogeneous coagulum, the net free charge has to achieve an equilibrium state to maintain the balance between attractive and repulsive forces on protein structures (Shimada and Matsushita, 1980). When the balance is attained, the number of net free charge is stable. Since the increasing temperature enhances the mobility of net free charges and molecules, the dielectric constants of egg whites in the RF range increases in the temperature range of 65 – 120 ºC. It is also reasonable to see major differences detected in the dielectric constants between liquid and pre-cooked egg whites at denaturation temperatures.

When correlating dielectric constant of pre-cooked egg with temperature, we observed that the standardized residuals larger than 2, indicating that a higher order regression analysis was necessary. The quadratic regression analysis results for the dielectric constants of precooked and liquid egg whites for selected frequencies are summarized in Table 3.1. At 915 and 1,800 MHz, the R^2 for quadratic regression of the liquid egg white dielectric constants with temperature were lower than 50%, indicating a higher order relationship. It is, therefore, more appropriate to use cubic regression to analyze the dielectric constant-temperature relationship to obtain the function with $R^2 \geq 0.8$ and standardized residual < 2.

Loss factor of pre-cooked egg whites and liquid egg whites

The loss factors of pre-cooked and liquid egg whites as influenced by temperature are presented in Figure 3.6 and 3.7, respectively. From 20 to 120 °C, the loss factor of both pre-cooked and liquid egg whites increased with increasing temperature at microwave frequencies and RF. But the loss factor of liquid egg whites increased more rapidly in the RF range with the increase of temperature than in the microwave frequency range. For example, at 27 and 40 MHz, the loss factor of egg whites at 120 °C was about four times the loss factor at 20 °C (Fig. 3.6A). At microwave frequencies of 915 and 1,800 MHz, the loss factor at 120 °C was two – three times the loss factor at 20 °C (Fig. 3.6 B). The faster increase of the loss factor at the RF range can be explained by the two mechanisms that affect the loss factor of aqueous ionic solutions, as shown by the following equation (Mudgett, 1986):

$$\varepsilon'' = \varepsilon''_d + \varepsilon''_\sigma \tag{3.3}$$

The dipole loss component, ε''_d, is due to the dipole rotation, while the ionic loss component, ε''_σ, results from the charge displacement and can be expressed as (Metaxas and Meredith, 1993):

$$\varepsilon''_\sigma = \frac{\sigma}{2\pi f \varepsilon_0} \tag{3.4}$$

where σ is electrical conductivity of the material and f is frequency of the EM wave. Taking the log value on both sides of Eq. (3.4) yields (Guan et al., 2004):

$$\log \varepsilon''_\sigma = -\log f + C \tag{3.5}$$

where constant $C = \log\sigma - \log 2\pi - \log\varepsilon_0$.

Therefore, according to Eq. (3.5), when the ionic loss component dominates the influence on the loss factor of material, there should be a linear relationship between loss factors and frequency on a log-log graph. The electric conductivities of egg products are summarized in Table 3.2. The electric conductivities of liquid egg whites and whole eggs were measured by a conductivity meter at 20 °C for four replicates. The calculated electric conductivities of pre-cooked and liquid egg whites and whole eggs at elevated temperatures were calculated from the measured loss factor at 19 MHz according to Eq. (3.4). The loss factors and their calculated ionic loss components for pre-cooked and liquid egg whites at selected temperatures as influenced by frequency are presented in Figure 3.8. The figures indicate that at frequencies from 10–100 MHz, the loss factors of pre-cooked and liquid egg whites were mainly contributed by the ionic loss components. But at frequencies higher than 100 MHz, the dipole loss component made an increasingly important contribution, increasing temperature reduced the importance of the dipole loss component at our measured microwave frequencies (Mudgett, 1986, Tang et al., 2002). Overall, the loss factor of egg whites increased rapidly with an increase of temperature at 27 and 40 MHz, but slowly at 915 and 1,800 MHz. The same phenomenon was reported by Guan et al. (2004) for mashed potatoes and Wang, et al. (2005) for tropical fruits.

There appeared no apparent influence ($p \leq 0.05$) of protein denaturation on the dielectric loss factor of egg whites between 20 and 100 °C. However, when temperatures increase from 100 – 120 °C, the dielectric loss factors of liquid egg whites are significantly larger than that of preheated denatured egg whites. The statistical differences observed in loss factors at elevated temperatures may be attributed to protein

denaturation, dipole alignment, and charge disposition leading to the differences in loss factors exhibited by liquid and predenatured pseudoplastic egg whites. Heating and cooling of pre-cooked egg whites results in partial denaturation of egg white protein and alignment and possibly agglomeration of the loosely structured mobile proteins, reducing the mobility of dipoles in denatured egg whites. Therefore, upon reheating of denatured egg white protein at high temperatures, the dielectric loss component of denatured egg whites is smaller than the dielectric loss factor of liquid egg whites.

Regression analysis for the loss factors of precooked and liquid egg whites at selected frequencies is summarized in Table 3.3. With R^2 larger than 0.96, the loss factors of pre-cooked and liquid egg whites have a quadratic relationship with temperature.

Dielectric properties of whole eggs

Dielectric constants of pre-cooked and liquid whole eggs

The dielectric constants of pre-cooked and liquid whole eggs as influenced by temperature are presented in Figure 3.9 and 3.10, respectively. With $p \leq 0.05$, there is a significant difference between the dielectric constants of pre-cooked and liquid whole eggs at 27 and 40 MHz from 40 to 70 ºC. However, there is no significant difference at 27 and 40 MHz for the rest of the temperatures, nor at 915 and 1,800 MHz from 20 – 120 ºC. The significant difference at 27 and 40 MHz at certain temperatures revealed the influence of denaturation on the dielectric constants of liquid whole eggs in the RF range (Figure 3.10).

In general, the dielectric constants of whole eggs are smaller than that of egg whites, but larger than that of egg yolk reported by Bircan and Barringer (2002) at

microwave frequencies and by Ragni et al. (2007) at room temperature. Due to the diluting effect of fat (Bircan and Barringer, 2002), the dielectric constants of liquid whole eggs (11.5% fat) are larger than the dielectric constants of liquid egg yolk (> 30% fat) (Stadelman and Cotterill, 1977), but smaller than the dielectric constants of liquid egg whites.

The dielectric constants for pre-cooked and liquid egg whites as influenced by frequency at the tested temperatures are presented in Figure 3.11. For whole eggs, the dielectric constants cross at 90 – 100 MHz. Above 100 MHz, the dielectric constants of egg whites decreased slightly with the increase of frequency, and decreased with increasing temperatures. From 10 – 90 MHz, the dielectric constants decreased with increasing frequencies and increased with increasing temperatures.

The regression analysis for the dielectric constants of precooked and liquid whole eggs for selected frequencies is summarized in Table 3.4. The R^2 for the quadratic regression of dielectric constants of pre-cooked whole eggs and liquid whole eggs with temperature were at least larger than 0.74, demonstrated quadratic relationships.

Loss factor of pre-cooked and liquid whole eggs

Figure 3.12 and 3.13 show, respectively, that the loss factors of pre-cooked liquid whole eggs increase with increasing temperature. In general, the loss factors of whole eggs are lower than that of egg whites but higher than that of egg yolk reported by Bircan and Barringer (2002) at microwave frequencies and by Ragni et al. (2007) at room temperature. The differences are attributed more to the higher electric conductivity (0.64

– 0.78 S/m at 20 °C) and higher water content (85%) of egg whites than lower electric conductivity (0.48–0.56 S/m at 20 ºC) and lower water content (73.7%) of whole eggs.

The loss factors and calculated ionic loss components of pre-cooked and liquid whole eggs at the tested temperatures are presented in Figure 3.14. From 10 – 100 MHz, the loss factors were primarily affected by the ionic loss components, but at frequencies higher than 100 MHz, the dipole loss component had an increasingly important contribution.

The loss factors of pre-cooked whole eggs were not significantly different ($p \leq 0.1$) from that of liquid egg whites at 27, 40, 915, and 1,800 MHz from 20 – 90 °C. However, from 90 – 120 °C, the loss factors of liquid whole eggs were larger than that of preheated egg whites. The similar phenomenon was observed and explained for egg whites, and should be applicable for whole eggs.

Regression analysis for the loss factors of precooked and liquid whole eggs for selected frequencies is summarized in Table 3.5. With R^2 larger than 0.88, the loss factors of pre-cooked and liquid whole eggs have a quadratic relationship with temperature.

Conclusions

The denaturation of egg products during heating resulted in noticeable influences on the dielectric constants of liquid egg whites and whole eggs. As influenced by temperature, the dielectric constants of pre-cooked egg whites and whole eggs increased with increasing temperatures at radio frequencies, but decreased with increasing temperatures at the microwave frequencies.

The loss factors of liquid whole eggs, pre-cooked whole eggs, liquid egg whites, and pre-cooked egg whites increased with increasing temperatures at both RF and microwave frequencies. The denaturation process of egg products did not show a significant effect on the ionic loss component of the loss factors, but did present an effect on the dipole loss components of the loss factors at temperatures above 100 °C.

References

Barber, H. 1983. Electroheat. Sheridan House, New York, NY, USA.

Bircan, C., Barringer, S.A., & Mangino, M.E. 2001. Use of dielectric properties to detect whey protein denaturation. Journal of Microwave Power and Electromagetic Energy, 36, 179–186.

Bircan, C., & Barringer, S.A. 2002. Use of dielectric properties to detect egg protein denaturation. Journal of Microwave Power and Electromagnetic Energy, 37, 89–96.

Cathcart, W.H., Parker, J.J., & Beattie, H.G. 1947. The treatment of packaged bread with high frequency heat. Food Technology, 1, 174–177.

Debye, P. 1929. Polar molecules.The Chemical Catalog Co., New York, NY, USA.

Donovan, J.W., Mapes, C.J., Davis, J.G., & Garibaldi, J.A. 1975. A differential scanning calorimetric study of the stability of egg white to heat denaturation. Journal of the Science of Food and Agriculture, 26, 73–83.

Gabriel, C., Gabriel, S., Grant, E.H., Halstead, B.S.J., & Mingos, D.M.P. 1998. Dielectric parameters relevant to microwave dielectric heating. Chemical Society Reviews, 27, 213–223.

Goldsmith, S.M., & Toledo, R.T. 1985. Kinetics of heat coagulation of egg albumin determined by water binding and rheological measurements. Journal of Food Processing and Preservation, 9, 241–251.

Guan, D., Cheng, M., Wang, Y., & Tang, J. 2004. Dielectric properties of mashed potatoes relevant to microwave and radio-frequency pasteurization and sterilization processes. Journal of Food Science, 69, 30–37.

Herve, A.G., Tang, J., Luedecke, L., & Feng, H. 1998. Dielectric properties of cottage cheese and surface treatment using microwaves. Journal of Food Engineering, 37, 389–410.

Kenyon, E.M., Westcott, D.E., Case, P.L., & Gould, J.W. 1971. A system for continuous thermal processing of food pouches using microwave energy. Journal of Food Science, 36, 289–293.

Kinn, T.P. 1947. Basic theory and limitations of high frequency heating equipment. Food Technology, 1, 161–173.

Lorrain, P., Corson, D.R., & Lorrain, F. 1988. Electromagnetic fields and waves. 3rd edition. W.H. Freeman and Company, New York, NY, USA.

Metaxas, A.C., & Meredith, R.J. 1993. Industrial microwave heating. Peter Peregrinus Ltd., London, U.K.

Meyer, R., & Potter, N.N. 1975. Ultrastructural changes in unwhipped and whipped egg albumen containing sodium hexametaphosphate and triethyl citrate plus trisodium citrate. Poultry Science, 54, 101–108.

Mudgett, R.E. 1986. Electrical properties of foods. In A. Mao, S.S.H. Rizvi, (Eds.), Engineering properties of foods. Marcel Dekker, New York, NY, USA.

Nakamura, R. 1964. Studies on the foaming properties of the chicken egg white. Part VII. On the foaming of denatured ovalbumin. Agricultural and Biological Chemistry, 28, 401–407.

Nelson, S.O. 1992. Measurement and applications of dielectric properties of agricultural products. IEEE Transactions on Instrumentation and Measurement, 41, 116–122.

Nyfors, E., Vainikainen, P. 1989. Industrial microwave sensors. Artech House, Norwood, MA, USA.

Ohlsson, T., Bengtsson, N.E., & Risman, P.O. 1974. The frequency and temperature dependence of dielectric food data as determined by a cavity perturbation technique. Journal of Microwave Power, 9, 129–145.

Parkinson, T.L. 1966. The chemical composition of eggs. Journal of the Science of Food and Agriculture, 17, 101–111.

Payawal, S.R., Lowe, B., & Stewart, G.F. 1946. Pasteurization of liquid-egg products. II. Effect of heat treatments on appearance and viscosity. Food Research, 11, 246–260.

Ragni, L., Al-Shami, A., Mikhaylenko, G., & Tang, J. 2007. Dielectric characterization of hen eggs during storage. Journal of Food Engineering, in press.

Seaman, R., & Seals, J. 1991. Fruit pulp and skin dielectric properties for 150 MHz to 6400 MHz. Journal of Microwave Power and Electromagnetic Energy, 26, 72–81.

Sheen, N., & Woodhead, I. 1999. An open-ended coaxial probe for broad-band permittivity measurement of agricultural products. Journal of Agricultural Engineering Research, 74, 193–203.

Shimada, K., & Matsushita, S. 1980. Thermal coagulation of egg albumin. Journal of Agriculutral Food Chemistry, 28, 409–412.

Stadelman, J.W., & Cotterill, J.O. 1977. Egg science and technology. 2nd edition. AVI Publishing Company, Inc. Westport, CT, USA.

Sipahioglu, O., & Barringer, S.A. 2003. Dielectric properties of vegetables and fruits as a function of temperature, ash, and moisture content. Journal of Food Science, 68, 234–239.

Tang, J., Feng, H., and Lau, M. 2002. Microwave heating in food processing, in Advances in Bioprocessing Engineering, (eds.) Young, X., Tang, J., World Scientific Publisher, River Edge, New Jersey, USA. 1-43.

Tinga, W.R., & Nelson, S.O. 1973. Dielectric properties of materials for microwave processing. Journal of Microwave Power, 8, 23–65.

Tong, C.H., & Lentz, R.R. 1993. Dielectric properties of Bentonite pastes as a function of temperature. Journal of Food Processing and Preservation, 17, 139–145.

Tran, V.N., & Stuchly, S.S. 1987. Dielectric properties of beef, beef liver, chicken and salmon at frequencies from 100 to 2500 MHz. 21st Symposium Proceedings of IMPI, 116.

Wang, S., Tang, J., Johnson, J.A., Mitcham, E., Hansen, J.D., Hallman, G., Drake, S.R., & Wang, Y. 2003a. Dielectric properties of fruits and insect pests as related to radio frequency and microwave treatments. Biosystems Engineering, 85, 201–12.

Wang, Y., Wig, T., Tang, J., & Hallberg, L.M. 2003b. Dielectric properties of food relevant to RF and microwave pasteurization and sterilization. Journal of Food Engineering, 57, 257–68.

Wang, S., Monzon, M., Gazit, Y., Tang J., Mitcham, E.J., & Armstrong, J.W. 2005. Temperature-dependent dielectric properties of selected subtropical and tropical fruits and associated insect pests. Transactions of the ASAE, 48, 1873–81.

Zhao, Y., Flugstad, B., Kolbe, E., Park, J.W., & Wells, J.H. 2000. Using capacitive (radio frequency) dielectric heating in food processing and preservation – a review. Journal of Food Process Engineering, 23, 25–55.

Tables

Table 3.1: Regression analysis for dielectric constants of pre-cooked and liquid egg whites

dielectric constants of pre-cooked egg whites		
Frequency (MHz)		R^2
27	$\varepsilon' = 94.22 - 0.31\ T + 4.58 \times 10^{-3}\ T^2$	0.94
40	$\varepsilon' = 83.87 - 0.11\ T + 2.22 \times 10^{-3}\ T^2$	0.74
915	$\varepsilon' = 70.56 - 0.32\ T + 1.26 \times 10^{-3}\ T^2$	0.85
1800	$\varepsilon' = 69.98 - 0.345\ T + 1.36 \times 10^{-3}\ T^2$	0.92
dielectric constants of liquid egg whites		
Frequency (MHz)		R^2
27	$\varepsilon' = 91.33 - 0.59\ T + 0.0081\ T^2$	0.93
40	$\varepsilon' = 84.08 - 0.56\ T + 0.0057\ T^2$	0.80
915	$\varepsilon' = 80.17 - 0.81\ T + 7.46 \times 10^{-3}\ T^2 - 2.12 \times 10^{-5}\ T^3$	0.82
1800	$\varepsilon' = 80.79 - 1.0\ T + 0.013\ T^2 - 4.27 \times 10^{-5}\ T^3$	0.89

Table 3.2: Summary of electric conductivities of egg whites and whole eggs (mean ± stand deviation) for four replicates*

Temperature (ºC)	Liquid egg whites	Pre-cooked egg whites	Liquid whole eggs	Pre-cooked whole eggs
20	0.71 ± 0.07 **	0.69 ± 0.09	0.52 ± 0.04 **	0.53 ± 0.05
60	1.01 ± 0.17	1.14 ± 0.12	0.95 ± 0.05	0.92 ± 0.06
100	1.90 ± 0.10	1.74 ± 0.10	1.48 ± 0.07	1.35 ± 0.10

* Conductivities were calculated based on Eq. (3.4) through the loss factor of egg products at 19 MHz, except liquid egg whites and whole eggs at 20 ºC.

** Measured with a conductivity meter.

Table 3.3: Regression analysis for loss factors of pre-cooked and liquid egg whites

loss factors of pre-cooked egg whites		
Frequency (MHz)		R^2
27	$\varepsilon'' = 324.71 + 3.85\ T + 4.69 \times 10^{-2}\ T^2$	0.99
40	$\varepsilon'' = 184.90 + 3.35\ T + 1.97 \times 10^{-2}\ T^2$	0.99
915	$\varepsilon'' = 16.70 + 8.20 \times 10^{-2}\ T + 1.75 \times 10^{-3}\ T^2$	0.99
1800	$\varepsilon'' = 14.87 - 3.99 \times 10^{-2}\ T + 1.25 \times 10^{-3}\ T^2$	0.98
loss factors of liquid egg whites		
Frequency (MHz)		R^2
27	$\varepsilon'' = 482.46 - 3.96\ T + 0.11\ T^2$	0.97
40	$\varepsilon'' = 239.96 + 0.11\ T + 5.14 \times 10^{-2}\ T^2$	0.98
915	$\varepsilon'' = 19.26 - 9.88 \times 10^{-2}\ T + 3.43 \times 10^{-3}\ T^2$	0.97
1800	$\varepsilon'' = 16.18 - 0.13\ T + 1.96 \times 10^{-3}\ T^2$	0.91

Table 3.4: Regression analysis for dielectric constants of pre-cooked and liquid whole eggs

pre-cooked whole eggs		
Frequency (MHz)		R^2
27	$\varepsilon' = 81.42 - 7.41 \times 10^{-2}\ T + 2.15 \times 10^{-3}\ T^2$	0.74
40	$\varepsilon' = 73.62 - 0.12\ T + 1.44 \times 10^{-3}\ T^2$	0.80
915	$\varepsilon' = 58.98 - 0.18\ T + 3.67 \times 10^{-4}\ T^2$	0.98
1800	$\varepsilon' = 57.39 - 0.17\ T + 2.40 \times 10^{-4}\ T^2$	0.94
liquid whole eggs		
Frequency (MHz)		R^2
27	$\varepsilon' = 79.31 - 0.22\ T + 3.79 \times 10^{-3}\ T^2$	0.88
40	$\varepsilon' = 72.65 - 0.24\ T + 2.77 \times 10^{-3}\ T^2$	0.80
915	$\varepsilon' = 61.25 - 0.22\ T + 7.60 \times 10^{-4}\ T^2$	0.76
1800	$\varepsilon' = 56.62 - 0.142\ T + 1.8 \times 10^{-4}\ T^2$	0.80

Table 3.5: Regression analysis for loss factors of pre-cooked and liquid whole eggs

pre-cooked whole eggs		
Frequency (MHz)		R^2
27	$\varepsilon'' = 199.19 + 6.43\ T + 3.51 \times 10^{-3}\ T^2$	0.94
40	$\varepsilon'' = 125.93 + 3.91\ T + 2.50 \times 10^{-3}\ T^2$	0.95
915	$\varepsilon'' = 12.76 + 0.15\ T + 6.12 \times 10^{-4}\ T^2$	0.96
1800	$\varepsilon'' = 11.98 - 1.79 \times 10^{-3}\ T + 6.93 \times 10^{-4}\ T^2$	0.95
liquid whole eggs		
Frequency (MHz)		R^2
27	$\varepsilon'' = 195.82 + 6.42\ T + 1.17 \times 10^{-2}\ T^2$	0.99
40	$\varepsilon'' = 123.46 + 3.88\ T + 7.67 \times 10^{-3}\ T^2$	0.99
915	$\varepsilon'' = 11.86 + 0.16\ T + 7.85 \times 10^{-4}\ T^2$	0.97
1800	$\varepsilon'' = 12.30 - 8.07 \times 10^{-3}\ T + 8.43 \times 10^{-4}\ T^2$	0.88

Figures

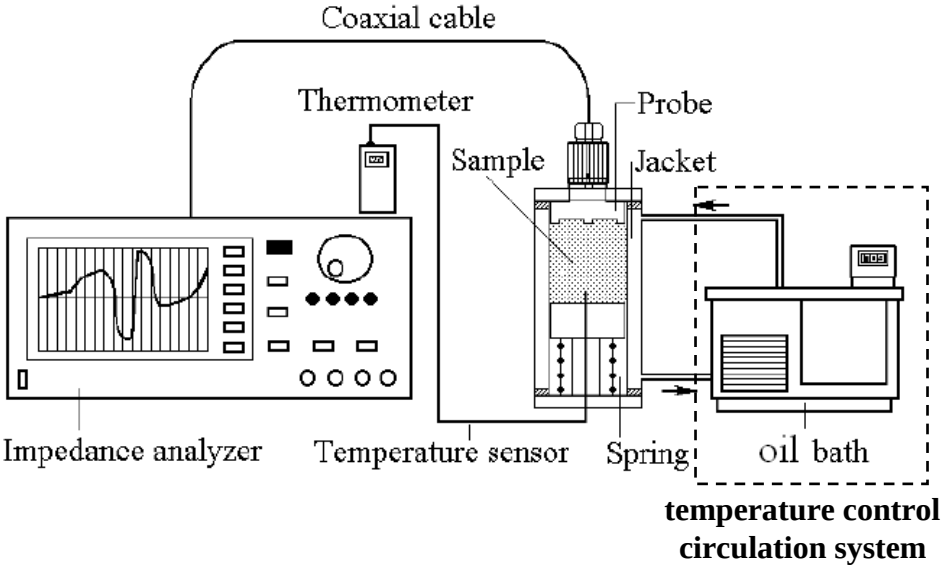

Figure 3.1: Diagram of a dielectric property measurement system (Wang et al., 2005)

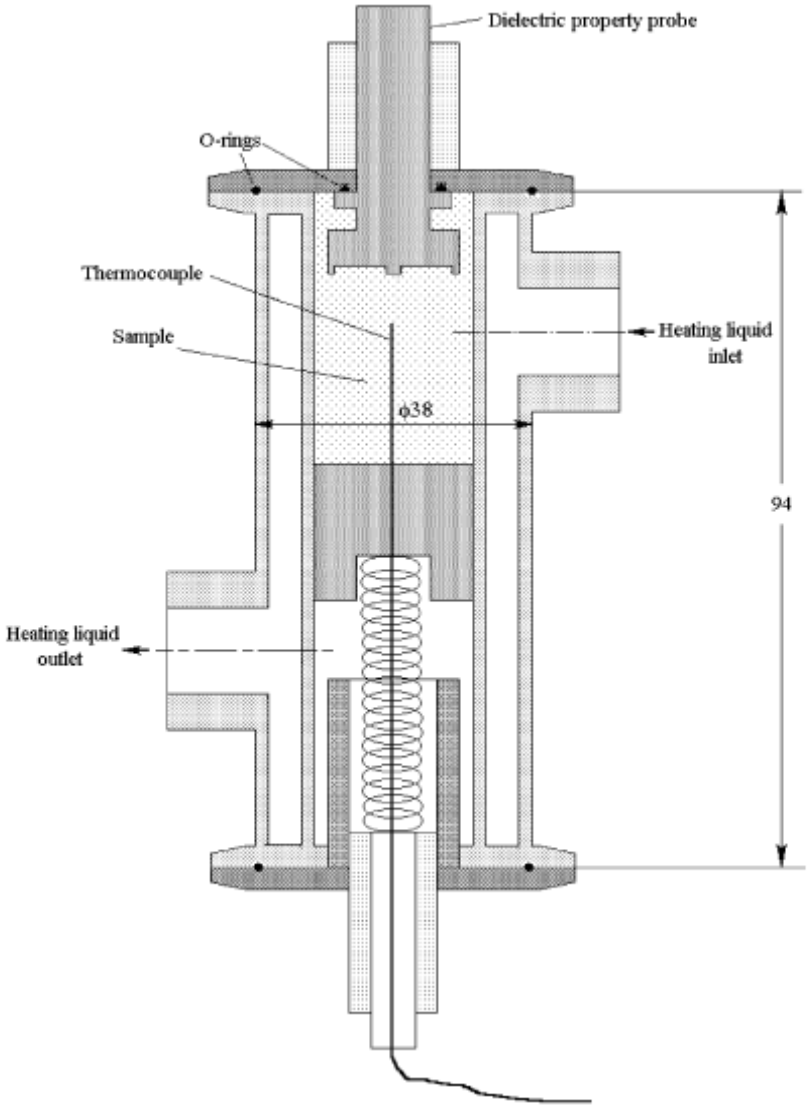

Figure 3.2: Diagram of a custom-built test cell, dimensions in mm (Wang et al., 2003b)

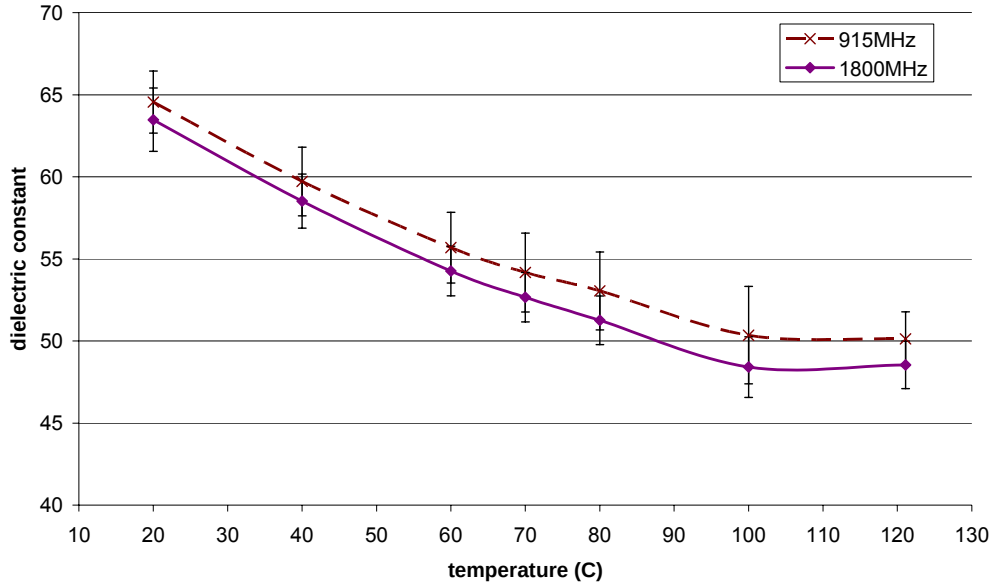

(A)

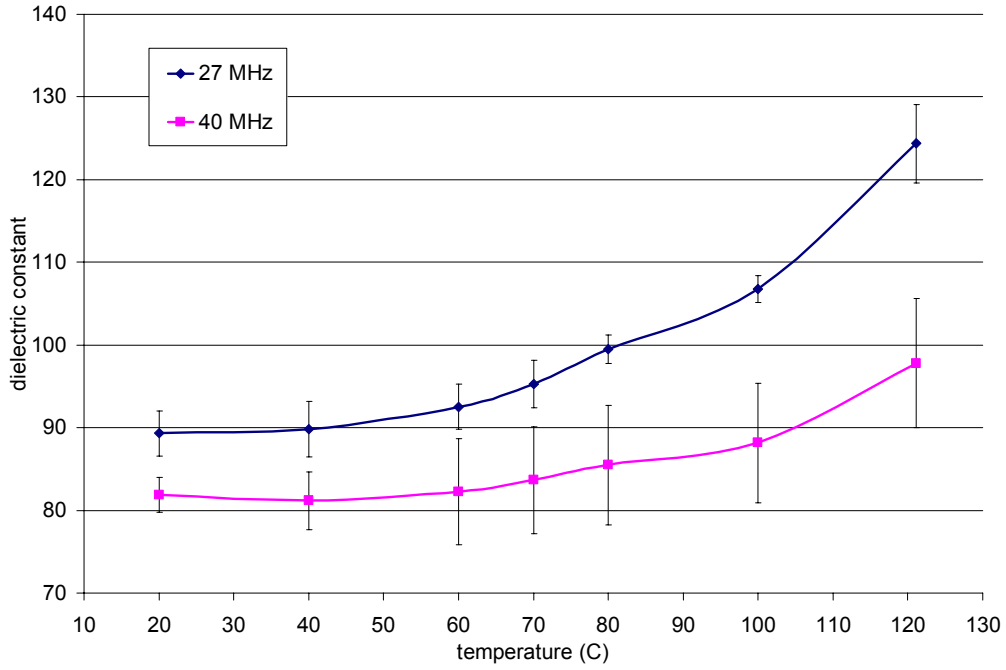

(B)

Figure 3.3 Dielectric constants of pre-cooked egg whites at (A) microwave frequencies and (B) radio frequencies

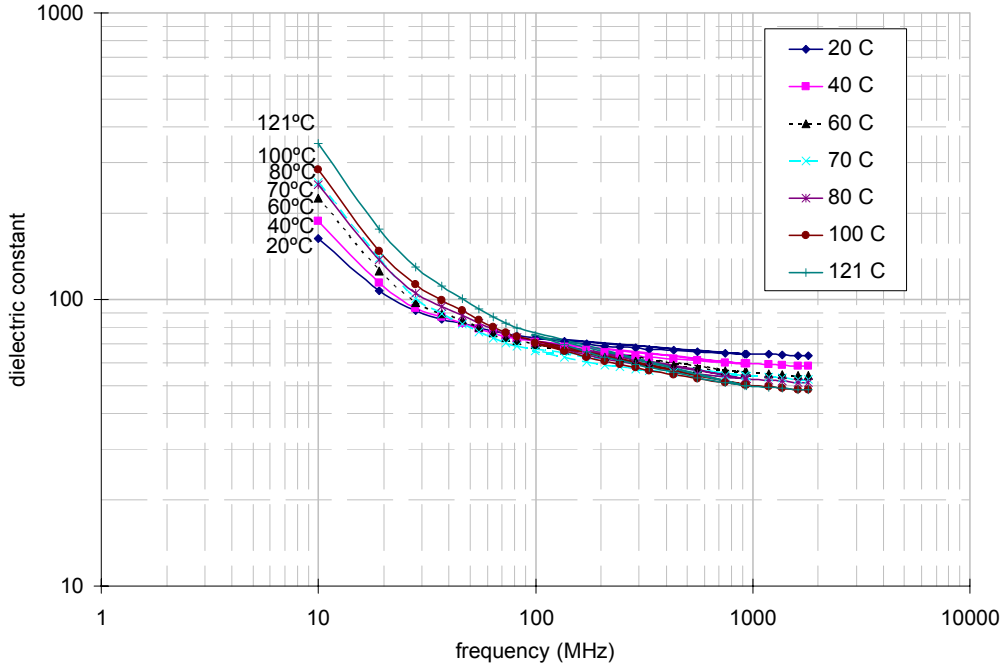

(A)

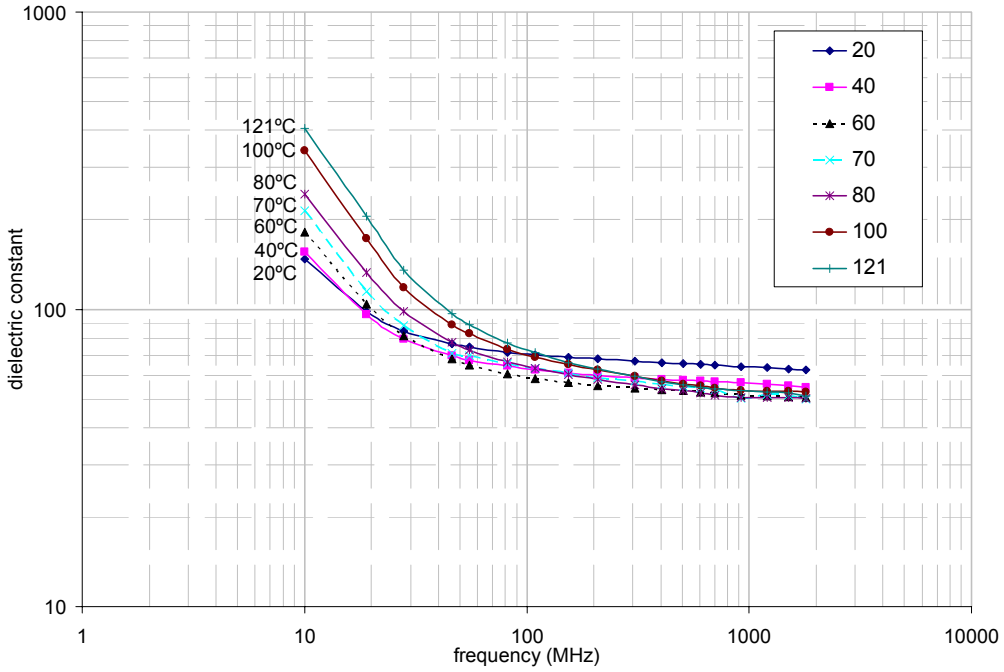

(B)

Figure 3.4: Dielectric constant of (A) pre-cooked and (B) liquid egg whites vs. frequency at different temperatures (the unit of temperature is ºC)

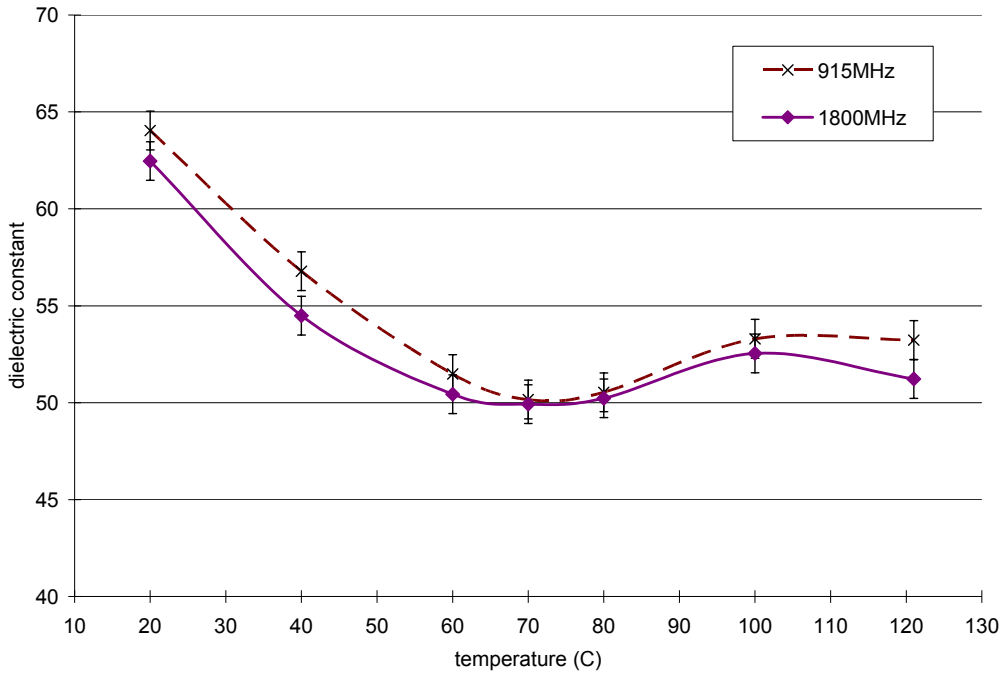

(A)

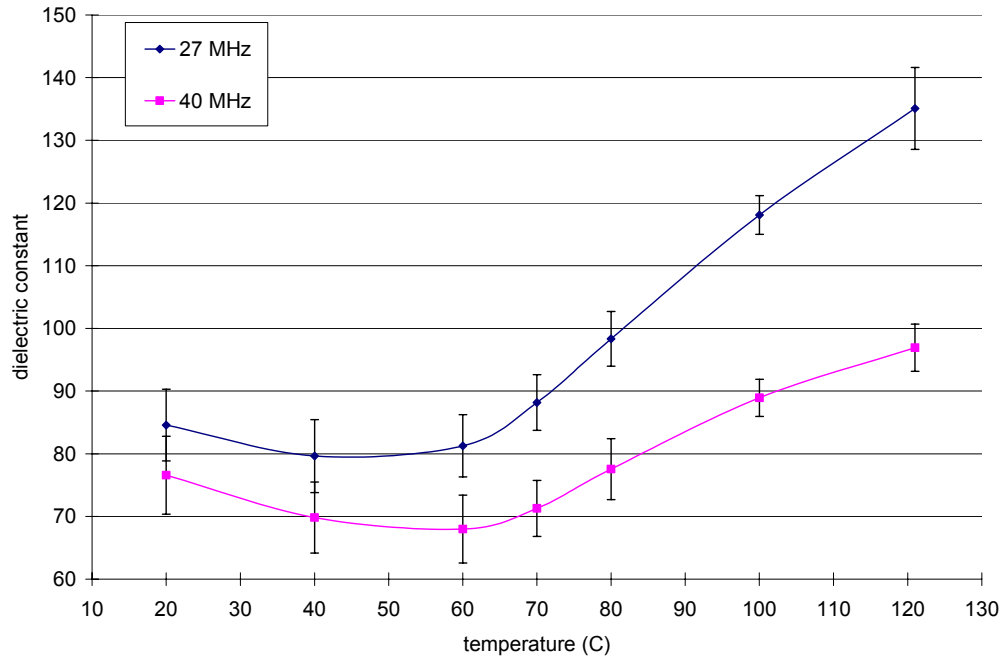

(B)

Figure 3.5: Dielectric constants of liquid egg whites at (A) microwave frequencies and (B) radio frequencies.

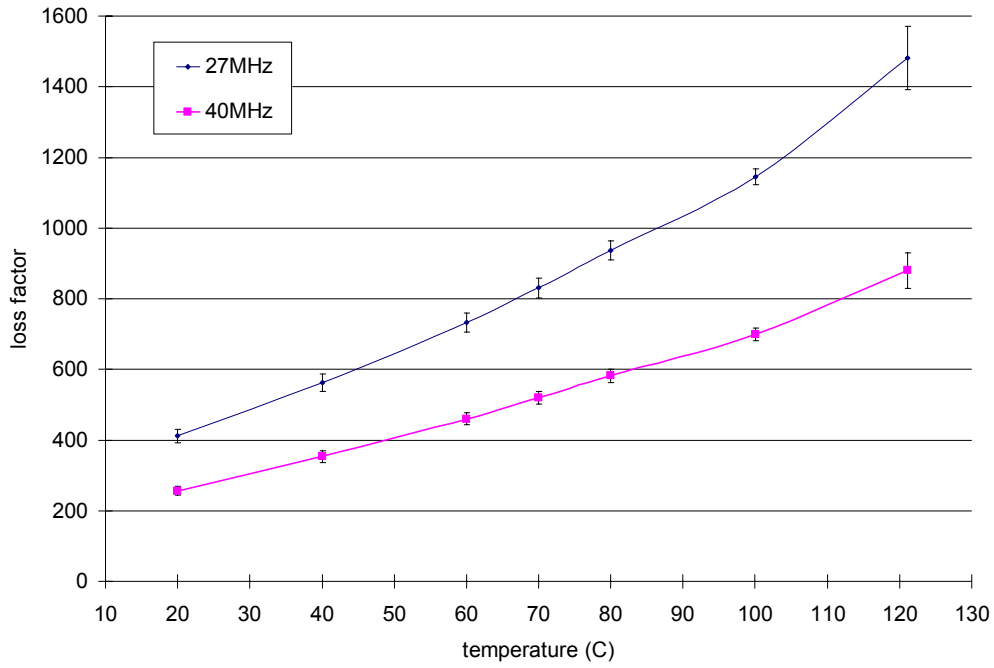

(A)

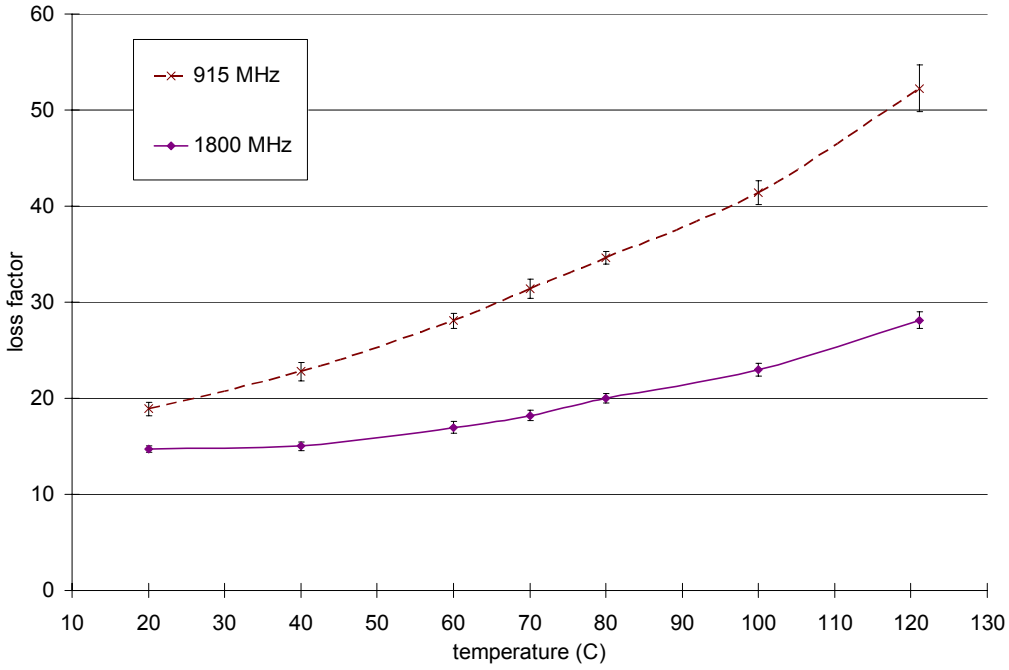

(B)

Figure 3.6: Loss factors of pre-cooked egg whites at (A) radio frequencies and (B) microwave frequencies.

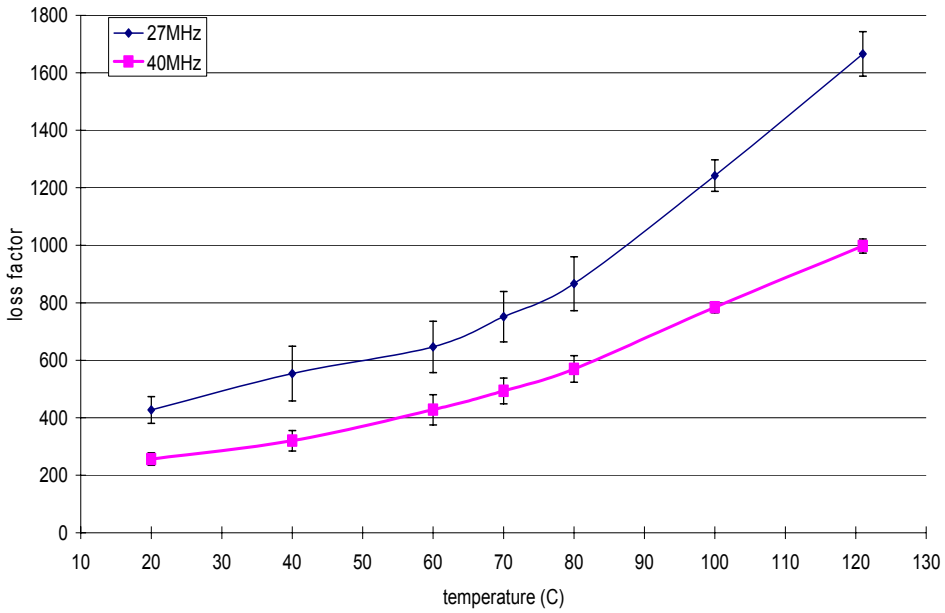

(A)

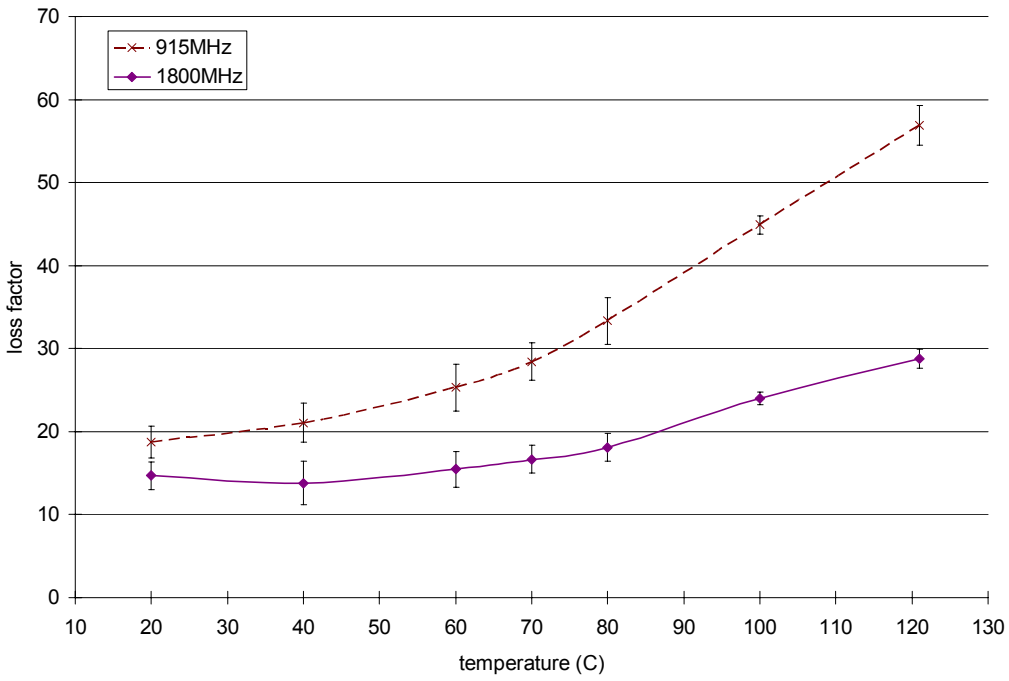

(B)

Figure 3.7: Loss factors of liquid egg whites at (A) radio frequencies and (B) microwave frequencies.

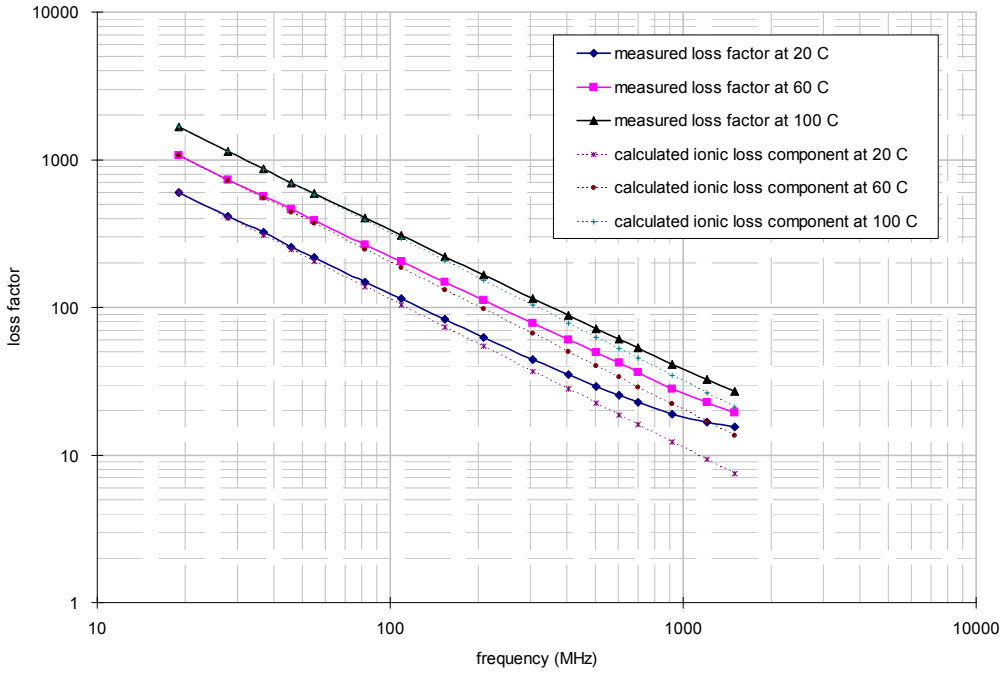

(A)

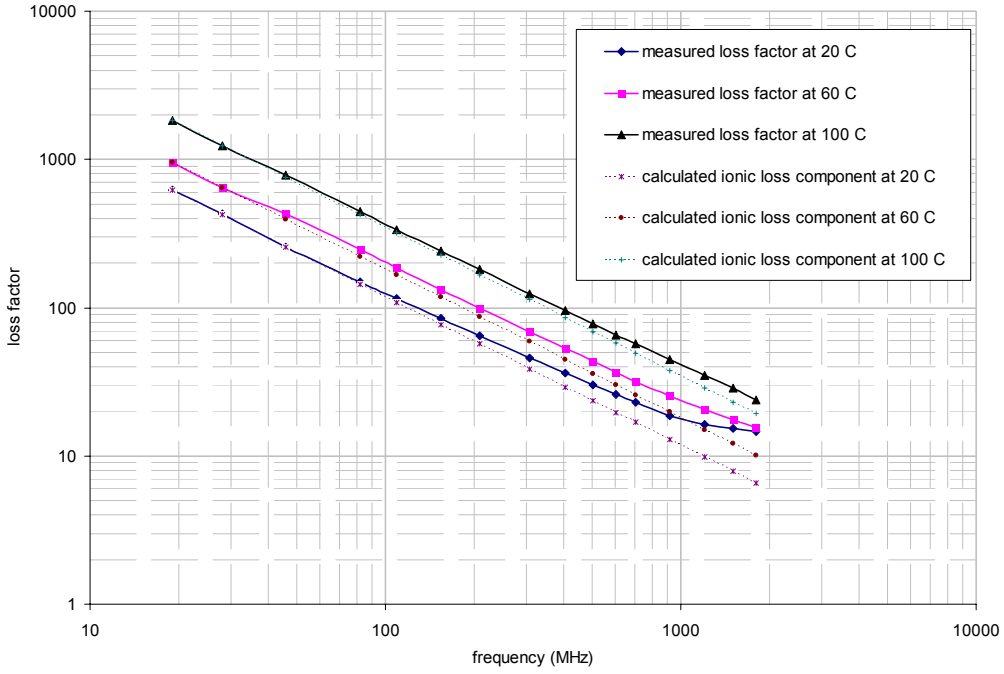

(B)

Figure 3.8: Loss factors and calculated ionic loss components of at (A) pre-cooked and (B) liquid egg whites vs. frequency at selected temperatures (the unit of temperature is

ºC).

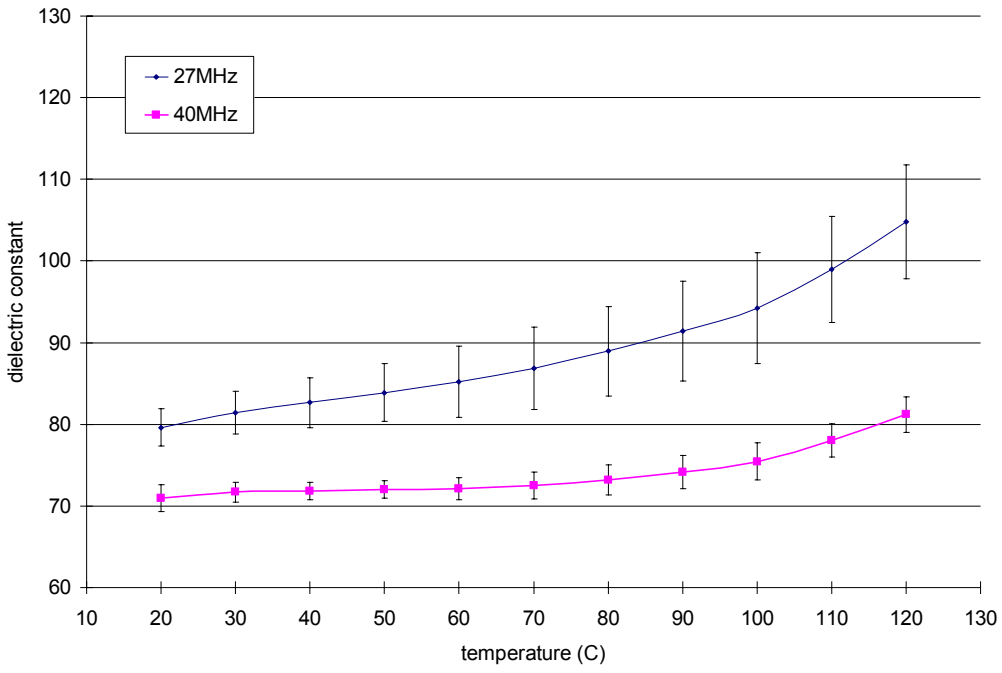

(A)

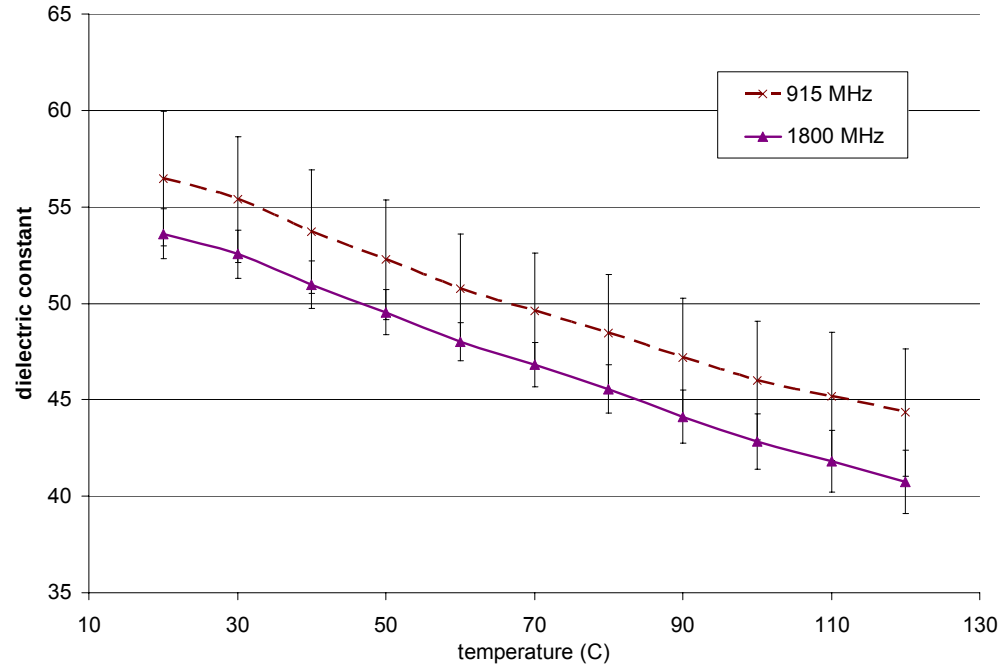

(B)

Figure 3.9: Dielectric constants of pre-cooked whole eggs at (A) radio frequencies, and (B) microwave frequencies.

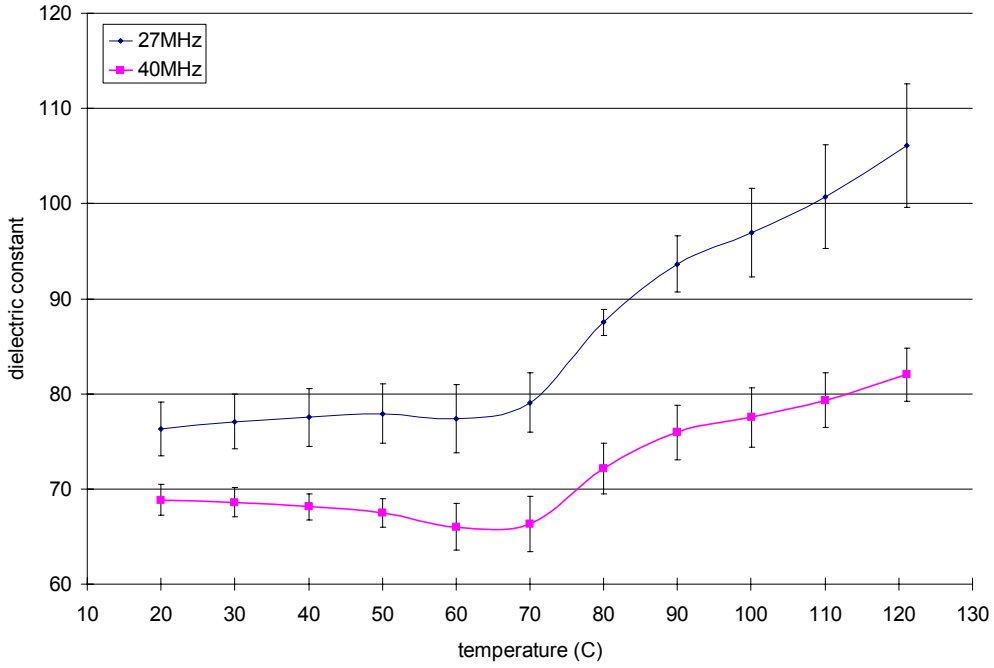

(A)

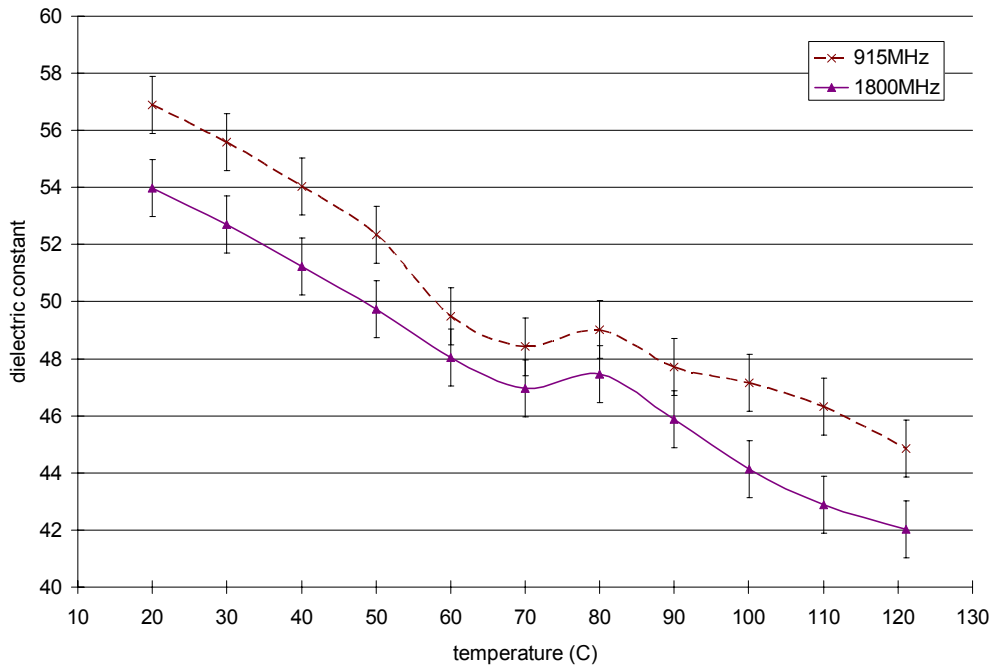

(B)

Figure 3.10: Dielectric constants of liquid whole eggs at (A) radio frequencies, and (B) microwave frequencies.

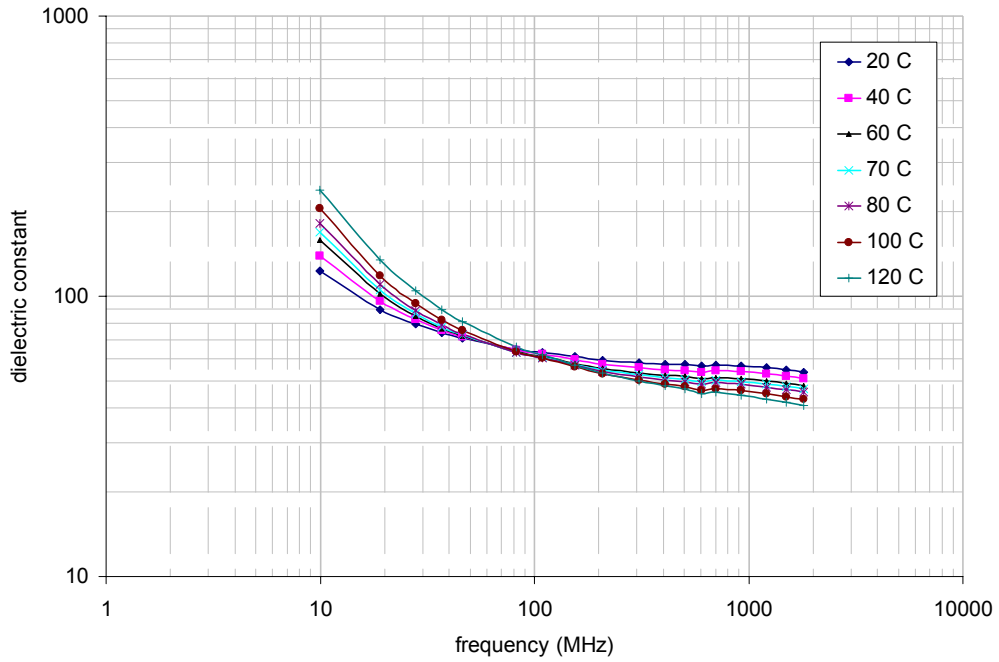

(A)

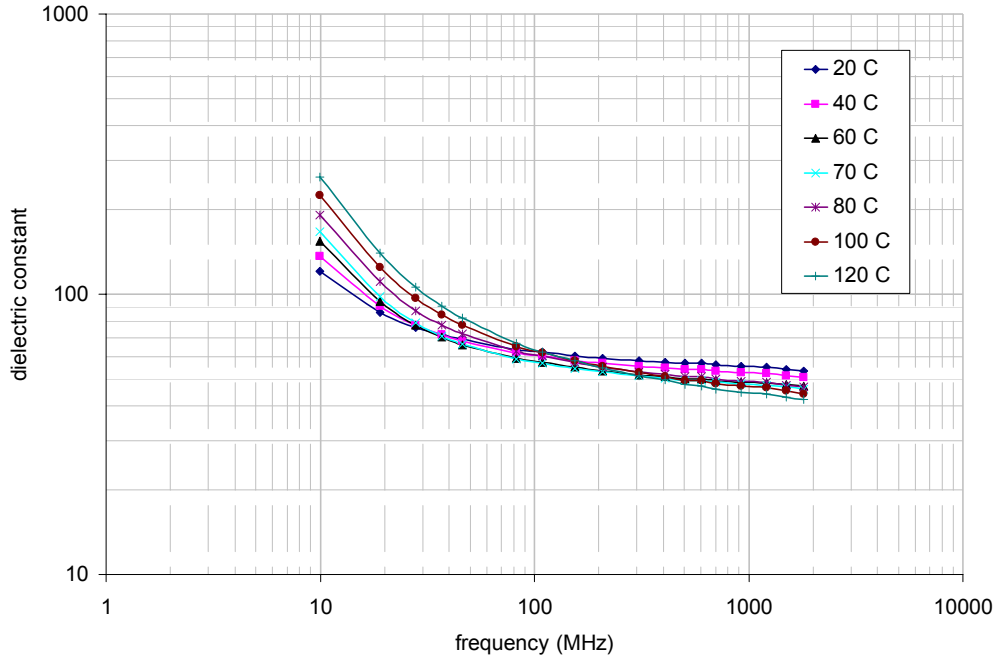

(B)

Figure 3.11: Dielectric constant of (A) pre-cooked and (B) liquid whole eggs vs. frequency at different temperatures (the unit of temperature is ºC).

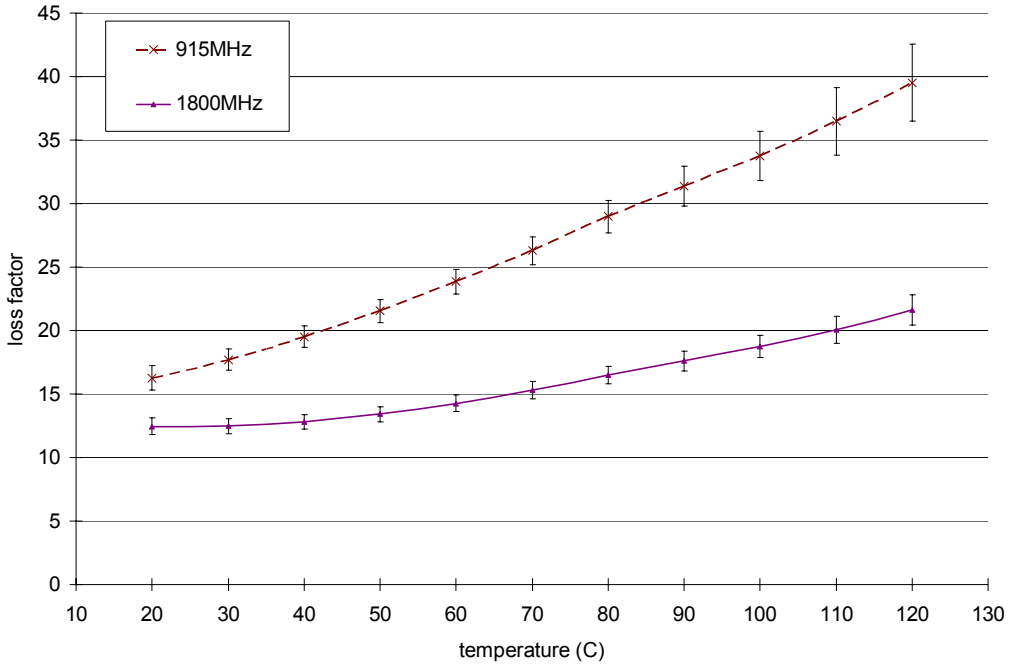

(A)

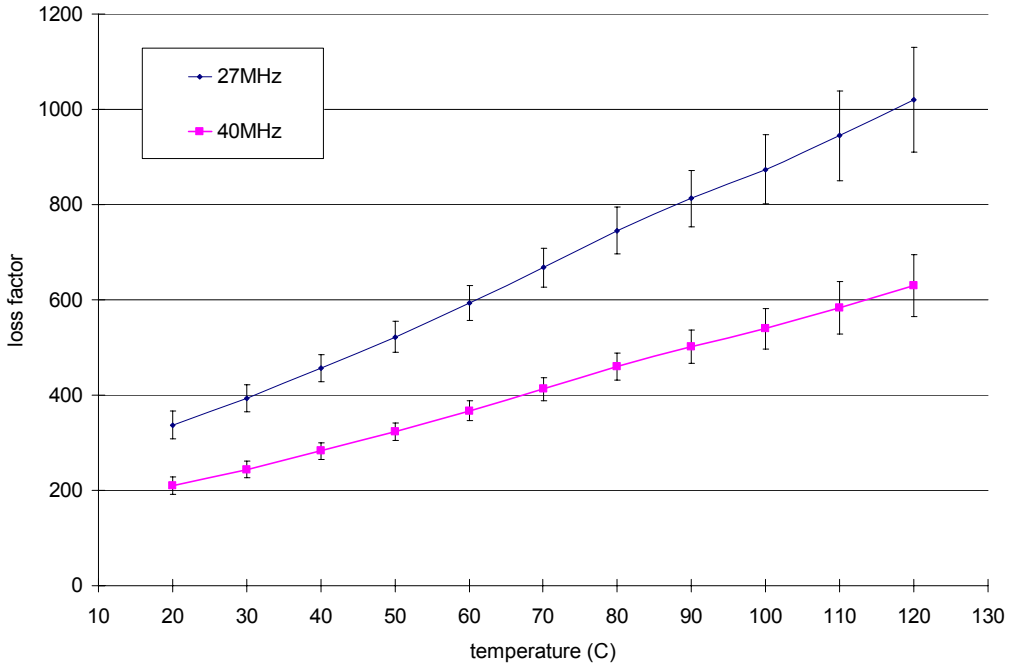

(B)

Figure 3.12: Loss factors of pre-cooked whole eggs at (A) microwave frequencies, and (B) radio frequencies.

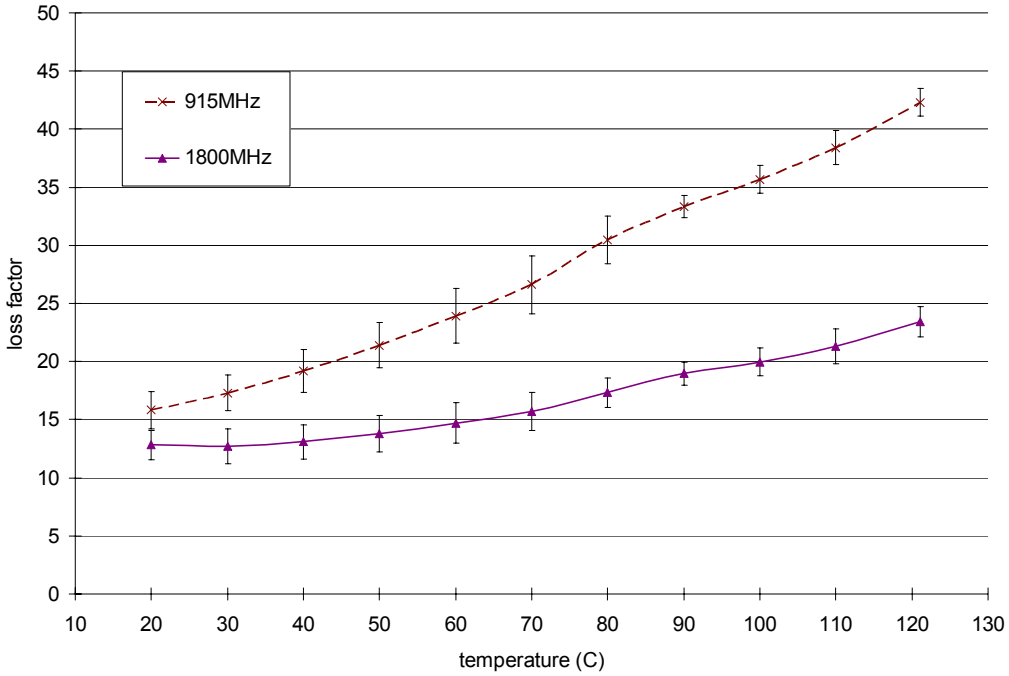
915MHz
1800MHz
loss factor
temperature (C)
0
5
10
15
20
25
30
35
40
45
50
10
20
30
40
50
60
70
80
90
100
110
120
130

(A)

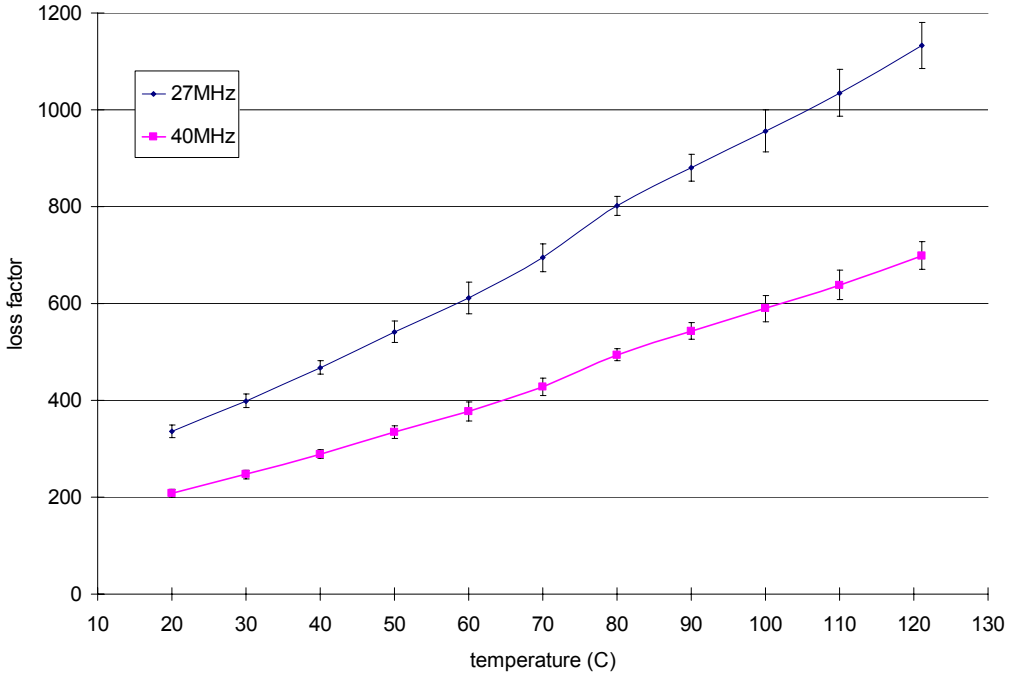
27MHz
40MHz
loss factor
temperature (C)
0
200
400
600
800
1000
1200
10
20
30
40
50
60
70
80
90
100
110
120
130

(B)

Figure 3.13: Loss factors of liquid whole eggs at (A) microwave frequencies, and (B) at radio frequencies.

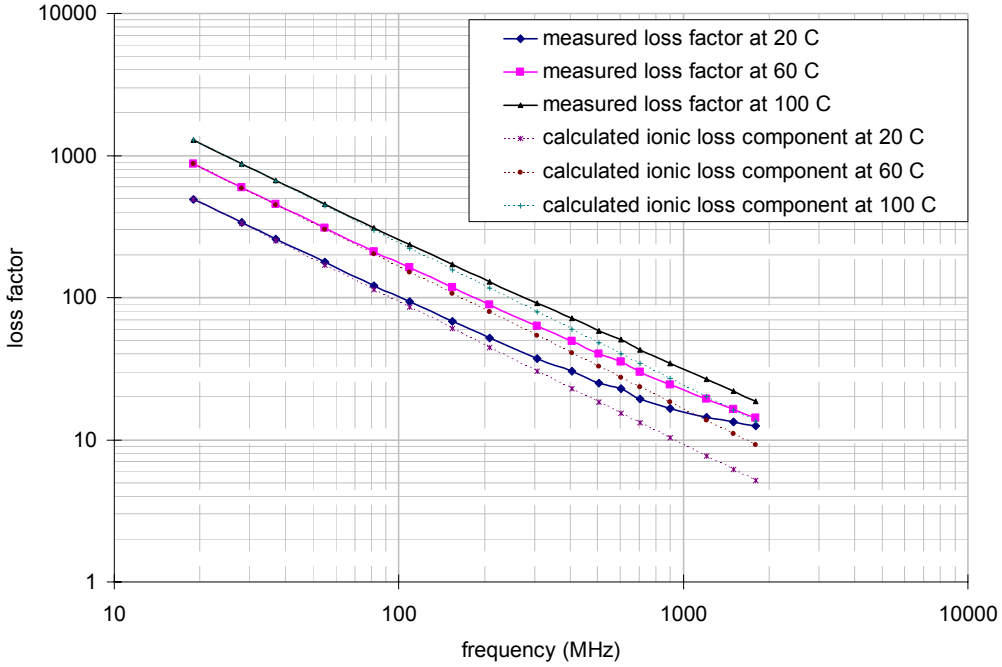

(A)

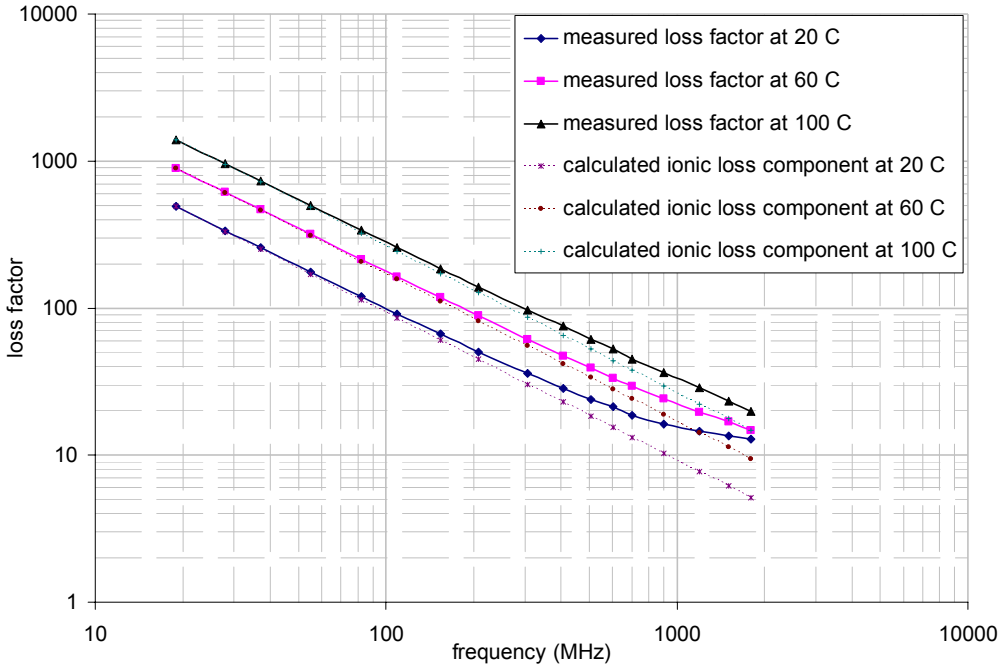

(B)

Figure 3.14: Loss factors and calculated ionic loss components of (A) pre-cooked and (B) liquid whole eggs vs. frequency at selected temperatures (the unit of temperature is ºC).

Appendixes

Appendix 3.1: Dielectric properties (mean ± standard deviation) of liquid egg whites (5 replicates)

	T (ºC)	27 MHz	40 MHz	915 MHz	1800 MHz
ε'	20	84.6 ± 5.7	76.6 ± 6.2	64.0 ± 5.5	62.5 ± 5.3
	40	79.6 ± 5.8	69.8 ± 5.7	56.8 ± 6.0	54.5 ± 5.0
	60	81.3 ± 5.0	68.0 ± 5.4	51.5 ± 4.4	50.4 ± 4.6
	70	88.2 ± 4.4	71.3 ± 4.5	50.2 ± 4.1	49.9 ± 4.1
	80	98.3 ± 4.4	77.6 ± 4.9	50.5 ± 3.6	50.2 ± 2.8
	100	118.1 ± 3.1	88.9 ± 3.0	53.3 ± 2.8	52.5 ± 1.3
	120	135.1 ± 6.5	96.9 ± 3.8	53.2 ± 2.7	51.2 ± 0.5
ε''	20	427.0 ± 46.7	256.4 ± 21.5	18.7 ± 1.9	14.7 ± 1.7
	40	553.6 ± 94.8	320.0 ± 35.8	21.1 ± 2.3	13.8 ± 2.6
	60	646.4 ± 89.4	427.7 ± 52.4	25.3 ± 2.8	15.5 ± 2.1
	70	751.7 ± 87.6	493.4 ± 44.7	28.4 ± 2.3	16.7 ± 1.7
	80	866.5 ± 93.9	569.6 ± 45.9	33.3 ± 2.8	18.1 ± 1.7
	100	1242.3 ± 54.6	784.3 ± 19.2	44.9 ± 1.1	24.0 ± 0.8
	120	1665.8 ± 77.1	997.5 ± 24.5	56.9 ± 2.4	28.8 ± 1.2

Appendix 3.2: Dielectric properties (mean ± standard deviation) of pre-cooked egg whites (5 replicates)

	T (ºC)	27 MHz	40 MHz	915 MHz	1800 MHz
ε'	20	89.3 ± 2.8	81.9 ± 2.1	64.5 ± 1.9	63.5 ± 1.9
	40	89.8 ± 3.3	81.2 ± 3.5	59.7 ± 2.1	58.5 ± 1.6
	60	92.5 ± 2.7	82.3 ± 6.4	55.7 ± 2.2	54.3 ± 1.5
	70	95.3 ± 2.9	83.7 ± 6.5	54.2 ± 2.4	52.7 ± 1.5
	80	99.5 ± 1.7	85.5 ± 7.2	53.0 ± 2.4	51.3 ± 1.5
	100	106.8 ± 2.6	88.2 ± 7.2	50.3 ± 3.0	48.4 ± 1.8
	120	124.4 ± 4.7	97.8 ± 7.8	50.1 ± 1.6	48.5 ± 1.5
ε''	20	411.8 ± 18.6	256.3 ± 13.1	18.9 ± 0.7	14.7 ± 0.3
	40	562.2 ± 25.4	353.1 ± 17.2	22.8 ± 0.9	15.0 ± 0.5
	60	732.1 ± 26.7	460.0 ± 17.0	28.1 ± 0.8	17.0 ± 0.6
	70	830.4 ± 27.7	520.1 ± 18.0	31.4 ± 1.0	18.2 ± 0.5
	80	937.1 ± 27.5	582.3 ± 18.8	34.6 ± 0.7	20.0 ± 0.5
	100	1145.0 ± 21.6	698.9 ± 8.4	41.4 ± 1.2	23.0 ± 0.7
	120	1480.5 ± 89.9	879.8 ± 50.8	52.2 ± 2.4	28.1 ± 0.9

Appendix 3.3: Dielectric properties (mean ± standard deviation) of liquid whole eggs (4 replicates)

	T (ºC)	27 MHz	40 MHz	915 MHz	1800 MHz
ε'	20	76.3 ± 2.8	68.8 ± 1.6	55.5 ± 1.9	53.1 ± 1.1
	30	77.1 ± 2.9	68.6 ± 1.5	54.2 ± 2.1	51.9 ± 1.0
	40	77.5 ± 3.0	68.1 ± 1.4	52.5 ± 2.5	50.4 ± 1.3
	50	77.9 ± 3.1	67.5 ± 1.5	50.9 ± 3.0	48.8 ± 1.9
	60	77.4 ± 3.6	66.0 ± 2.5	48.6 ± 3.7	47.0 ± 2.9
	70	79.1 ± 3.1	66.3 ± 2.9	47.8 ± 3.8	45.9 ± 2.5
	80	87.5 ± 1.4	72.2 ± 2.7	48.9 ± 2.7	46.6 ± 1.2
	90	93.7 ± 2.9	75.9 ± 2.8	47.6 ± 1.2	45.7 ± 1.0
	100	96.9 ± 4.6	77.5 ± 3.1	47.1 ± 2.2	44.2 ± 1.1
	110	100.7 ± 5.4	79.3 ± 2.9	46.1 ± 1.9	43.0 ± 1.0
	120	106.1 ± 6.5	82.0 ± 2.8	44.7 ± 1.0	42.1 ± 0.9
ε''	20	335.9 ± 12.9	208.4 ± 7.8	15.8 ± 1.6	12.8 ± 1.3
	30	398.5 ± 13.8	246.8 ± 8.5	17.3 ± 1.6	12.7 ± 1.5
	40	467.8 ± 14.4	289.1 ± 9.0	19.2 ± 1.8	13.1 ± 1.5
	50	541.8 ± 21.6	334.2 ± 13.5	21.4 ± 2.0	13.8 ± 1.5
	60	612.0 ± 32.7	377.1 ± 19.9	23.9 ± 2.4	14.7 ± 1.7
	70	694.9 ± 28.7	427.8 ± 17.8	26.6 ± 2.5	15.7 ± 1.6
	80	801.8 ± 20.2	494.0 ± 12.5	30.5 ± 2.0	17.3 ± 1.3
	90	880.1 ± 28.4	542.9 ± 17.4	33.3 ± 1.0	19.0 ± 1.0
	100	956.4 ± 44.1	589.8 ± 26.9	35.7 ± 1.2	20.0 ± 1.2
	110	1035.1 ± 49.1	638.5 ± 29.6	38.4 ± 1.5	21.3 ± 1.5
	120	1132.7 ± 48.0	698.7 ± 28.8	42.3 ± 1.2	23.4 ± 1.3

Appendix 3.4: Dielectric properties (mean ± standard deviation) of pre-cooked whole eggs (4 replicates)

	T (ºC)	27 MHz	40 MHz	915 MHz	1800 MHz
ε'	20	79.6 ± 2.2	71.0 ± 1.6	56.5 ± 3.5	53.6 ± 1.3
	30	81.5 ± 2.6	71.7 ± 1.2	55.4 ± 3.2	52.5 ± 1.2
	40	82.7 ± 3.0	71.8 ± 1.0	53.7 ± 3.2	51.0 ± 1.2
	50	83.9 ± 3.6	72.0 ± 1.1	52.3 ± 3.1	49.5 ± 1.2
	60	85.2 ± 4.4	72.1 ± 1.4	50.8 ± 2.8	48.0 ± 1.0
	70	86.9 ± 5.1	72.5 ± 1.7	49.6 ± 3.0	46.8 ± 1.2
	80	89.0 ± 5.5	73.2 ± 1.8	48.5 ± 3.0	45.6 ± 1.3
	90	91.4 ± 6.1	74.1 ± 2.0	47.2 ± 3.1	44.1 ± 1.4
	100	94.2 ± 6.8	75.4 ± 2.3	46.0 ± 3.1	42.9 ± 1.4
	110	99.0 ± 6.5	78.1 ± 2.0	45.2 ± 3.3	41.8 ± 1.6
	120	104.8 ± 7.0	81.2 ± 2.2	44.3 ± 3.3	40.7 ± 1.6
ε''	20	336.8 ± 29.2	209.5 ± 18.2	16.3 ± 1.0	12.5 ± 0.7
	30	393.1 ± 27.9	244.2 ± 16.9	17.7 ± 0.9	12.5 ± 0.6
	40	456.0 ± 28.4	282.8 ± 17.0	19.5 ± 0.8	12.8 ± 0.6
	50	522.0 ± 32.2	323.2 ± 19.0	21.5 ± 0.9	13.4 ± 0.6
	60	594.1 ± 36.6	367.4 ± 21.4	23.9 ± 1.0	14.3 ± 0.6
	70	667.8 ± 41.3	412.6 ± 24.0	26.3 ± 1.1	15.3 ± 0.7
	80	745.8 ± 48.5	460.5 ± 28.3	29.0 ± 1.3	16.5 ± 0.7
	90	813.0 ± 59.3	501.9 ± 34.7	31.4 ± 1.6	17.6 ± 0.8
	100	874.1 ± 73.0	539.5 ± 42.8	33.8 ± 1.9	18.7 ± 0.9
	110	944.5 ± 93.8	583.3 ± 55.6	36.5 ± 2.6	20.1 ± 1.1
	120	1020.0 ± 109.8	630.4 ± 65.0	39.5 ± 3.0	21.6 ± 1.2

CHAPTER FOUR

INFLUENCE OF DIELECTRIC PROPERTIES OF MASHED POTATO AND CIRCULATING WATER ON RADIO FREQUENCY HEATING

Abstract

Experiments and computer simulations were conducted to systematically investigate the influence of mashed potato dielectric properties and circulating water electric conductivity on electromagnetic field distribution, heating rate, and heating pattern in packaged food during radio frequency (RF) heating processes. Both experimental and simulation results indicated that for the selected food (mashed potato) in this study, the heating rate decreased with an increase of water conductivity and salt content (loss factor). Simplified theoretical calculations were carried out to verify the simulation results, which further indicated that the electric field distribution in the mashed potato samples was also influenced by their dielectric properties and the electric conductivity of the surrounding circulating water. Knowing the influence of water electric conductivity and mashed potato dielectric properties on the heating rate and heating pattern is helpful in optimizing the radio frequency heating process by appropriate adjustment of these factors. The results demonstrate that computer simulation has the potential to aid the construction, modification, and expanded application of RF heating.

Introduction

Sterilization is used to reduce spoilage, eliminate pathogenic microorganisms, and prolong the shelf-life of packaged foods. Conventional sterilizing methods such as steam

retorting are time consuming. Since the surface of packaged food is normally exposed to high temperature for a long time, the food quality degradation at the container periphery is severe, especially for heat-sensitive foods (Meredith, 1998; Priestley, 1979). Thermal processes that utilize high temperatures for short duration can produce a better quality food product while ensuring food safety (Banwart, 1989). Radio frequency (RF) heating has this potential. It may also use less energy than conventional processes. As such, it may be an improved means for producing higher quality, shelf-stable foods for civilian and military uses (Wang et al., 2003a). Since power penetration depths in the RF range are several times deeper than at microwave frequencies, RF heating has an obvious advantage to process institutional-size packaged food over microwave heating (Wang et al., 2003b). Previous works involving inoculated pack studies and instrumental quality measurements reveal that sterilization using RF energy can produce shelf-stable foods with better quality than retort-treated food products in large polymeric trays (Luechapattanaporn et al., 2004; 2005).

Although RF heating processes have several advantages over conventional and microwave heating processes, we are still facing challenges in determining the positions of cold and hot spots in packaged foods and in improving heating uniformity. Both challenges are related to the electromagnetic field distribution within dielectric heating equipment. In early studies, predication of the electromagnetic field distribution and heating pattern associated with RF heating was mainly based on experiments.

Lengthy experimentation times, high operational costs, and lack of flexibility are major problems in experimental research. With the rapid development of numerical simulation techniques, computer modeling has great potentials in predicting

electromagnetic field distribution and heating patterns inside heating oven and foods. Several previous studies were conducted to numerically simulate RF heating processes. Neophytou and Metaxas (1998; 1999) demonstrated the capability of the finite element method (FEM) for modeling an RF heating system, they suggested the possibility of simulating an entire RF heating system with both generator and applicator circuits, thus opened opportunity for analyzing the structure and circuit design of an RF heating system to optimize its effectiveness via tuning and design of the RF heating system. Chan et al. (2004) predicted RF heating patterns in foods due to electromagnetic field distribution. Baginski et al. (1990) and Marshall and Metaxas (1998) showed the potential of computer simulation to model RF drying processes and the associated electromagnetic and thermodynamic phenomena. However, few systematic studies have focused on the specific application of RF energy to food sterilization processes nor on the influence of variation in food dielectric properties and electric conductivity of circulating water that used to mitigate the fringing field and edge heating effects, leading to a lack of information electromagnetic field distribution, heating rate, and heating patterns in packaged foods during RF heating.

Thermal effects analysis, besides electromagnetic field investigation, is essential for simulating RF heating processes. During RF heating, two physical factors, temperature and electric field intensity, interrelate with each other. In particular, the dissipated energy provided by electric fields heats those materials with temperature-dependent dielectric properties. The variation, caused by temperature change and heat transfer of the dielectric properties, influences the electromagnetic field distribution. So the coupling of two physical phenomena becomes one of the most critical factors for the

successful simulation of RF heating process (i.e., requires software with the ability to handle multiphysical problems).

The objectives of this research were to 1) investigate the influence of the electric conductivity of circulating water and dielectric properties of mashed potatoes on the food's heating rate and pattern, and 2) simulate RF heating processes using commercial simulation software (COMSOL Multiphysics, Burlington, MA). COMSOL Multiphysics, a modeling package for the simulation of physical processes that can be described with partial differential equations, enabled the modeling and coupling of the electric field distribution and heat transfer phenomena through predefined modeling templates (COMSOL, 2005a).

Experimental Procedures

Materials and Experimental Procedure

A simplified schematic diagram of the pilot-scale 6 kW 27 MHz RF heating system used in the experiments is shown in Figure 4.1. The system consists of a RF power generator, an applicator, a pressure-proof vessel to hold packaged foods (Figure 4.2), a water conditioning system, a temperature monitoring system, and a data collecting system.

The water conditioning system consisting of buffer tanks, heat exchangers, pumps and connecting pipers was used to circulate water through the pressure-proof vessel and adjust the electric conductivity, pressure, temperature, and flow rate of circulating water. The circulating water was used to improve the heating uniformity in the sample food, including reduction of edge heating.

The pressure-proof vessel (as shown in Figure 4.2) was developed at Washington State University (Pullman, WA, USA) to provide an overpressure of up to 0.276 MPa (40 psi) that allowed foods in large polymeric trays to be heated up to 135 ºC without bursting. The vessel was constructed with Ultem (polyetherimide, or PEI) plastic walls and 2 parallel aluminum plates as upper and lower covers. Several probe ports were drilled on one side of the wall to allow insertion of fiber optic sensors (UMI; FISO Technologies Inc., Quebec, Canada) that were used to detect the real-time temperatures of the food samples. A computer was used to record the data measured by the sensors.

The dielectric properties of mashed potato were adjusted by changing salt content. Mashed potato samples consisted of mashed potato flakes (from Oregon Potato Co., Broadman, OR., USA), deionized water, and table salt (NaCl). Non-salted samples consisted of mashed potato flakes and deionized water at 5.5:1 water/potato mass ratios; the corresponding moisture content was 85.9% (wet basis), with a 0.8% (w.b.) salt content. Salt-enriched samples had the same moisture content, but by adding salt solution with 0.63% salt concentration, samples had a 1.3% (w.b.) salt content.

About 2600 g of mashed potatoes samples were filled in each of 6-pound capacity polymeric trays (295 × 235 × 42 mm) commonly used as packages for U.S. military group rations. The trays were heat-sealed under about 61 kPa (18 inHg) below atmospheric vacuum with a 0.15-mm-thick aluminum foil lid (Jefferson Smurfit, Dublin, Ireland) in a laboratory vacuum tray sealer (Rexam Containers, Union, MO, USA). The trays were then placed in the pressure-proof vessel positioned at the center of the bottom plate in the RF heating oven. Circulating water was pumped through the vessel before and during the heating process. The inlet temperature of the circulating water was

controlled by the water conditioning system. During RF processing, the flow rate of the circulating water was controlled at approximately 10 L/min, the pressure at 13.8 kPa (2 psi), and the temperature at 40 °C. Two fiber optic sensors, placed in the sample trays as illustrated in Figure 4.3, were used to monitor the sample temperatures at sensor tips. The average temperature of the two sensors was used to characterize the heating rate.

Immediately after each test run, the sample trays were removed from the pressure-proof vessel and thermal images at the intersection of the horizontal plane, in which fiber optic sensors were placed, were taken by a ThemaCAM® infrared camera (FLIR System Inc., Sweden) that had been set up and calibrated before the experiment. Temperature differences at random positions checked by the thermal images and a thermocouple were controlled within ± 1 °C. It normally took 3 to 4 min from turning off the RF power to take the thermal image. Four different circulating water electrical conductivities, 20, 64, 140, and 220 μS/cm at 23°C were used.

Numerical Model

Figure 4.4 illustrates computer simulation procedures. An appropriate simulation module was chosen based on governing equations that revealed the physical basis of simulated physical phenomena. The constants and variables were then predefined. After the geometry of the model was built, the sub-domain properties and boundary conditions were assigned. A convergence study was conducted to investigate convergence of the simulation and to determine the optimized meshing that comprises the calculation time and accuracy of simulation. Finally, the computing solution was calculated and the simulation results were analyzed.

Governing Equations

The electromagnetic field patterns in RF systems are governed by Maxwell's equations (Balanis, 1989):

$$\nabla \times \mathbf{H} = \sigma \mathbf{E} + \frac{\partial(\varepsilon \mathbf{E})}{\partial t} \tag{4.1}$$

$$\nabla \times \mathbf{E} = -\frac{\partial \mathbf{B}}{\partial t} = -\frac{\partial(\mu \mathbf{H})}{\partial t} \tag{4.2}$$

$$\nabla \bullet \mathbf{D} = \nabla \bullet \varepsilon \mathbf{E} = 0 \tag{4.3}$$

$$\nabla \bullet \mathbf{B} = \nabla \bullet \mu \mathbf{H} = 0 \tag{4.4}$$

where **E** is electric field intensity, **H** is magnetic field intensity, **D** is electric flux density, **B** is magnetic field density, and ε and μ are, respectively, dielectric constant and permeability of the material.

The dielectric properties of food materials can be described as (Sadiku, 2001):

$$\varepsilon_c = \varepsilon - j\varepsilon'' = \varepsilon_0(\varepsilon_r' - j\varepsilon_r'') = \varepsilon_0(\varepsilon_r' - j\frac{\sigma}{\omega\varepsilon_o}) \tag{4.5}$$

where, ε_c is complex permittivity of the material, ε_0 is permittivity of free space, ε_r' is relative dielectric constant, ε_r'' is relative loss factor of the material, and σ is electrical conductivity of the material.

Quasi-static analysis is applicable when the coupling between electric and magnetic fields is negligible under the condition that that all dimensions are small compared to the wavelength in any relevant medium. Therefore (COMSOL, 2005b),

$$\nabla \times \mathbf{E} = -\frac{\partial \mathbf{B}}{\partial t} = 0 \tag{4.6}$$

Hence, **E** can be derived from a scalar electric potential V and magnetic vector potential **A** as:

$$\mathbf{E} = -\nabla V - \frac{\partial \mathbf{A}}{\partial t} \tag{4.7}$$

Eq. (4.3) can be rewritten as:

$$\nabla \bullet \varepsilon\left(-\nabla V - \frac{\partial \mathbf{A}}{\partial t}\right) = -\varepsilon\left[\nabla^2 V + \frac{\partial}{\partial t}(\nabla \bullet \mathbf{A})\right] \tag{4.8}$$

Considering that when $\partial \mathbf{B}/\partial t = 0$ (Sadiku, 2001),

$$\nabla \bullet \mathbf{A} = 0 \tag{4.9}$$

Therefore, Eq. (4.8) can be rearranged as:

$$\nabla^2 V = 0 \tag{4.10}$$

which is Laplace's equation.

In our simulation, by solving Eq. (4.10), the electric potential (V) and electric field intensity (E) were obtained. The time-averaged power density, P, was generated by transferring the electric energy to heat the food material as shown by (Barber, 1983):

$$P = \omega \mathbf{E}^2 \varepsilon_0 \varepsilon_r'' \tag{4.11}$$

Note that the time interval over which the power is calculated (one cycle of the electromagnetic field) is less than 0.04 μSec (27 MHz). Since the time interval is very small compared to the thermal changes, it can be used as a time varying quantity, *P(t)*, in the thermal problem.

The power density in Eq. (4.11) was then treated as the heat source of the heat transfer phenomena to couple the electromagnetic field with the thermal field. The governing equation for heat transfer by conduction is expressed as:

$$\rho C_p \frac{\partial T}{\partial t} - \nabla \bullet (k \nabla T) = P(t) \tag{4.12}$$

where ρ is density, C_p is heat capacity, k is thermal conductivity, $P(t)$ is average power density, and T is temperature.

Assumptions

In order to accomplish the simulation with acceptable accuracy under the constrained memory capability of the computer, assumptions were used to simplify the heating system. A quasi-static analysis was assumed because the wavelength of the electromagnetic wave (27 MHz) in our research (> 10 m in air and > 1.5 m in food) was much larger than the dimension of our equipment (< 1 m) and food (< 0.3 m). In addition, the flow of circulating water inside the pressure-proof vessel and the heat transfer between the circulating water and food were neglected because we concentrated on the heating distribution at the center layer of the sample trays; the influence from the circulating water was small.

Modelling

The geometry of the RF heating system is shown in Figure 4.7. The electric potential of the aluminum cavity was set to 0, and a 5 kV electric potential (RMS at 27 MHz) was applied to the feeder plate. The dielectric properties of the mashed potatoes were determined from calculations in Guan et al. (2004), while a linear regression analysis was used to determine the relation between temperature and dielectric properties (Table 4.1). The electrical conductivity of circulating water were measured by a

conductivity analyzer model 53 (GLI International, Milwaukee, WI, USA) at the beginning of each experiment at 23 ºC. In the heat transfer analysis, heat effects were only considered in the food sample domain to simplify the model. The thermal conductivity and specific heat of the mashed potatoes were measured by a KD2 Pro Thermal Properties Analyzer (Decagon Devices, Pullman, WA, USA) in triplicate at room temperature (Table 4.2). Since the flow of circulating water was ignored, no heat convection was assumed between the circulating water and sample trays. The boundary conditions for the surface of the sample trays were set to 40 °C.

Convergence study

Preliminary simulations were conducted to acquire appropriate meshing density and element numbers. The average power density at cold and hot spots and sensors were monitored to check the accuracy of the simulation results. As presented in Figure 4.5, increasing number of elements stabilized average power density at the three locations. When the number of elements reached 417,881, there was no more than a 3.4% difference in the average power density with a 47% increase in the number of elements, indicating a stabilization of the average power density and the number of elements was reasonable to conduct further simulation.

Solution computation

The procedures for computing the solution are shown in the flow chart in Figure 4.6. The initial condition was assigned to the model at time zero. The FEM was then

applied to obtain electric potential and electric field distributions. After the average power density was calculated based on the material properties and electric field intensity, the FEM heat transfer simulation module was used to investigate the heat generation and transfer condition. The temperature-dependant variables were modified according to the renewed temperature distribution, applied to the model, and then a renewed electric field distribution was calculated. Iterations were continued until the final time step was reached. Variable time steps were automatic selected by simulation software to determine the optimal simulation process.

A Dell Precision 870 workstation with two Dual-Core 2.80GHz Intel® Xeon™ processors and a 12 GB memory was utilized to perform the simulation, which took about 1 h.

Results

Experimental Results

The heating times and final temperatures at the hot spot and cold spots and sensor tips of the mashed potato samples are summarized in Table 4.3. The temperature profile at the sensor tip is plotted in Figure 4.9, which shows that with an increase in the electrical conductivity of the circulating water, the heating rate decreased at the sensor tips. For the same temperature, the mashed potatoes with 1.3% salt content took longer to heat than those with 0.8% salt content.

Simulation Results

In order to verify the simulation results, three positions in the sample were chosen to compare the numerical solutions with the experimental results. The first position was at the sensor tip, and the other two positions were at the hot and cold spots within the horizontal central layer of the sample tray, where both fiber optic sensors were placed and thermal images taken to evaluate the uniformity of the heating process. Digitized by the ThermaCAM Researcher 2001, the software provided by FLIR System Inc., the thermal images provided the final heating pattern and temperatures at the hot and cold spots at the central layer of the sample tray. As shown in Figure 4.10, the hot spots were located at the places near the corner of the sample, and the cold spots were at the center of the sample. Temperatures at the same positions, as shown in Figure 4.11, were determined from the numerical solution.

Figure 4.12 indicates that both the increase in conductivity of the circulating water and increase in mashed potato salt content reduced the heating rates. The simulation results confirmed the temperature change trends observed in the experiments (Figure 4.9).

Discussions

The temperature differences, which were controlled within ± 13%, between the experimental and simulation results at the mashed potato cold and hot spots and sensor tips under different conditions are summarized in Table 4.4.

The sterilization effects of thermal treatment on food are commonly determined by sterilization value (F_0) (min) (Stumbo 1973):

$$F_0 = \int_0^t 10^{\left(\frac{T-121.1}{z}\right)} dt \tag{4.13}$$

where T is temperature (°C), t is processing time (min), and z is 10 °C for *Clostridium botulinum* spores, which are target microorganisms in commercial thermal processes for low-acid foods (pH>4.5). Generally, a minimum safe public health sterilization value (F_0) for low-acid canned foods based on inactivation of *C. botulinum* is 3.0 min (Frazier and Westhoff, 1988). Most food companies used a minimum process sterilization value of 5.0 min (Teixeira, 1992).

During the food sterilization process, due to the exponential nature of the sterilization calculation, a small difference at temperatures above 121 ºC can introduce a large variation in sterilization value. For example, a ±13% temperature difference at 121 ºC represent a 15 ºC temperature difference between experiment and simulation, which in term would cause a significant error in predicting the F_0 by simulation result. In order to guarantee the safety of commercially sterilized food, it is necessary to assure that the F_0 of cold spot reaches the designated value. In this study, the temperature differences between the simulation and experimental at cold spots were within ± 5% (i.e., 6 ºC at 120 ºC) which limited the F_0 value error to 3 min.

Although further improvement to simulation accuracy is needed to make a completely substitution of experimentation by computer simulation possible when predicting sterilization values, simulation alone can give a reasonable indication of heating pattern and sterilization value in food packages. Computer simulation also makes it much more convenient than laboratory experimentation to adjust physical properties and equipment to improve heating uniformity during RF heating

Several reasons may account for the differences between the experimental and simulation temperature values. Measurement error is one of the distinct possibilities causing the difference, because the linear regression analysis for the temperature-dielectric properties relationship was based on mean values without considering the 10% standard deviation (Guan et al., 2004). Simplification of the model could be another reason that caused the differences. Without considering the flow of circulating water and convection between water and the sample food, the heating pattern could have been affected by the simplified heat transfer condition. Adding more details to the model would improve the precision of the simulation results, but also require much more computer memory and a faster CPU.

At RF, the loss factor of mashed potatoes increases with the rise of temperature and salt content (Guan et al., 2004). As shown in Eq. (4.11), the dissipated power density is proportional to the loss factor of food. Thus, if the electric field intensity, **E**, were fixed, the increasing temperature at certain points of the food sample would lead to a rise in the local loss factor and increase heat generation at these positions, suggesting that the heating rate at positions with high temperature should be higher than those at low temperature. It is, therefore, commonly believed in the literature that a positive correlation between dielectric loss factor and temperature for foods contribute to significant runaway heating during RF heating causing overall nonuniform heating. However, both the experiments and simulations results in our studies revealed that an increase in salt content (i.e., sample loss factors) resulted in a reduced heating rate, opposite to what we originally anticipated.

In order to investigate the above stated paradox, several simulations were performed to study the electric field distributions in samples with different salt contents. During the simulation, all the physical constants (i.e., 40 °C temperature and 85.9% moisture content) of the mashed potatoes were kept the same except for the salt content, which varied from 0.8, 1.3, 1.8, to 2.8%.

According to the numerical solution summarized in Figure 4.5, the average electric field intensity in the circulating water was relatively stable at around 3 kV/m, even though the salt content of the mashed potato changed. Since the water conductivity was fixed, the energy absorbed by the water remained steady at around 16 kW/m^3. The average electric field intensity in the sample food, on the other hand, decreased from 1.1 to 0.23 kV/m, while the loss factor increased from 383 to 1906. The sample loss factors, which are proportional to the power produced in the food, increased almost five times, but due to the dramatic decrease of electric field intensity, thermal energy conversion in the samples actually decreased. Since the average power density dropped from 347 to 85 kW/m^3, the heating rate declined with the rise in salt content of the mashed potatoes.

To better understand these phenomena, a simplified theoretical calculation was conducted using an RF heating system with only a pressure-proof vessel, circulating water, and food (Figure 4.13).

The electric potential between the two metal plates can be calculated from:

$$V_0 = d_w E_w + d_f E_f \tag{4.14}$$

where E_w is the electric field intensity in circulating water, E_f is the electric field intensity in food, d_w is the thickness of water, and d_f is the thickness of food.

Assuming the electrostatic field, the electric field is uniform in the material and with only considering the electric field in y-direction (as shown in Figure 4.13), the boundary condition at interface between water and food is:

$$\varepsilon_w E_w = \varepsilon_f E_f \tag{4.15}$$

where ε_w is the is the permittivity of circulating water, and ε_f is the is the permittivity of food. According Eq. (4.5), (4.15) can be rewritten as:

$$\varepsilon'_{rw} E_w = \varepsilon'_{rf} E_f \tag{4.16}$$

where ε'_{rw} is the dielectric constant of circulating water, and ε'_{rf} is the dielectric constant of food.

Combining Eqs. (4.14) and (4.16),

$$E_f = \frac{V_0 \varepsilon'_{rw}}{\varepsilon'_{rw} d_f + \varepsilon'_{rf} d_w} \tag{4.17}$$

Finally with considering about Eq. (4.11), the power density inside the food can be approximated to

$$P_f \approx \omega \varepsilon_0 \varepsilon''_{rf} V_0^2 \left[\frac{\varepsilon'_{rw}}{\varepsilon'_{rw} d_f + \varepsilon'_{rf} d_w} \right]^2 \tag{4.18}$$

The theoretical calculations based on Eq. (4.18), as shown in Table 4.6, present a clear similarity to the simulation results of the average electric field intensity and power density in water and mashed potato with different salt contents. According to Eq. (4.18), the power density inside the food is not only proportional to its loss factor, but also influenced by the food thickness, circulating water, and dielectric properties.

Conclusions

Both experimental and simulation results indicated that with an increase of water electric conductivity or salt content (loss factor) in mashed potato samples, their heating rate decreased. The simulation results further demonstrated that although the dissipated power in the mashed potatoes was proportional to their loss factor, the decreased electric field intensity caused by the increased loss factor not only compensated for the influences brought by the increase in loss factor, but actually reduced the dissipated power. According to our theoretical calculations, the power density inside mashed potatoes is not simply proportional to their dielectric loss factor, but influenced by the thickness of mashed potato and circulating water and their dielectric properties and electric conductivity, respectively. Although several assumptions affected the simulation accuracy, a reasonable indication of mashed potato heating pattern and heating rate was obtained. COMSOL Multiphysics has the potential to further improve similar simulations and aid the construction and modification of RF heating systems.

References

Baginski, M., Broughton, R., Hall, D., and Christman, L. 1990. Experimental and Numerical Characterization of the Radio-Frequency Drying of Textile Materials (II). Journal of Microwave Power and Electromagnetic Energy, 25(2), 104-113.

Balanis, C.A. 1989. Advanced Engineering Electromagnetics. John Wiley & Sons, New York, NY, USA.

Banwart, G.J. 1989. Basic Food Microbiology. Van Nostrand Reinhold, New York.

Barber, H. 1983. Electroheat. Sheridan House, Inc., Dobbs Ferry, NY, USA.

COMSOL 2005a. Electromagnetics Module User's Guide. COMSOL Multiphysics, Burlington, MA, USA.

COMSOL 2005b. COMSOL Multiphysics User's Guide. COMSOL Multiphysics, Burlington, MA, USA.

Chan, T.V.C.T., Tang, J.M., and Younce, F. 2004. Three-Dimensional Numerical Modeling of an Industrial Radio Frequency Heating System using Finite Elements. Journal of Microwave Power and Electromagnetic Energy. 39(2), 87-106.

Frazier, W.C. and Westhoff, D.C. 1988. Food Microbiology. 4th ed. McGraw-Hill, New York, NY, USA.

Guan, D., Cheng, M., Wang, Y., and Tang, J. 2004. Dielectric Properties of Mashed Potatoes Relevant to Microwave and Radio-Frequency Pasteurization and Sterilization Processes. Journal of Food Science. 69(1), 30-37.

Luechapattanaporn, K., Wang, Y., Wang, J., Al-Holy, M., Kang, D.H., Tang, J., and Hallberg, L.M. 2004. Microbial Safety in Radio Frequency Processing of Packaged Foods. Journal of Food Science. 69(7), 201-206.

Luechapattanaporn, K., Wang, Y., Wang, J., Tang J., Hallberg, L.M., and Dunne, C.P. 2005. Sterilization of Scrambled Eggs in Military Polymeric Trays by Radio Frequency Energy. Journal of Food Science. 70(4), 288-294.

Marshall, M.G. and Metaxas, A.C. 1998. Modeling of the Radio Frequency Electric Field Strength Developed during the RF Assisted Heat Pump Drying of Particulates. Journal of Microwave Power and Electromagnetic Energy, 33(3), 167-177.

Meredith, R., ed. 1998. Engineers' Handbook of Industrial Microwave Heating. The Institution of Electrical Engineers, London.

Neophytou, R.I. and Metaxas, A.C. 1998. Combined 3D FE and circuit modeling of radio frequency heating systems. Journal of Microwave Power and Electromagnetic Energy, 33(4), 243-262.

Neophytou, R.I. and Metaxas, A.C. 1999. Combined Tank and Applicator Design of Radio Frequency Heating Systems. IEE Proceedings – Microwaves, Antennas, and Propagation, 146(5), 311-318.

Priestley, R.J. 1979. Vitamins. In: Priestley, R.J., ed. Effects of Heating on Foodstuffs, pp. 121-156. Applied Science Publishers, Essex, UK.

Sadiku, M.N.O. 2001. Elements of Electromagnetics, 3rd edition. Oxford University Press Inc., New York, USA.

Stumbo, C.R. 1973. Thermobacteriology in food processing, 2nd edition. Academic Press, London, UK.

Teixeira, A. 1992. Thermal Process Calculation. In: Heldman D.R. and Lund, D.B., eds. Handbook of Food Engineering. Marcel Dekker, New York, NY, USA. 563-565.

Wang, Y., Wig, T., Tang, J., and Hallberg, L.M. 2003a. Radio Frequency Sterilization of Packaged Foods, Journal of Food Science, 68(2), 539-544.

Wang, Y., Wig, T., Tang, J., and Hallberg, L.M. 2003b. Dielectric Properties of Food Relevant to RF and Microwave Pasteurization and Sterilization, Journal of Food Engineering. 57, 257-268.

Tables

Table 4.1: Summary of temperature-dielectric properties relationship of mashed potatoes samples (ε = interception + slope × temperature) (Guan et al., 2004)

Mashed potatoes with salt content		Interception	Slope	R^2
0.8%	ε'	84.7	0.13	0.86
	ε''	78.7	7.8	0.98
1.3%	ε'	83.3	0.14	0.85
	ε''	173.2	16.4	0.99

Table 4.2: Summary of mashed potatoes sample thermal properties (mean of 3 replicates)

Mashed potatoes with salt content	Thermal conductivity (W/m·K)	Heat capacity (kJ/kg·K)	Approximate density (kg/m^3)
0.8%	0.545 ± 0.007	3.743 ± 0.068	1000
1.3%	0.548 ± 0.025	3.763 ± 0.112	1000

Table 4.3: Summary of experimental heating times and final temperatures

Mashed potatoes with salt content	Circulating water electric conductivity at 23ºC (µS/cm)	Heating time (seconds)	Temperature (ºC) at		
			Cold spot	Hot spot	Sensor tip
0.8%	20	320	51.6	80.3	61.4
	64	390	48.6	79.5	60.3
	140	630	58.7	81.1	62.5
	220	660	55.3	79.5	58.5
1.3%	20	570	53.7	76.1	68.2
	64	660	53.0	68.1	61.2
	140	1020	54.6	70.6	60.5
	220	1200	53.2	66.8	58.4

Table 4.4: Summary of temperature differences between the experimental and simulation results

Mashed potato salt content	Circulating water electric conductivity at 23ºC (μS/cm)	Temperature difference (ºC) at			Temperature difference (%) at		
		Cold spot	Hot spot	Sensor tip	Cold spot	Hot spot	Sensor tip
0.8%	20	-1.4	-0.8	5.8	-2.7	-1.0	9.5
	64	-2.4	1.0	4.8	-4.9	1.3	8.0
	140	2.2	2.9	5.2	3.8	3.6	8.3
	220	-2.8	6.5	3.8	-5.1	8.2	6.4
1.3%	20	2.8	-2.9	7.6	5.2	-3.8	11.2
	64	2.5	-6.9	6.8	4.7	-10.1	11.1
	140	2.2	-2.4	7.1	4.0	-3.4	11.6
	220	0.6	-1.8	5.3	1.1	-2.7	9.1

Table 4.5: Simulation results of average electric field intensity and power density in water and food with different salt content

Mashed potato salt content		0.8%	1.3%	1.8%	2.8%
Dielectric constant of mashed potato at 40°C		90	89	79	105
Loss factor of mashed potato at 40°C		383	817	1000	1906
Average electric field intensity in	food (kV/m)	1.1	0.5	0.5	0.2
	water (kV/m)	3.06	2.99	2.99	2.98
Average power density in	food (kW/m^3)	347	193	163	85
	water (kW/m^3)	16.4	16.1	16.1	16.1

Table 4.6: Simulation results of average electric field intensity and power density in water and food with different salt content

Mashed potato salt content		0.8%	1.3%	1.8%	2.8%
Dielectric constant of mashed potato at 40°C		90	89	79	105
Loss factor of mashed potato at 40°C		383	817	1000	1906
Average power density in food (kW/m^3)	Simulation	347	192.5	162.5	85
	Theoretical	366	179	148	79

Figures

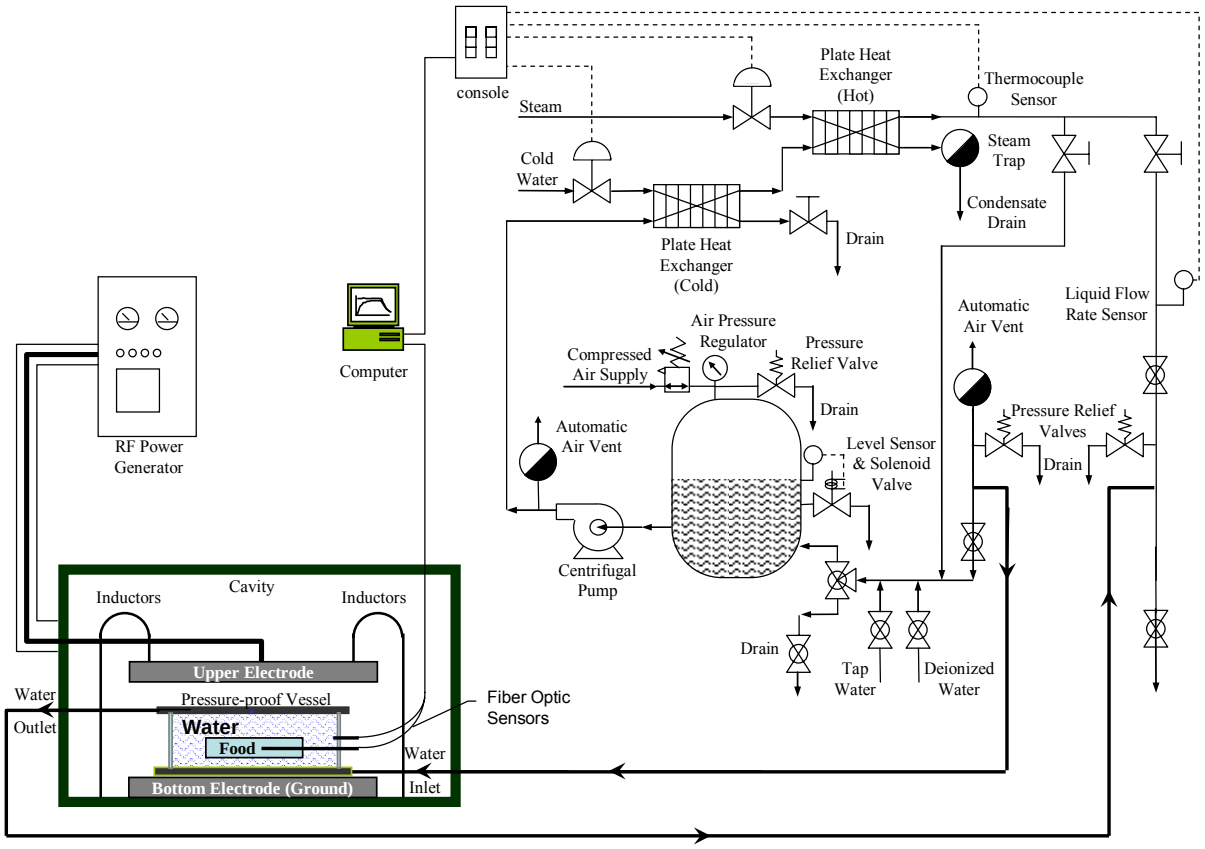

Figure 4.1: Simplified schematic diagram of the Washington State University RF heating system

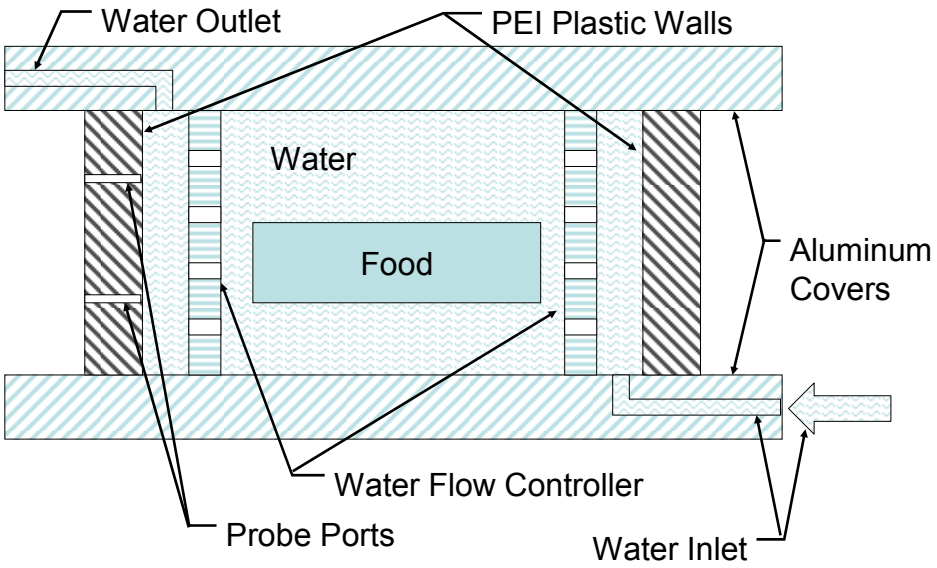

Figure 4.2: Diagram of the pressure-proof vessel cross section (not to scale)

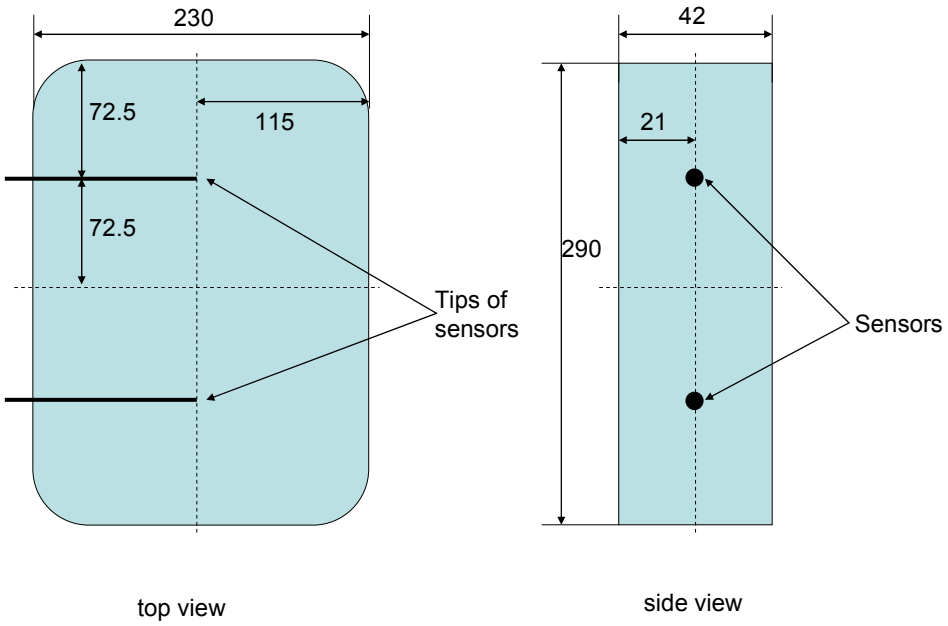

Figure 4.3: Positions of fiber optic sensors in the tray (units in the figure are mm)

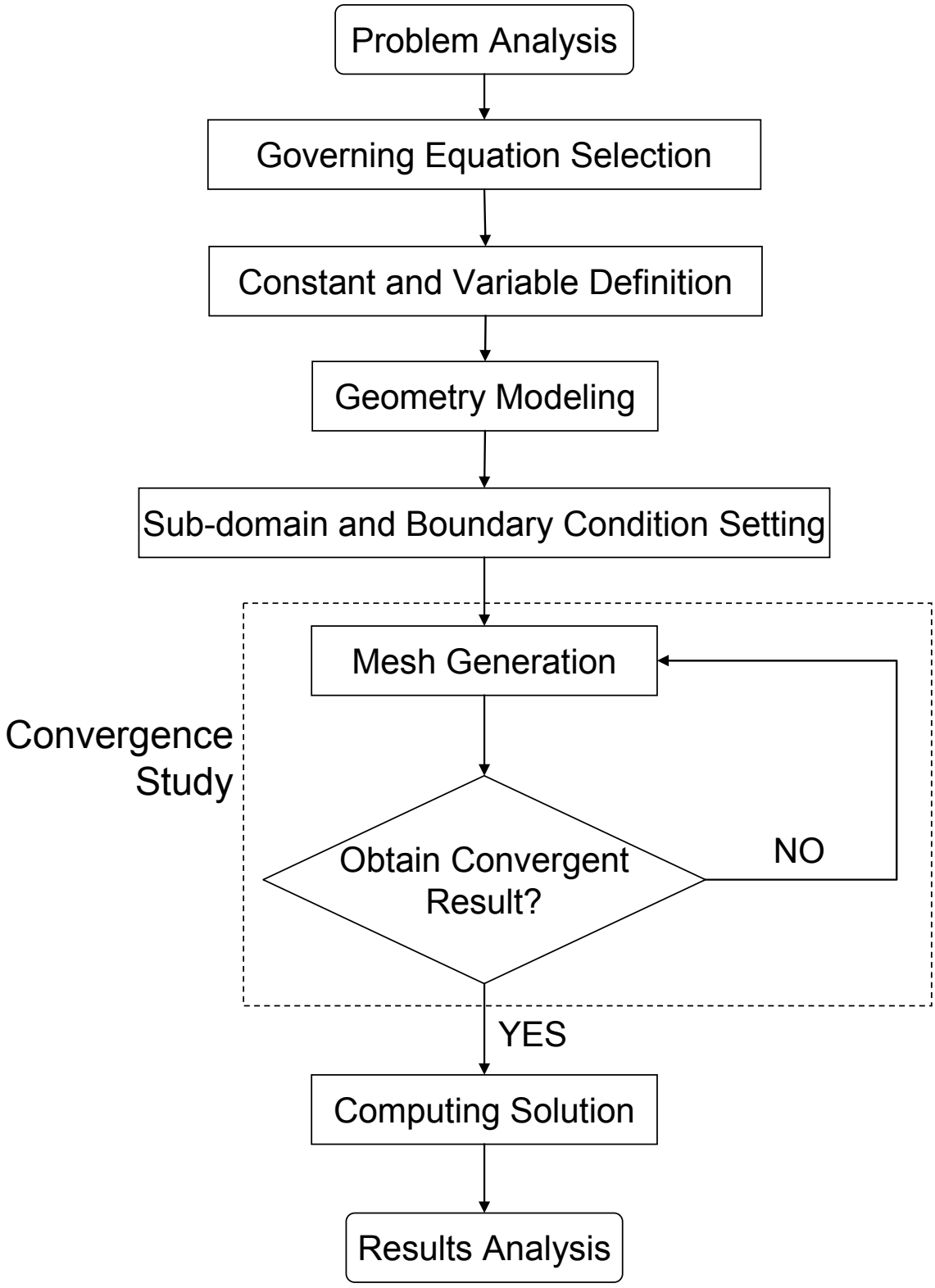

Figure 4.4: Flow chart of the computer simulation procedure

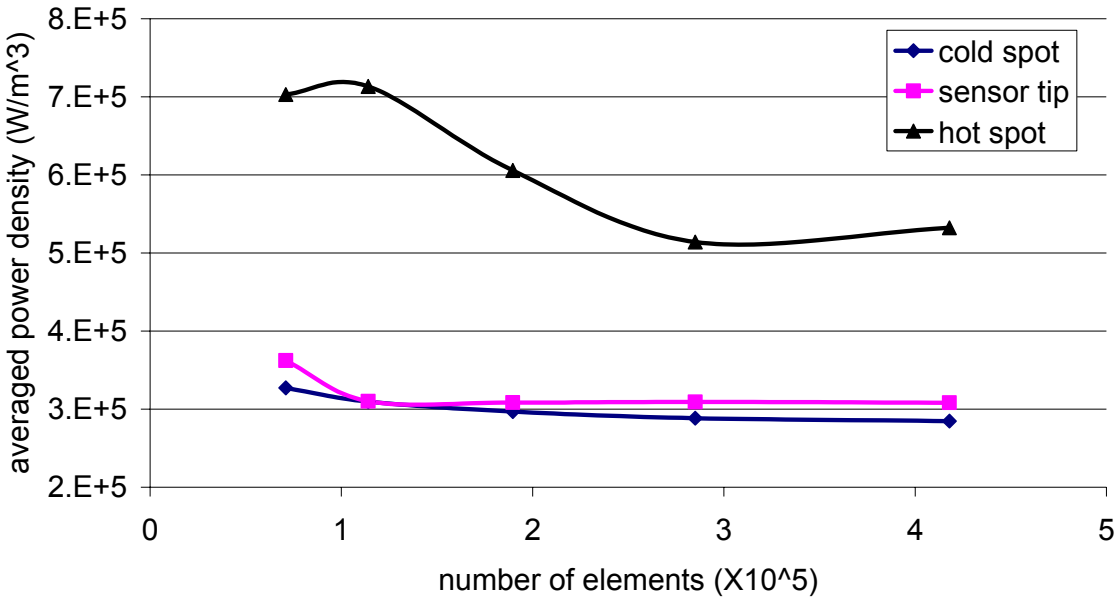

Figure 4.5: Effects of number of elements on the accuracy of average power density

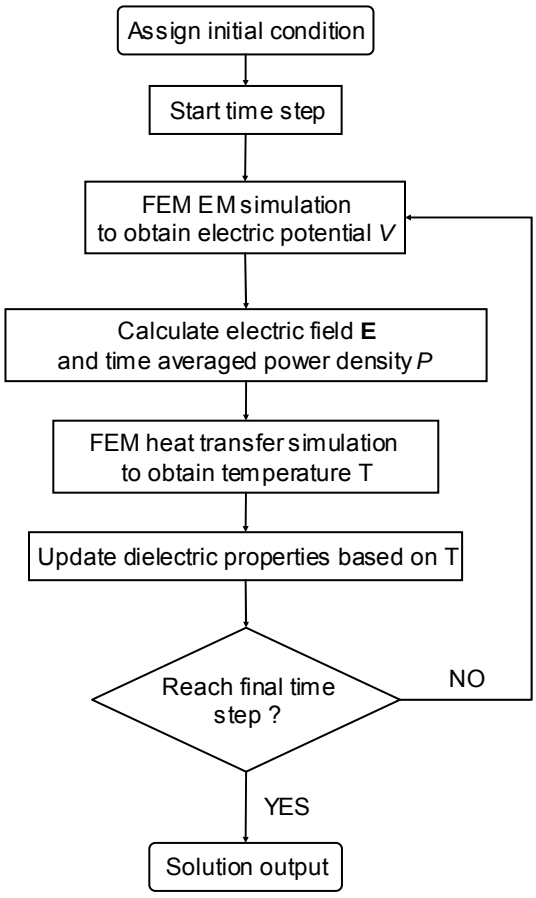

Figure 4.6: Flow chart of the procedure in solution calculation

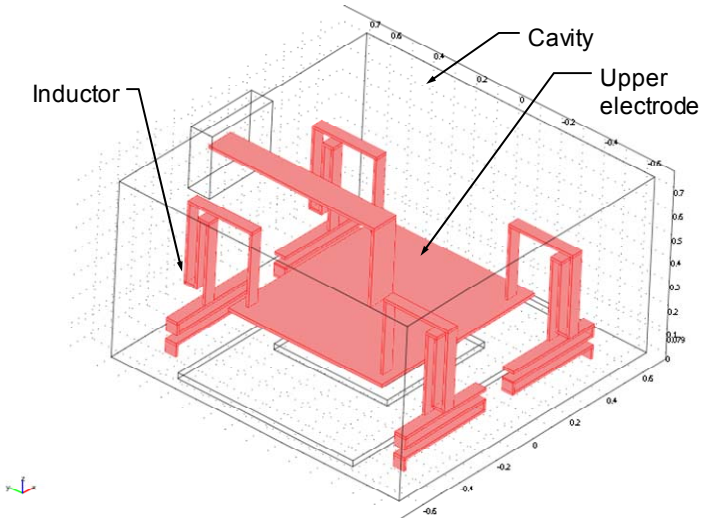

Figure 4.7: Geometry model of the RF heating system

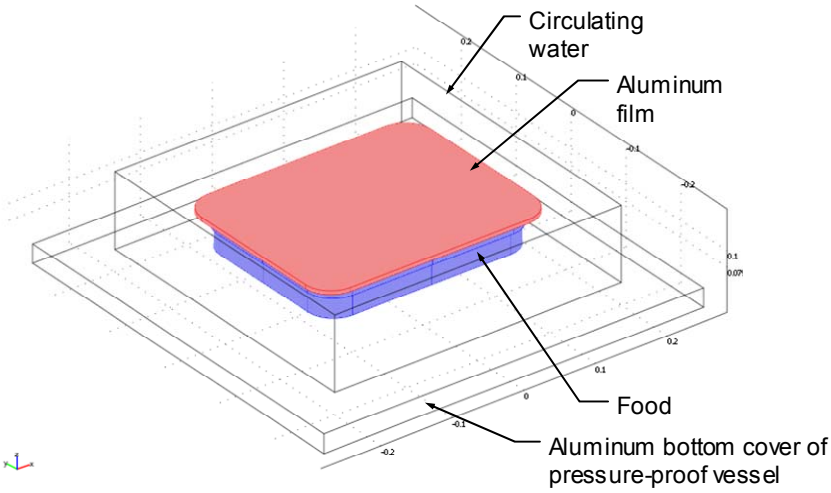

Figure 4.8: Geometry model of vessel and food

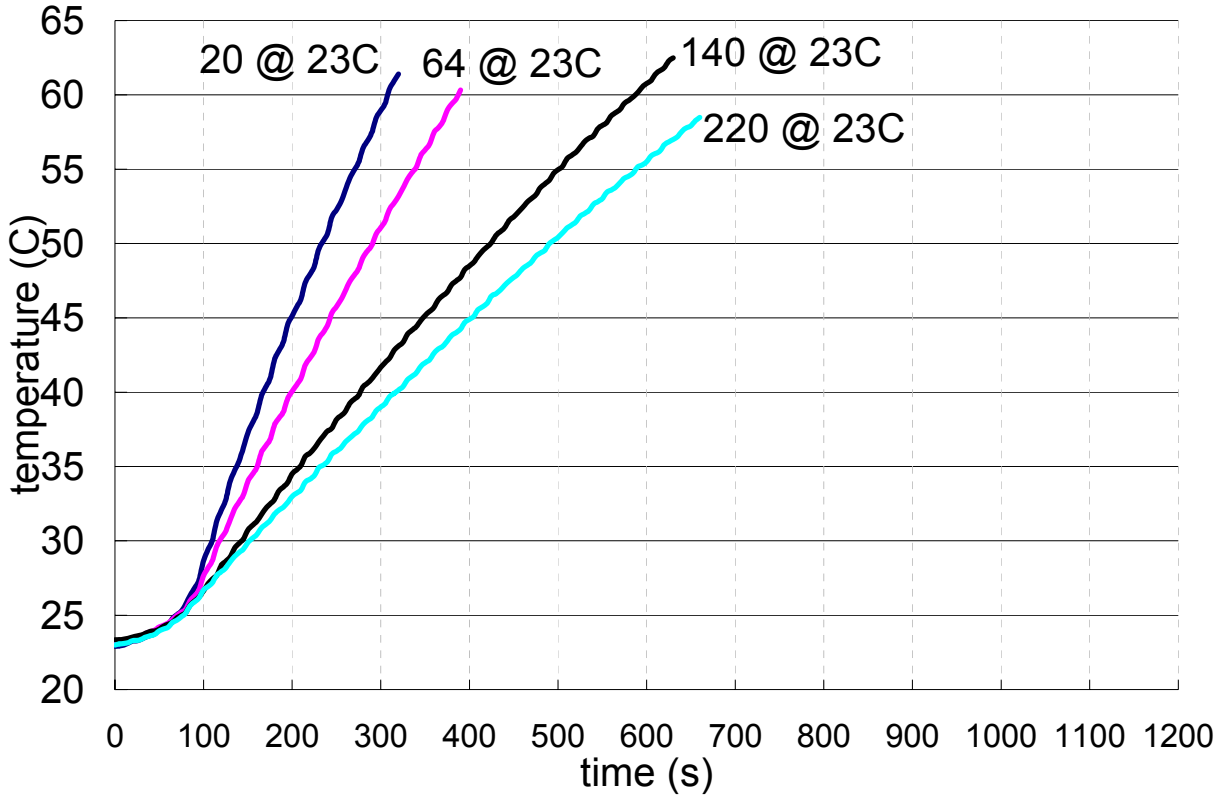
20 @ 23C
64 @ 23C
140 @ 23C
220 @ 23C
temperature (C)
time (s)
65
60
55
50
45
40
35
30
25
20
0
100
200
300
400
500
600
700
800
900
1000
1100
1200

(a)

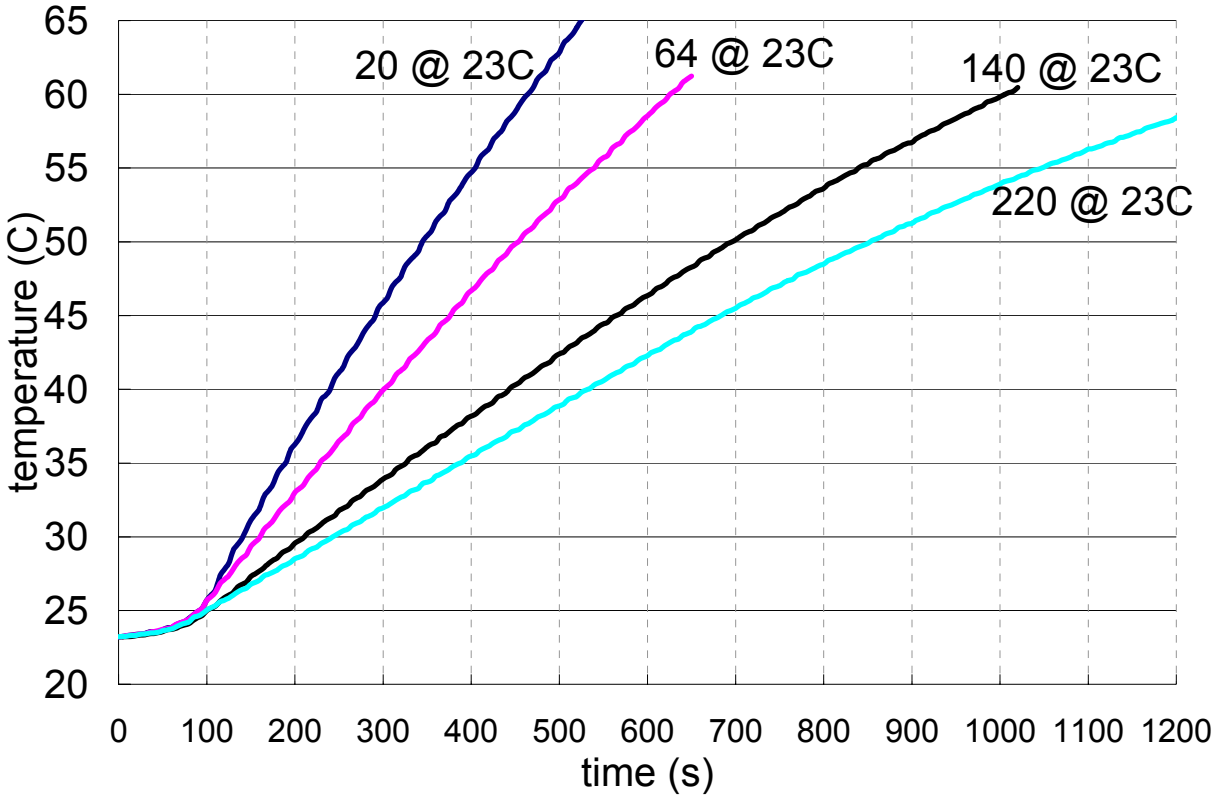

(b)

Figure 4.9: Measured heating profile at the mashed potato sample sensor tips with (a) 0.8% and (b) 1.3% salt content under different circulating water (unit of water conductivity in the figure is μS/cm)

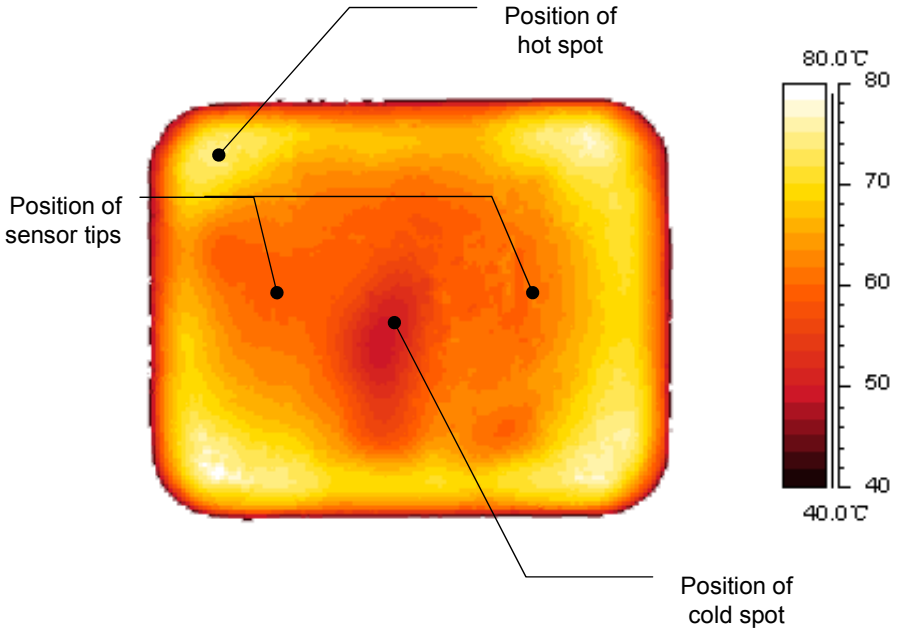

Figure 4.10: Typical thermal image of the central layer of an RF processed mashed potato sample

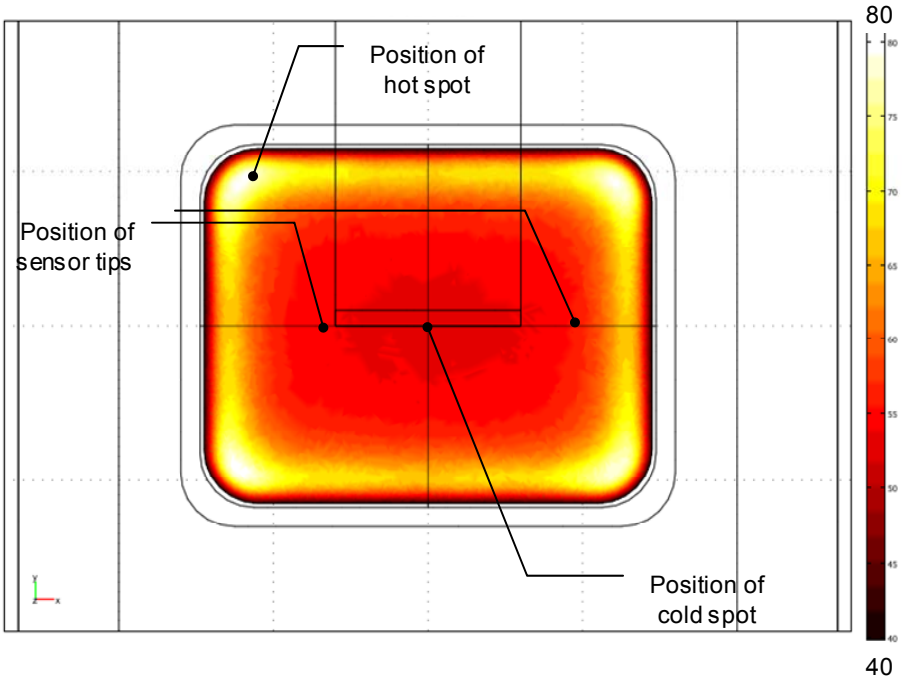

Figure 4.11: Typical numerical solution of the central layer of an RF processed mashed potato sample

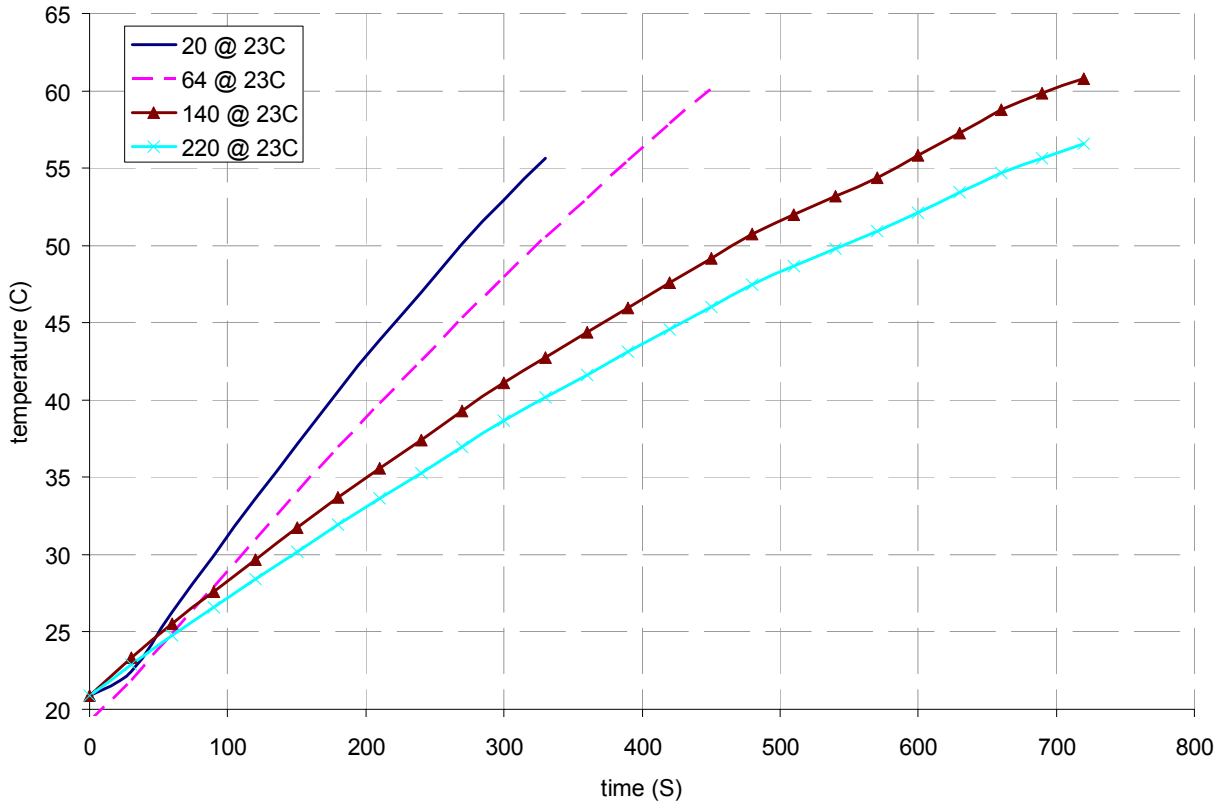
20 @ 23C
64 @ 23C
140 @ 23C
220 @ 23C
temperature (C)
time (S)
65
60
55
50
45
40
35
30
25
20
0
100
200
300
400
500
600
700
800

(a)

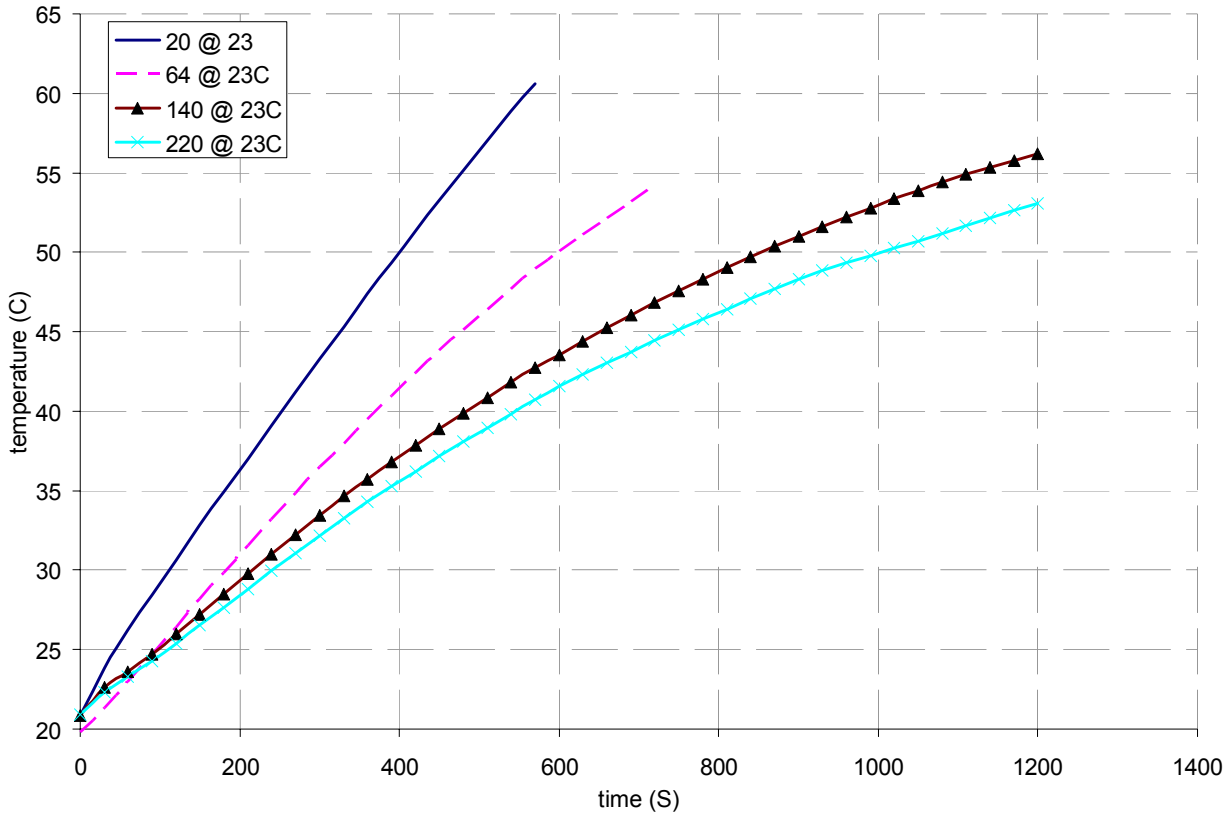

(b)

Figure 4.12: Simulation results of the heating profiles at the mashed potato sample sensor tips with (a) 0.8% and (b) 1.3% salt content under different surrounding water (unit of water conductivity in the figure is μS/cm)

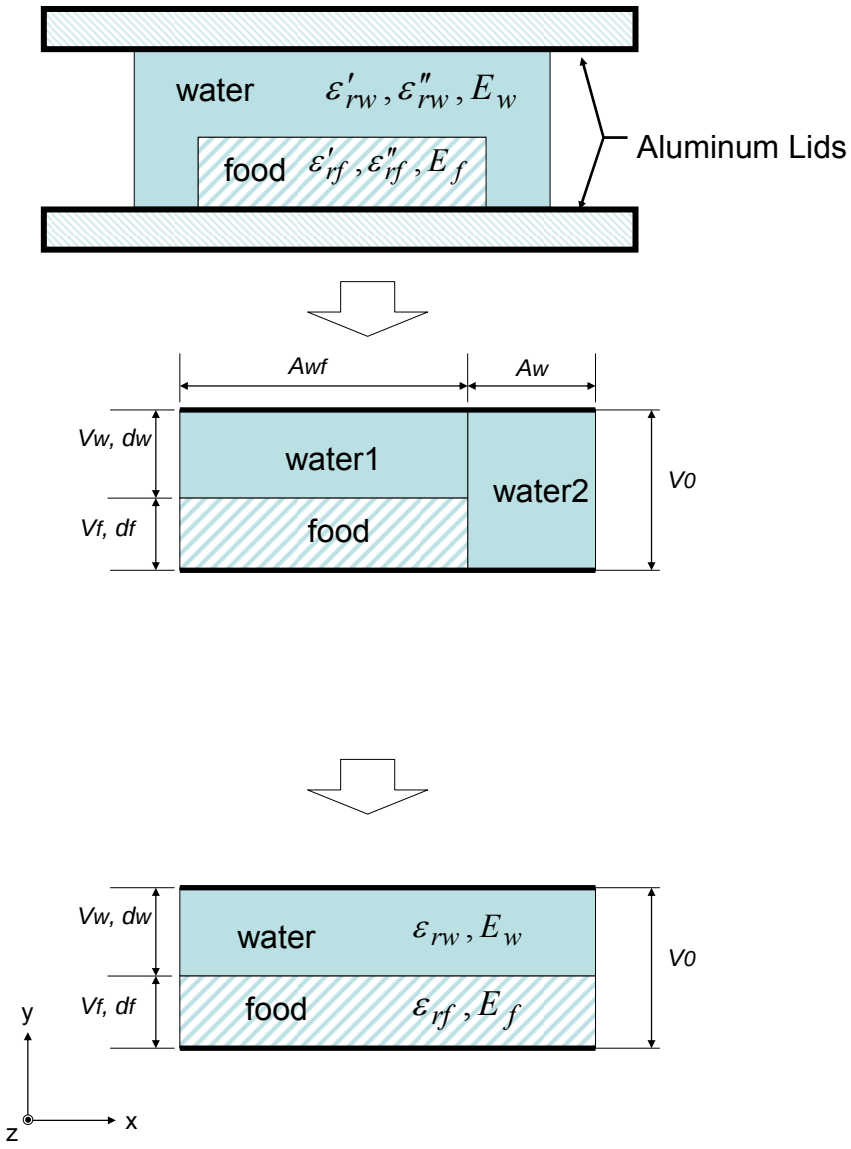

Figure 4.13: Simplified diagram for calculating the electric field distribution inside the RF heating system

CHAPTER FIVE

COMPUTER SIMULATION OF RADIO FREQUENCY HEATING FOR HETEROGENEOUS FOOD

Abstract

A pilot-scale 6 kW 27 MHz radio frequency (RF) heating system was used to sterilize packaged meat lasagna as a sample heterogeneous food. Computer simulations were conducted to study the influence of each food component's dielectric properties on the electric field distribution and heating pattern during RF heating. The experiments indicated relatively uniform heating in the lasagna using RF energy at 27 MHz when beef meatballs, mozzarella cheese and sauce were properly distributed between layers of noodles inside 6-pound capacity combat group ration polymeric trays. The greatest temperature difference among the different ingredients at close proximity (2 cm) inside the trays was within 2 °C once the cold spots' temperate achieved 121 °C. Simulation results indicated that despite the vastly different dielectric properties and electric field intensities of the different food components, due to adequate heat transfer, heating was still rather uniform, conforming to the experimental observations. This study therefore suggests that RF heating has the potential to safely process pre-packaged heterogeneous food and retain product quality, and computer simulation can facilitate the refinement of RF technology.

Introduction

Dielectric properties describe the ability of a food to store and dissipate electrical energy in response to an alternating electromagnetic field (Mudgett, 1986). Dielectric properties, which are described by the complex permittivity of material, ε_c, and can be expressed as (Mohsenin, 1984):

$$\varepsilon_c = \varepsilon_0 \varepsilon_r = \varepsilon_0 (\varepsilon_r^{'} - j\varepsilon_r^{''}) \tag{5.1}$$

where $j = \sqrt{-1}$, and ε_0 = 8.854 × 10^{-12} (F/m), the permittivity of free space (Sadiku, 2001). The relative dielectric constant, ε_r', describes the ability of a food to store electromagnetic energy. The relative loss factor, ε_r'', describes the ability of a food to dissipate electromagnetic energy to heat (Nyfors and Vainikainen, 1989; Lorrain et al., 1998).

The dielectric constant, ε, and loss factor, ε'', of a food can be shown as (Sadiku, 2001):

$$\varepsilon = \varepsilon_0 \varepsilon_r' \tag{5.2a}$$

$$\varepsilon'' = \varepsilon_0 \varepsilon_r'' \tag{5.2b}$$

The loss factor of the food, ε'', has two components that affect the loss factor, as shown by the following equation (Mudgett, 1986):

$$\varepsilon'' = \varepsilon_d'' + \varepsilon_\sigma'' \tag{5.3}$$

The dipole loss component, ε_d'', is due to dipole rotation. The ionic loss component, ε_σ'', results from charge displacement and can be expressed as (Metaxas and Meredith, 1993):

$$\varepsilon_\sigma'' = \frac{\sigma}{2\pi f} \tag{5.4}$$

where σ is electrical conductivity (S/m) of the food and f is frequency (Hz).

Since the loss factors of food material at radio frequencies (e.g., at 27 MHz) are mainly affected by their ionic loss components (Guan et al., 2004; Mudgett, 1986; Wang et al., 2005), by substituting Eq. (5.4) into (5.1), the complex permittivity of a food in the RF range can be simplified as:

$$\varepsilon_c = \varepsilon_0(\varepsilon_r' - j\varepsilon_r'') = \varepsilon_0(\varepsilon_r' - j\frac{\sigma}{\omega\varepsilon_o}) \tag{5.5}$$

The frequency, temperature, moisture content, chemical composition and physical state of foods affect their dielectric properties (Decareau, 1985). Although many dielectric property prediction models have been studied (Nelson and Datta, 2001), it is still difficult to precisely predict the dielectric properties of compound foods because of their variable composition (Datta et al., 1995; Mudgett, 1986). In general, accurate dielectric properties can be obtained only by direct measurement under specified conditions (Nelson, 1999; Guan et al., 2004).

Differences in loss factors among the components of heterogeneous food may result in non-uniform heating in an RF heating system. Preferential heating of certain components within heterogeneous material may be useful for some applications such as post-harvest pest control and lumber drying (Luechapattanaporn, 2005b; Zhao et al., 2000). Wang et al. (2003a) reported greater heating rates of insect larvae compared to infested dried nuts in RF systems, which would lead to a lower product temperature yet high insect larvae temperature, and thus less degradation of product quality. However, for sterilization of packaged food, non-uniform heating is not desirable because it tends to sacrifice food safety and quality. Most experiments on RF sterilization have been conducted on homogeneous foods such as mashed potato (Luechapattanaporn et al.,

2004) and scrambled eggs (Luechapattanaporn et al., 2005a). Macaroni and cheese is one of few heterogeneous foods in the literature on RF sterilization (Wang et al., 2003b) even though heterogeneous foods are more common in the food market.

The objectives of this research were to: (1) study the feasibility of using RF heating to process a selected heterogeneous food, meat lasagna; (2) investigate how the different dielectric properties of the various components in meat lasagna influenced its overall heating pattern by using computer simulation; and (3) explore the ability of computer simulation to predict RF heating patterns in meat lasagna.

Materials and Methods

Dielectric properties measurement

Dielectric properties were determined by Luechapattanaporn (2005b) for four different major ingredients of thawed frozen meat lasagna (Chefs Circle™, Supervalu Inc., Eden Prairie, MN, USA). The data are presented in Appendices 5.1 to 5.4. The meat lasagna ingredients and their proportions were 38.7% beef meatballs, 7.3% grated mozzarella cheese, 38.1% noodles and 13.9% sauce on a wet basis. Proximate compositions of each component are presented in Table 5.1.

RF heating of lasagna

A pilot-scale 6 kW 27 MHz RF heating system was used to perform the experiments. The RF sterilization system was developed at Washington State University,

along with a water circulating system. Detailed information of the RF heating system is described in Chapter 4.

Frozen lasagna was placed at room temperature for at least 24 hours to defreeze and then was placed in 6-pound capacity polymeric combat group ration trays (295 × 235 × 45 mm). Beef meatballs (9.4 mm in diameter), grated mozzarella cheese and sauce were mixed well before being evenly distributed between each of two layers of noodles (107.9 × 254 × 1.5 mm). Trays containing about 2600 g of meat lasagna were vacuum-sealed with a 0.15 mm thick laminated PET/Nylon/Aluminum/PP lid (Jefferson Smurfit, Dublin, Ireland) in a laboratory vacuum tray sealer (Reynolds Metals Company, Richmond, VA, USA).

The filled trays were placed in the center of the custom-designed pressure-proof vessel, which was positioned at the center of the bottom plate of an RF heating oven. Preheated circulating water was pumped through the vessel before and during the heating process. The inlet temperature of the circulation water was controlled by a water conditioning system with a heat exchanger. The core temperature in the trays was preheated by circulating water from room temperature to 65 °C. The temperature of the circulating water was maintained at 65 °C for 2 hours to ensure uniform temperature distribution before the RF heating process, in order to simulate industrial hot fill. The food was then processed with RF heating, during which the flow rate of the circulating water was controlled at approximately 10 L/min. The gauge over-pressure from 34 kPa (5 psi) to 138 kPa (20 psi) depended on the temperature of the food to prevent bursting of packages. The inlet temperature was regulated to increase linearly with time from 65 to 120 °C during 30 min of RF heating. Pre-calibrated fiber optic temperature sensors (FISO

technologies, Inc., Que., Canada) were inserted into different locations within the lasagna to monitor the time-temperature profile under RF heating.

Two different sets of experiments were conducted in which temperature distributions were measured in: 1) different food ingredients (beef meatballs, noodles, mixture of cheese and sauce) in close proximity within 2 cm of each other inside trays (Figure 5.1a), and 2) the same food ingredient (beef meatballs) at different locations inside trays (Figure 5.1b). The experiments were conducted in duplicate. The recorded temperature profile was used to calculate the sterilization value (F_0) (Stumbo, 1973):

$$F_0 = \int_0^t 10^{\left(\frac{T-121.1}{z}\right)} dt \tag{5.6}$$

where T is product temperature (°C), t is processing time (min), and z is 10 °C for *Clostridium botulinum* spores, which are target microorganism in commercial thermal processes for low acid foods (pH > 4.5).

Generally, a minimum safe public health sterilization value (F_0) for low acid canned foods based on inactivation of *C. botulinum* is 3.0 min (Frazier and Westhoff, 1988). Most food companies use a minimum process sterilization value of 5.0 min (Teixeira, 1992). The RF sterilization process for the 6-pound capacity trays with meat lasagna was conducted based on the temperature profile of the fiber optic probe at the cold spots to reach a sterilization value (F_0) of ~5.0 min.

Numerical Model

Computer simulation was conducted to help visualize heating patterns in the above experiments and investigate the influence of various dielectric properties associated with each food component on electric field distribution and heating pattern.

The same procedures detailed in the previous chapter (Figure 4.4 flow chart) were used in this simulation. Similarly, the commercial simulation software COMSOL Multiphysics (Burlington, MA, USA) was chosen to simulate the models in this study because of its ability to describe physical processes with partial differential equations.

Governing equations

The governing equations for electromagnetic field distribution in RF applicators are described by the Maxwell's equations (Balanis, 1989):

$$\nabla \times \mathbf{H} = \sigma \mathbf{E} + \frac{\partial(\varepsilon \mathbf{E})}{\partial t} \tag{5.7a}$$

$$\nabla \times \mathbf{E} = -\frac{\partial \mathbf{B}}{\partial t} = -\frac{\partial(\mu \mathbf{H})}{\partial t} \tag{5.7b}$$

$$\nabla \bullet \mathbf{D} = \nabla \bullet \varepsilon \mathbf{E} = 0 \tag{5.7c}$$

$$\nabla \bullet \mathbf{B} = \nabla \bullet \mu \mathbf{H} = 0 \tag{5.7d}$$

where **E** is electric field intensity (V/m), **H** is magnetic field intensity (A/m), **D** is electric flux density (C/m^2), **B** is magnetic field density (Wb/m^2), ω is angular frequency (radians/second) and μ is food permeability (H/m).

Quasi-static analysis is applicable when the coupling between electric and magnetic fields can be neglected and all dimensions are small compared to the wavelength in any relevant medium. Therefore (COMSOL, 2005b):

$$\nabla \times \mathbf{E} = -\frac{\partial \mathbf{B}}{\partial t} = 0 \tag{5.8}$$

where **E** can be derived from a scalar electric potential V and magnetic vector potential **A** as:

$$\mathbf{E} = -\nabla V - \frac{\partial \mathbf{A}}{\partial t} \tag{5.9}$$

Eq. (5.7c) can now be rewritten as:

$$\nabla \bullet \varepsilon\left(-\nabla V - \frac{\partial \mathbf{A}}{\partial t}\right) = -\varepsilon\left[\nabla^2 V + \frac{\partial}{\partial t}(\nabla \bullet \mathbf{A})\right] \tag{5.10}$$

Considering that when $\partial \mathbf{B} / \partial t = 0$ (Sadiku, 2001)

$$\nabla \bullet \mathbf{A} = 0 \tag{5.11}$$

Therefore Eq. (5.10) can be rearranged as:

$$\nabla^2 V = 0 \tag{5.12}$$

which is the Laplace equation. Solving Eq. (5.12), the electric potential (V) and electric field intensity (**E**) are obtained and the average power density, P, generated by transferring electric energy to heat inside a food can be calculated from (Barber, 1983):

$$P = \omega \mathbf{E}^2 \varepsilon_0 \varepsilon_r'' \tag{5.13}$$

The time interval for a complete wave to pass a stationary point (one cycle of the electromagnetic field) is less than 0.04 μSec for 27 MHz. This interval is very small compared to the thermal changes, the average power density can be used as a time varying quantity, *P(t)*, in the thermal problem.

The power density in Eq. (5.13) is then treated as the heat source in the heat transfer phenomena to couple the electromagnetic field with the thermal field, and the governing equation for heat transfer by conduction is expressed as:

$$\rho C_p \frac{\partial T}{\partial t} - \nabla \bullet (k \nabla T) = P(t) \tag{5.14}$$

where ρ is density, C_p is heat capacity, k is thermal conductivity, $P(t)$ is average power density and T is temperature.

Assumptions

In order to accomplish the simulation with an acceptable accuracy with the computer available for this simulation, Dell Precision 870 workstation, 2 Dual-Core 2.80GHz Intel® Xeon™ Processors and 12GB memory, several assumptions were made to simplify the heating system. First, a quasi-static analysis was assumed. Second, the flow of circulating water inside the pressure-proof vessel and the heat transfer between circulating water and food were neglected. Third, only 6 meat balls and two layers of noodles were placed in the model as shown in Figure 5.2.

Model

By using the finite element method (FEM), the COMSOL Multiphysics software modeled the quasi-static electric and heat transfer phenomena through predefined modeling templates (COMSOL, 2005a). The geometry of the overall RF heating system is presented in Figure 5.3.

Sub-domain and boundary condition setting

Regression analyses of the dielectric properties of the lasagna components are summarized in Table 5.2. The equations were obtained based on the mean values of the dielectric properties found in Appendices 5.1 – 5.4. The electric conductivity value of the circulating water was set as a function of time according to the measured value by a model 53 conductivity analyzer (GLI International, Milwaukee, WI, USA) during a complete 30 min RF heating process expressed as:

$$\sigma = (0.2688 \times t + 337.14) \times 10^{-4} \text{ (S/m)} \tag{5.15}$$

where t is time from 0 to 1800 seconds. The electric potential of the aluminum cavity was set to 0, and a 5 kV electric potential (RMS at 27 MHz) was applied to the feeder plate.

In the heat transfer analysis, heat effects were only considered in the food sample domain to simplify the model. The thermal conductivity and specific heat of each four components of the meat lasagna at room temperature were measured with a KD2 pro thermal properties analyzer (Decagon Devices, Pullman, WA, USA), as shown in Table 5.3. The density of the components was measured by sinking the pre-weighted samples in pure Wesson canola oil (ConAgra Foods, Omaha, NE, USA) to determine the volume and then density. The measurements were conducted in triplicate and results presented in Table 5.3. Since the flow of circulating water was ignored, we accordingly assumed there was no heat convection between the circulating water and sample trays. The boundary conditions for the temperature at the surface of the sample trays were increasingly linear with time from 65 to 120 °C in 30 min.

Convergence study

Preliminary simulations were conducted to acquire an appropriate meshing density and element number. The average power density at three selected elements at the sensor tips of 2, 3, and 4 (as shown in Figure 5.1b) were monitored to check the accuracy of the simulation result and summarized in Table 5.4. As presented in Figure 5.4, with an increase in number of elements, the average power density at the three locations stabilized. In addition, according to the varying percentages between the different meshes (Table 5.5), when the number of elements reached 30624, there was no more than 0.7% difference in the average power density with a 27.5% increase in elements. Stabilization of the average power density value indicated that the number of elements, 30624, was reasonable for further simulation runs.

The time step of simulation was automatically selected by the simulation software to optimize the simulation process while maintaining calculation accuracy. In our model, it took 4 to 5 hours for one simulation run.

Solution computation

Procedures for obtaining the simulation solution are shown in the flow chart in Figure 5.5. At time zero, the initial condition was assigned to the model. The FEM was then used to calculate the electric potential and electric field distribution. The average power density was calculated based on the properties of the materials and electric field distribution. The FEM heat transfer simulation module was used to calculate heat generation and heat transfer. The temperature-dependant dielectric property values were then updated based on renewed temperature distribution. The time-varied temperature

and electric conductivity of circulation water were also changed. The updated variables were applied to the model, and a renewed electric field distribution was calculated. The iterations continued until the final time step was reached.

Results and Discussion

A measured temperature-time history of RF heating applied to four different ingredients in close proximity (Figure 5.1a) within a tray is shown in Figure 5.6. The greatest temperature difference among the beef meatballs, mozzarella cheese, noodles and sauce within 2 cm of each other was 2 °C, with the cold spot temperature reaching 121 °C. Computer simulation of the same conditions as the experiment is shown in Figure 5.7, which shows a similar temperature profile (differing by 4 °C).

The relatively uniform heating results from both the experiment and computer simulation suggests potential for attaining safety along with high quality when heating heterogeneous food with RF as long as the different components are in close proximity to each other and have sufficient heat transfer.

The simulation results were checked at two planes (Figure 5.8). The electric field distribution in planes 1 and 2 (Figure 5.9) indicated a concentration at the tray corners and inside the noodles. Accordingly, the power density (Figure 5.10) at these locations was higher than the rest of the food. However, there was no apparently severe overheating at the noodle and corner of tray (Figure 5.11). Sufficient heat transfer among the sauce, noodles, cheese and beef mitigated the power density concentration that caused by the electric field intensity concentration.

A time-temperature profile of the beef meatballs at four different locations (Figure 5.1b) within a tray was monitored during RF and retort heating (Figure 5.12). In RF heating, the greatest temperature difference among the four locations was less than 5 °C. The time to reach ~121 °C was 35 min compared to 95 min with retort heating.

Similarly, the greatest temperature difference among meatballs indicated by the computer simulation of the RF heating process (Figure 5.11) was 5 °C. The hottest parts of the food were at the corners of the trays, caused by edge heating effects. However, according to Figure 5.12, the experiment exhibited center heating instead.

Three reasons may cause the disagreement between the experiment and simulation. First, the simplification of boundary conditions at the interface between food and circulating water diminished the cooling effect of the circulating water to the food surface. Secondly, the linear regression analysis applied to draw the relationship between the dielectric properties of the food components and their temperatures was based on the mean values of the measurement results, which inevitably included measurement errors due to approximations. Thirdly, deformation of the trays during RF heating may have caused center heating.

In some cases during the heat-hold-cool process of conventional retort heating, the end of heating or beginning of cooling contributes as much as 90% of the cumulative F_0 obtained by heated food (Pflug and Esselen, 1963). Comparatively, the hold-cool stage in RF heating contributed ~80-90% of the cumulative F_0 (Table 5.6).

Conclusions

The results from this study show that RF heating has a potential to produce safe, high quality pre-packaged heterogeneous food. RF heating has advantages over retort heating when processing semi-solid food such as meat lasagna due to its short heat-up time and relatively uniform temperature distribution, resulting in less degraded food products (Luechapattanaporn et al., 2005a). Proper distribution and suitable amounts and sizes of each component, though with vastly different dielectric properties, can provide relatively uniform RF heating. This study also demonstrated that investigations of RF heating can be facilitated by computer simulation to further improve RF heating systems. But inoculated studies of packaged RF-treated meat lasagna are needed to ensure that the target level of sterility is achieved.

References

Balanis, C.A. 1989. Advanced engineering electromagnetics. John Wiley & Sons, New York, NY, USA.

Barber, H. 1983. Electroheat. Sheridan House, Dobbs Ferry, NY, USA.

COMSOL. 2005a. Electromagnetics module user's guide. COMSOL Multiphysics, Burlington, MA.

COMSOL. 2005b. COMSOL multiphysics user's guide. COMSOL Multiphysics, Burlington, MA.

Datta, A.K., Sun, E. and Solis, A. 1995. Food dielectric property data and their composition-based prediction. In: Rao, M.A. and Rizvi, S.S.H., editors. Engineering properties of foods. Marcel Dekker, New York, NY, USA. 457-493

Decareau, R.V. 1985. Microwaves in the food processing industry. Academic Press, Orlando, FL, USA. 15-37.

Frazier, W.C. and Westhoff, D.C. 1988. Food microbiology. 4th ed. McGraw-Hill, New York, NY, USA.

Guan, D., Cheng, M., Wang, Y. and Tang, J. 2004. Dielectric properties of mashed potatoes relevant to microwave and radio frequency pasteurization and sterilization process. Journal of Food Science, 69(1): 30-37.

Lorrain, P., Corson, D.R., and Lorrain, F. 1988. Electromagnetic Fields and Waves, 3rd edition. W.H. Freeman and Company, New York, NY. 192-210.

Luechapattanaporn, K., Wang, Y., Wang, J., Al-Holy, M., Kang, D.H., Tang, J. and Hallberg, L.M. 2004. Microbial safety in radio frequency processing of packaged foods. Journal of Food Science, 69(7): 201-206.

Luechapattanaporn, K., Wang, Y., Wang, J., Tang, J., Hallberg, L.M. and Dunne, C.P. 2005a. Sterilization of scrambled eggs in military polymeric trays by radio frequency energy. Journal of Food Science, 70(4): 288-294.

Luechapattanaporn, K. 2005b. Microbial safety of radio frequency sterilization process. Doctor of philosophy dissertation. Department of Biological System Engineering. Washington State University, Pullman, WA, USA.

Metaxas, A.C., & Meredith, R.J. 1993. Industrial microwave heating. Peter Peregrinus Ltd., London, UK.

Mohsenin, N.N. 1984. Electromagnetic radiation properties of foods and agricultural products. Gordon and Breach Science Publishers, New York, NY, USA.

Mudgett, R.E. 1986. Electrical properties of foods. In: Mao, A. and Rizvi, S.S.H., editors. Engineering properties of food. Marcel Dekker, New York, NY, USA.

Nelson, S.O. 1999. Dielectric properties measurement techniques and applications. Transactions of the ASAE, 42(2): 523-9.

Nelson, S.O. and Datta, A.K. 2001. Dielectric properties of food materials and electric field interactions. In: Datta, A.K. and Anantheswaran, R.C., editors. Handbook of microwave technology for food applications. Marcel Dekker, New York, NY, USA. 69-114.

Nyfors, E. and Vainikainen, P. 1989. Industrial Microwave Sensors. Artech House, Norwood, Norwood, MA, USA.

Pflug, I.J. and Esselen, W.B. 1963. Food processing by heat sterilization. In: Heid, J. and Joslyn, M.A., editors. Food processing operations: their management, machines, materials and methods. Volume 2. AVI Publishing, Westport, CT, USA. 410-479.

Sadiku, M.N.O. 2001. Elements of electromagnetics, 3rd ed. Oxford University Press, New York, NY, USA.

Stumbo, C.R. 1973. Thermobacteriology in food processing. 2nd ed. Academic Press, New York, NY, USA.

Teixeira, A. 1992. Thermal process calculation. In: Heldman, D.R. and Lund, D.B., editors. Handbook of food engineering. Marcel Dekker, New York, NY, USA. 563-65.

Wang, S., Tang, J., Cavalieri, R.P. and Davis, D.C. 2003a. Differential heating of insects in dried nuts and fruits associated with radio frequency and microwave treatments. Transaction of the ASAE. 46(4): 1175-82.

Wang, Y., Wig, T.D., Tang, J. and Hallberg, L.M. 2003b. Dielectric properties of foods relevant to RF and microwave pasteurization and sterilization. Journal of Food Engineering. 57: 257-68.

Wang, S., Monzon, M., Gazit, Y., Tang, J., Mitcham, E.J. and Armstrong, J.W. 2005. Temperature-dependent dielectric properties of selected subtropical and tropical fruits and associated insect pests. Transaction of the ASAE. 48(5): 1873-1881.

Zhao, Y., Flugstad, B., Kolbe, E., Park, J.W. and Wells, J.H. 2000. Using capacitive (radio frequency) dielectric heating in food processing and preservation – a review. Journal of Food Process Engineering .23: 25–55.

Tables

Table 5.1: Composition of each ingredient in the RF heated meat lasagna (Luechapattanaporn, 2005b)

Ingredient	% (wb)				
	CHO	Fat	Protein	Moisture	Ash
Beef meatballs	1.33	12.74	18.01	66.93	0.99
Noodles	30.64	0.98	7.14	60.71	0.53
Cheese	6.36	15.70	15.76	59.05	3.13
Sauce	5.37	0.00	1.24	91.96	1.43

Table 5.2: Regression analysis of the dielectric properties of lasagna components based on the mean values in Appendices 5.1–5.4

Meatballs	ε_r' = 62.63 + 0.29 T
	ε_r'' = 198.42 + 12.57 T
Noodles	ε_r' = 98.87 – 0.34 T + 2 × 10^{-3} T^2
	ε_r'' = 203.09 + 12.96 T
Cheese	ε_r' = 54.63 + 0.28 T
	ε_r'' = 160.57 + 11.19 T
Sauce	ε_r' = 101.77 – 0.9315 T + 1.16 × 10^{-2} T^2 – 4× 10^{-5} T^3
	ε_r'' = 418.26 + 25.92 T

Table 5.3: Summary of the thermal properties of lasagna components at 20 °C (mean ± standard deviation of triplicate)

	Meatballs	Noodles	Cheese	Sauce
Thermal conductivity (W/m·K)	0.479 ± 0.026	0.515 ± 0.021	0.478 ± 0.007	0.512 ± 0.015
Heat capacity (kJ/kg·K)	3.597 ± 0.188	3.687 ± 0.145	3.702 ± 0.039	3.728 ± 0.112
Density (kg/m^3)	1144.7 ± 26.5	977 ± 16.7	1013.2 ± 3.7	905.6 ± 10.1

Table 5.4: Summary of the meshing effects on the average power density

Meshing	Number of elements	Number of freedom	Average power density (W/m^3)		
			Position 2	Position 3	Position 4
1	10095	25544	171290.8	160746.2	237773.3
2	10151	25650	155552.6	145718.5	215245.2
3	10985	27003	151258.3	141834.9	208279.9
4	16022	36898	146654.6	139148.8	201837.6
5	24019	52743	142917.1	135796.5	196675.2
6	30624	65462	141962.7	134866.2	195436.1

Table 5.5: Summary of the difference in percentages between the meshing

Difference between	Percentage (%) differencse between number of elements	Percentage (%) difference		
		Position 2	Position 3	Position 4
1 and 2	0.6	10.1	10.3	10.5
2 and 3	8.2	2.8	2.7	3.3
3 and 4	45.9	3.1	1.9	3.2
4 and 5	49.9	2.6	2.5	2.6
5 and 6	27.5	0.7	0.7	0.6

Table 5.6: Sterilization values (F_0) during different periods of RF heating

(Luechapattanaporn, 2005b)

		Cumulative F_0 (min)					
		RF heating		Holding		Cooling	
Sensor positions*	Temperature probe	Test 1**	Test 2	Test 1	Test 2	Test 1	Test 2
A	1	2.9	1.0	8.1	4.9	13.5	10.8
	2	1.2	0.6	4.1	2.9	7.9	6.7
	3	7.2	1.0	17.5	4.9	23.5	10.6
	4	1.1	0.7	3.5	3.2	7.0	6.9
B	1	2.8	3.6	6.4	6.9	9.9	9.4
	2	4.2	8.3	9.5	15.5	16.6	19.9
	3	2.1	2.3	3.0	4.8	6.2	6.8
	4	1.1	1.5	4.8	4.0	7.3	5.1

* two sets of experiments with the sensor positions arranged according to Figure 5.1

** data shown are from two separate tests

Figures

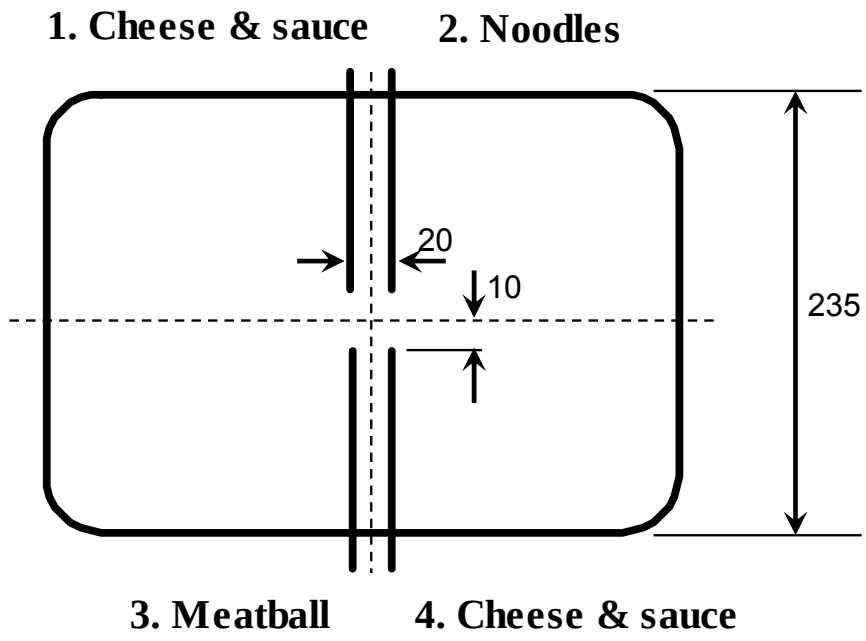
1. Cheese & sauce
2. Noodles
20
10
235
3. Meatball
4. Cheese & sauce

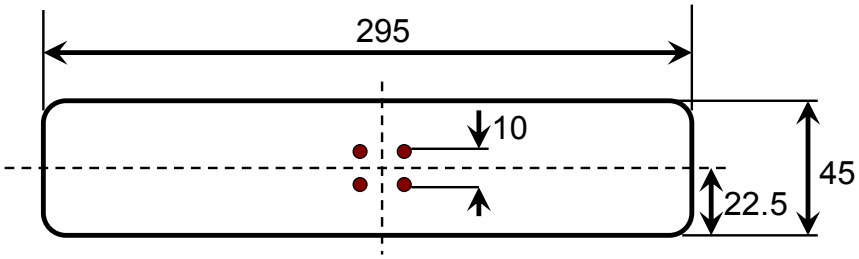
295
10
45
22.5

(a)

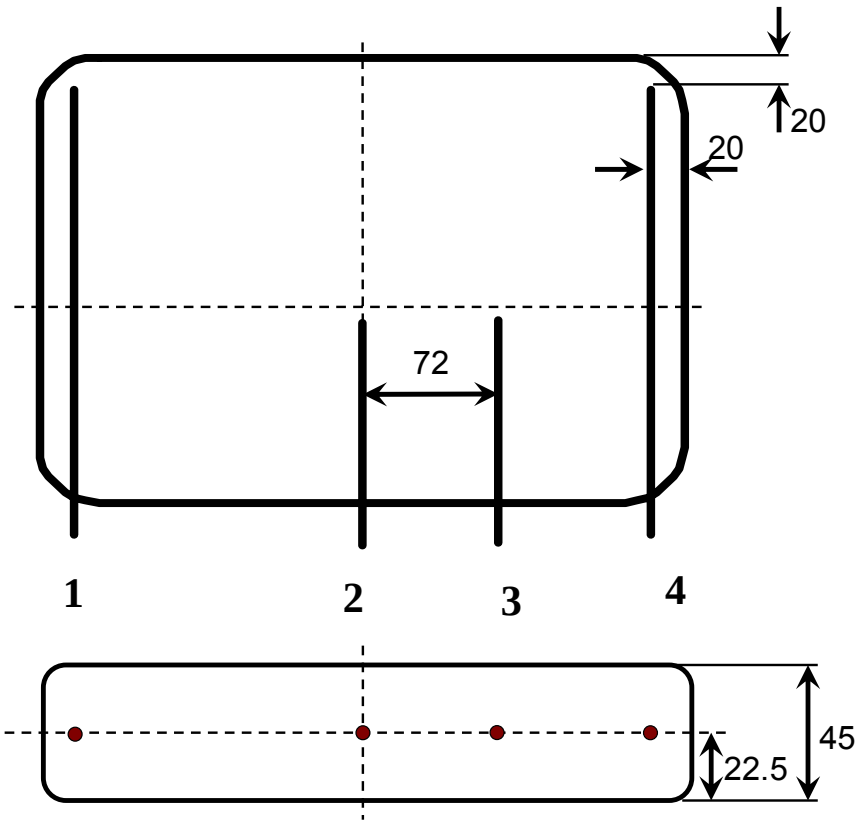

(b)

Figure 5.1: Positions of fiber optic probes inside polymetric trays inserted in: (a) different lasagna components: beef meatballs, noodles, mixture of cheese and sauce within close proximity; and (b) beef meatballs at different locations. Unit in the diagram is in mm (not to scale).

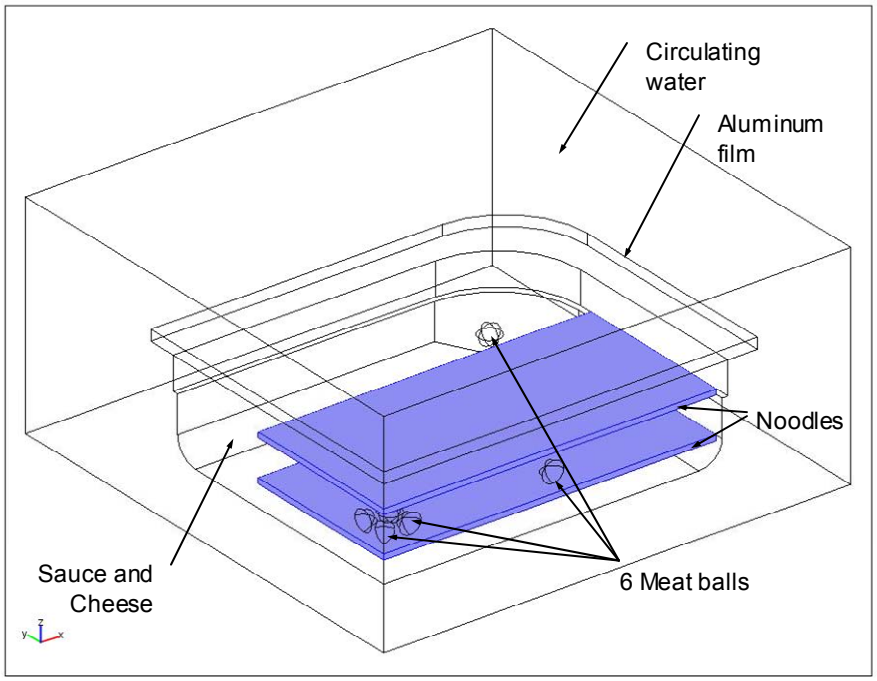

Figure 5.2: Detailed geometry used in the computer simulation model for a quarter of the packaged lasagna and circulating water

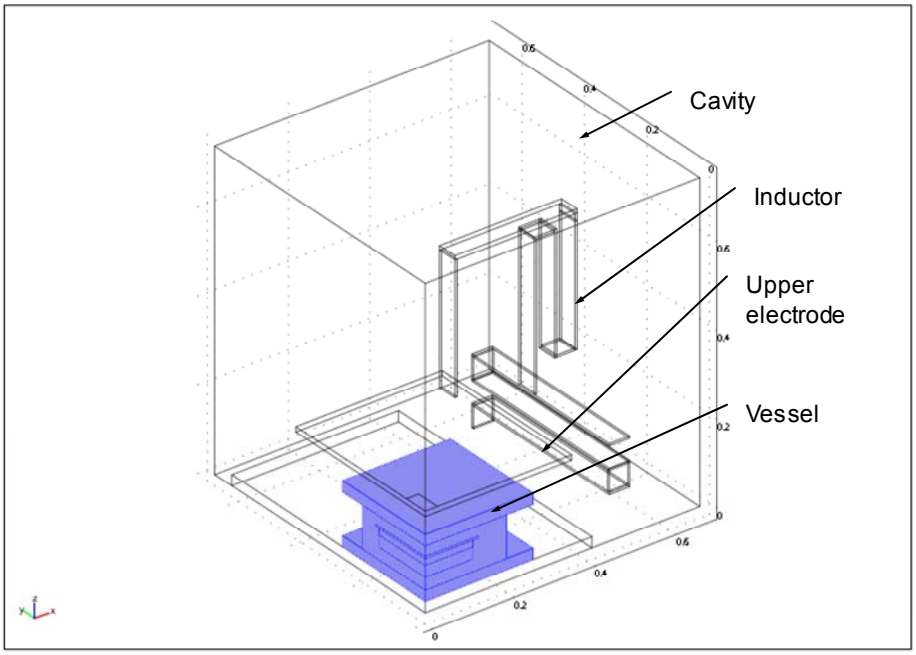

Figure 5.3: Detailed geometry used in the model of a quarter of the RF heating cavity

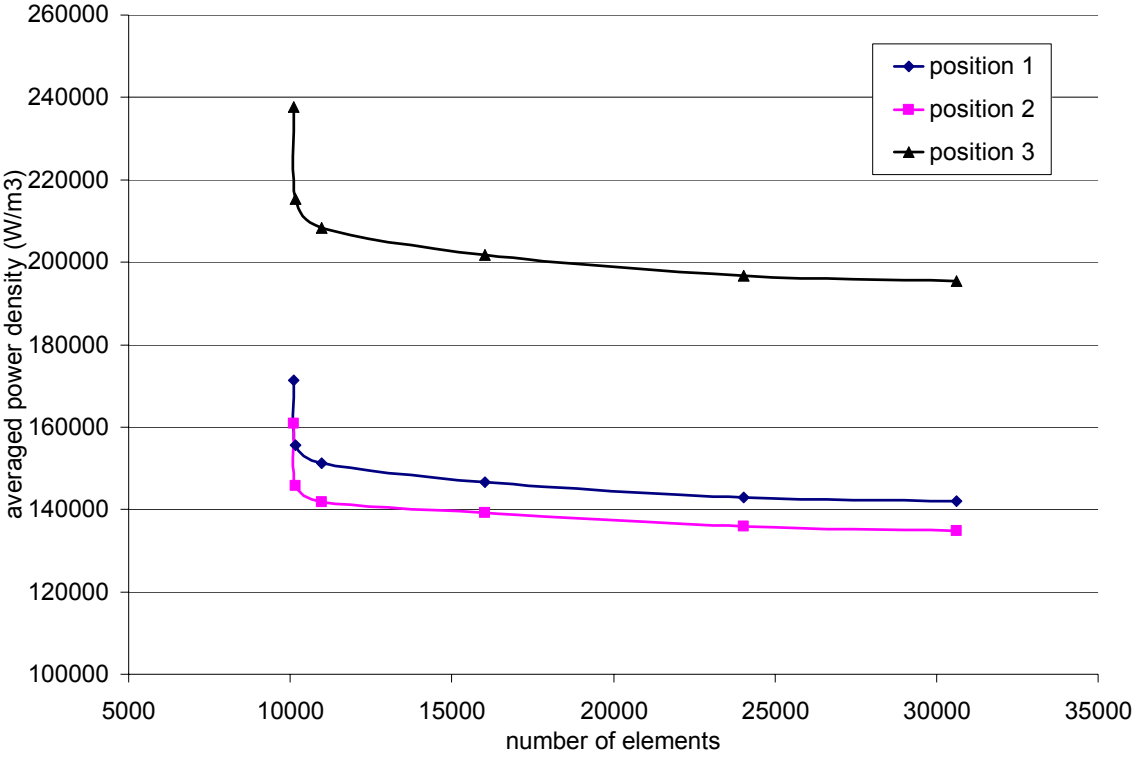

Figure 5.4: Effects of the number of elements on the accuracy of the average power density

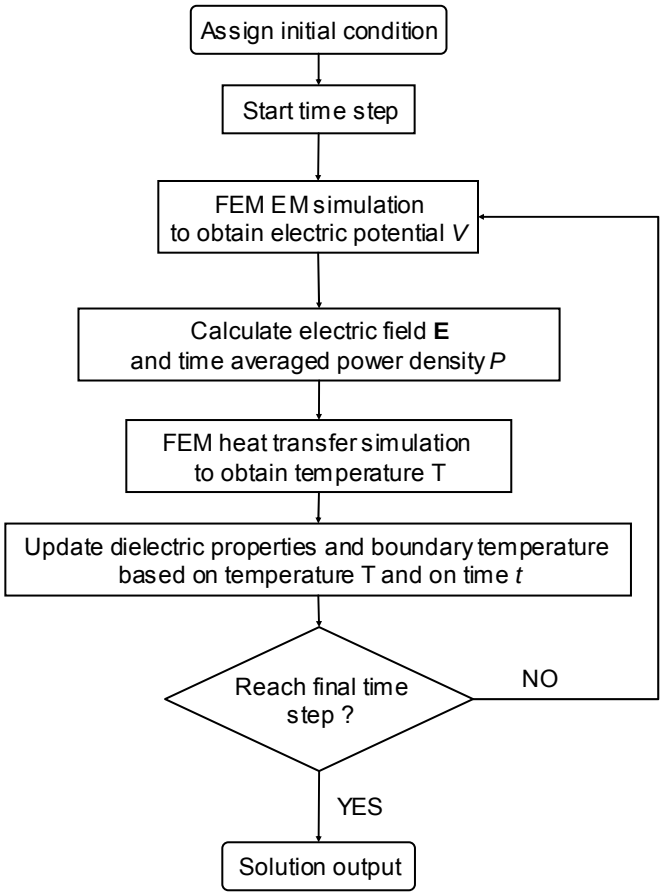

Figure 5.5: Flow chart of the solution computation procedure

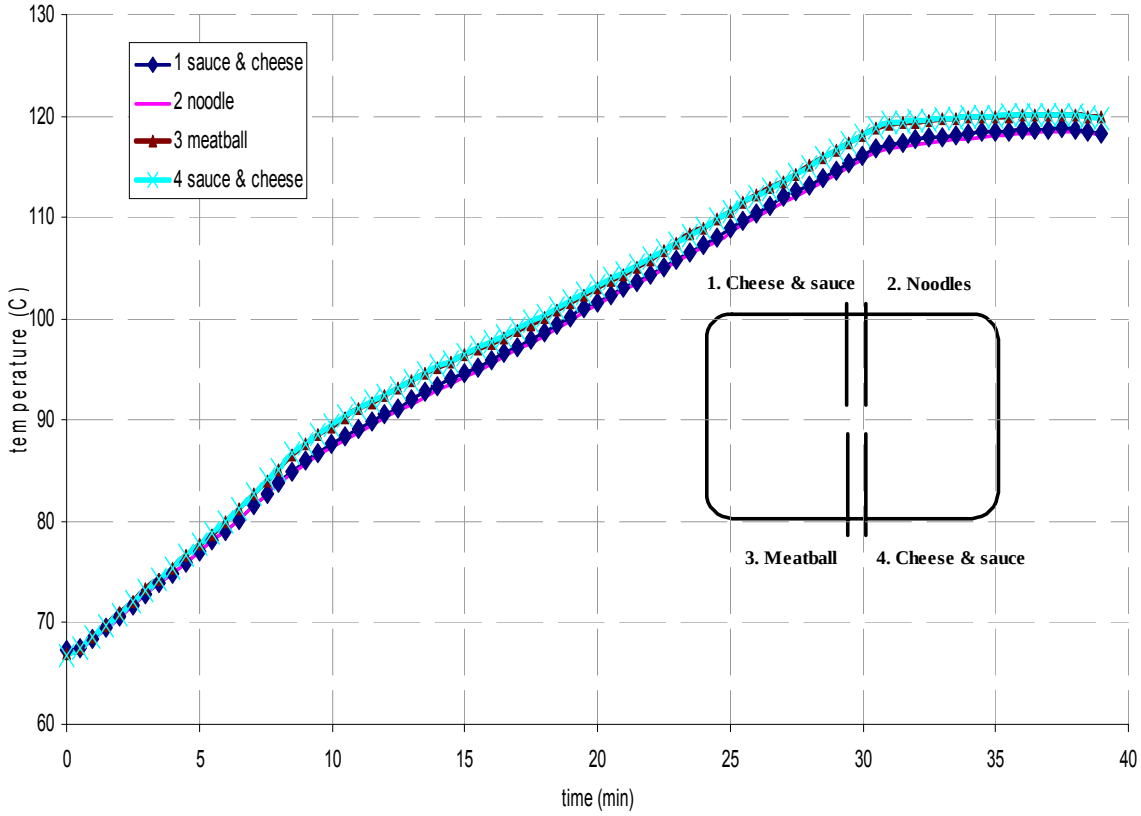

Figure 5.6: Measured time-temperature profile of lasagna ingredients inside a polymeric tray thermally processed by RF based on the measurement in Figure 5.1a.

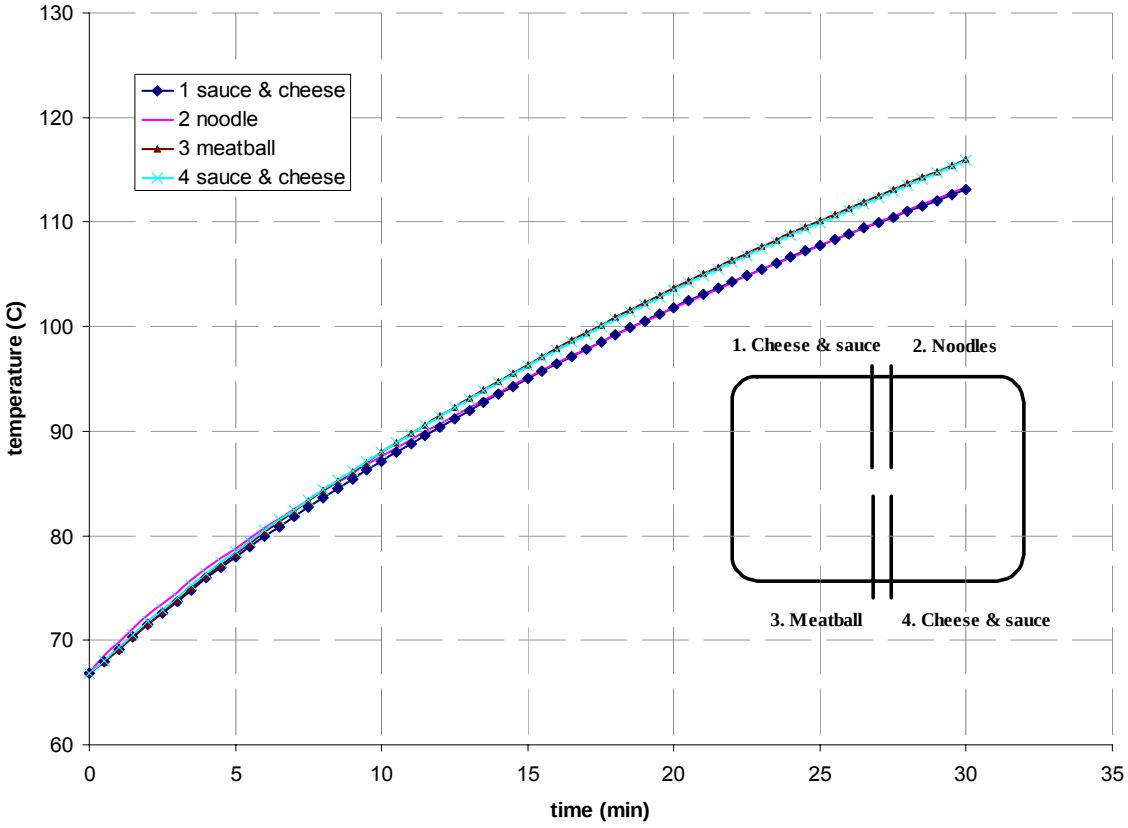

Figure 5.7: Simulated time-temperature profile of lasagna ingredients inside a polymeric tray thermally processed by RF based on the measurement in Figure 5.1a.

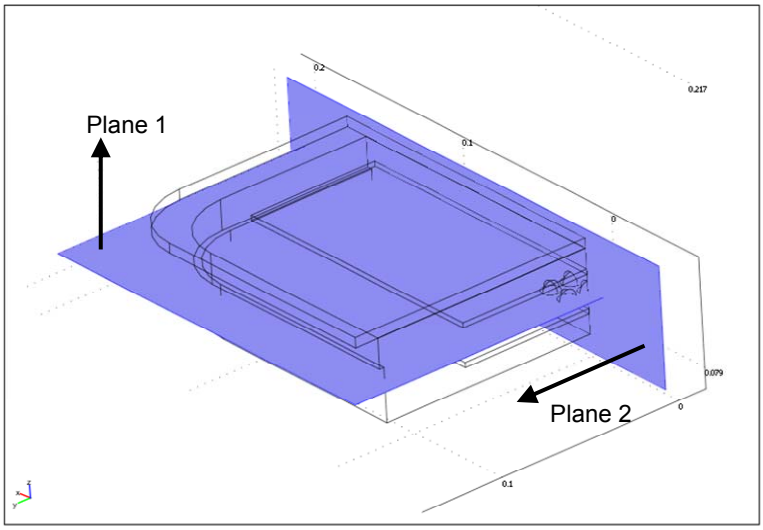

Figure 5.8: Two planes for checking the numerical solutions

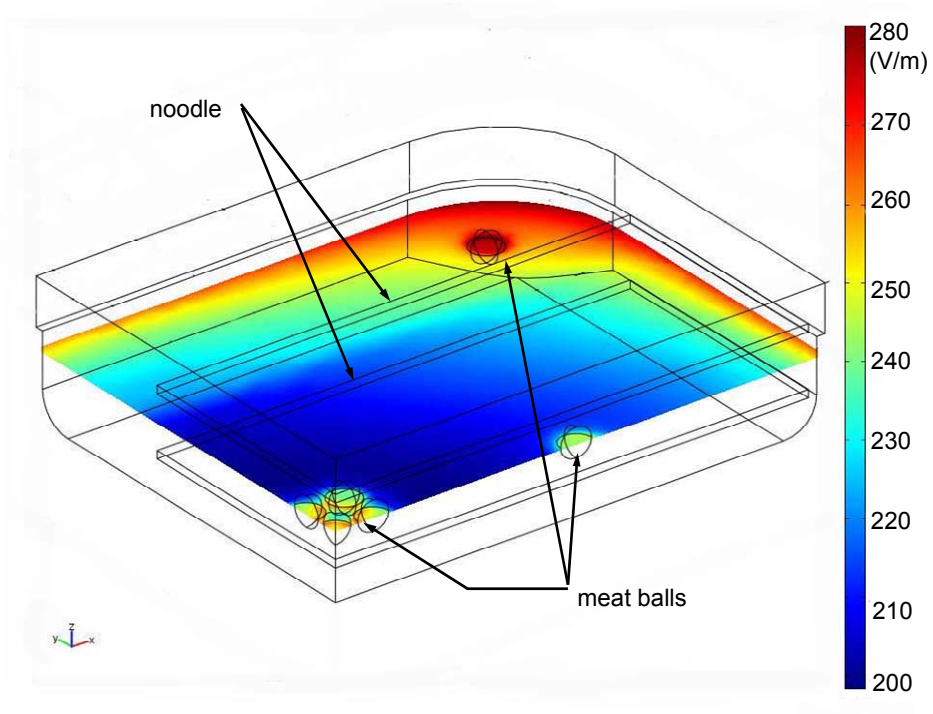

(a)

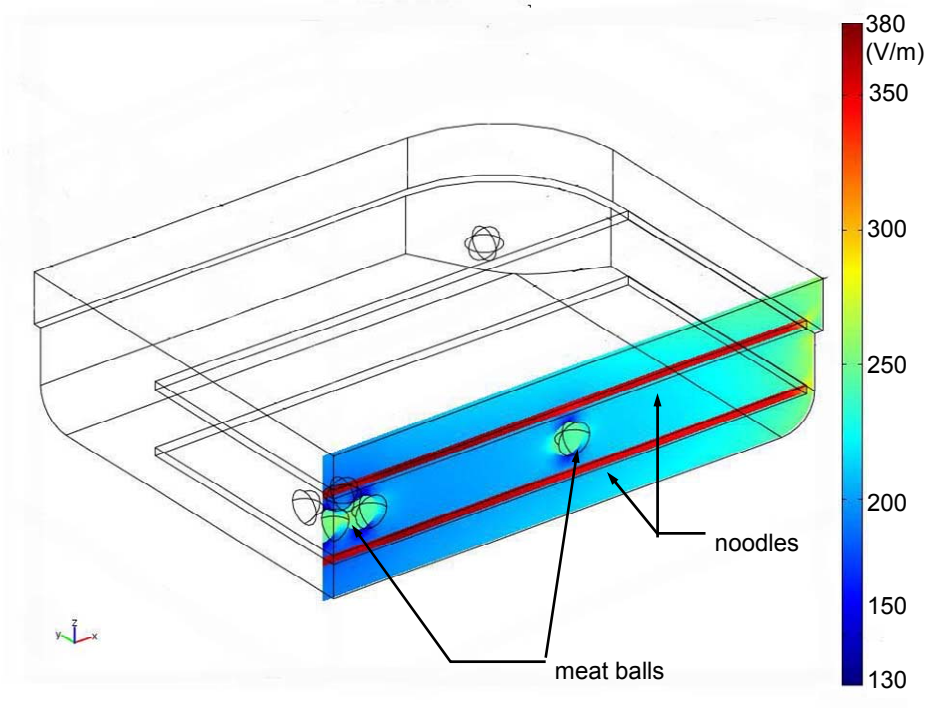

(b)

Figure 5.9: Electric field distribution at a) plane 1 and b) plane 2 (Figure 5.8)

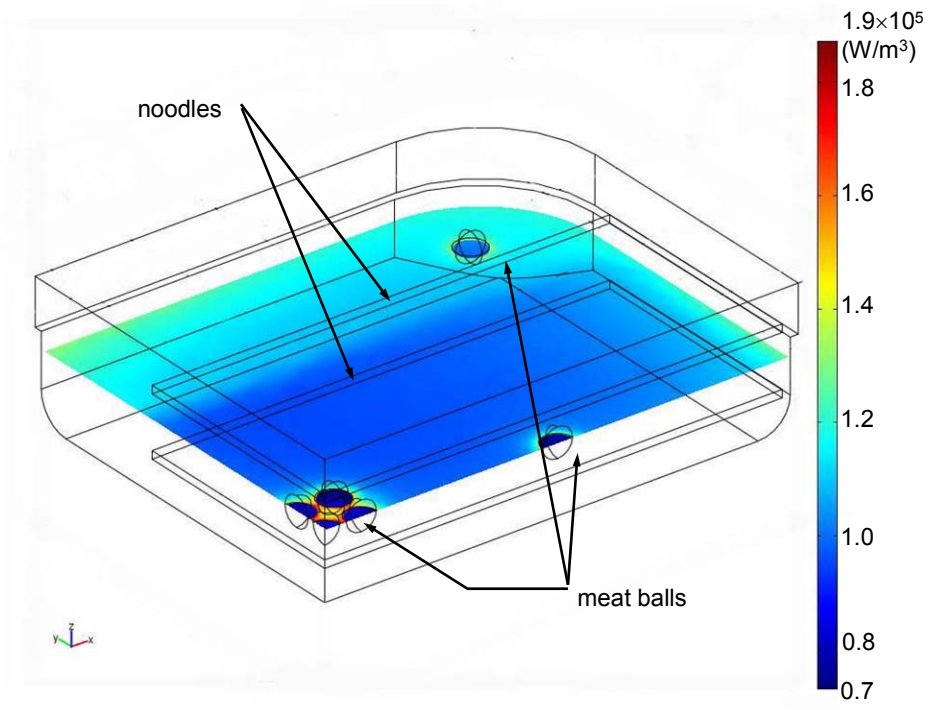

(a)

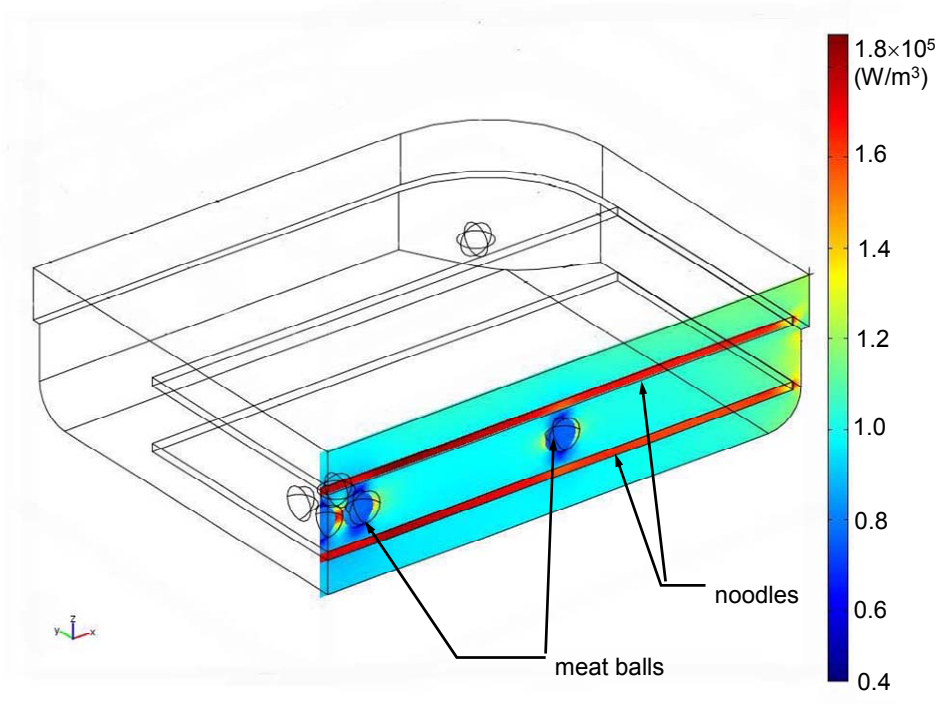

(b)

Figure 5.10: Power density distribution at a) plane 1 and b) plane 2 (Figure 5.8)

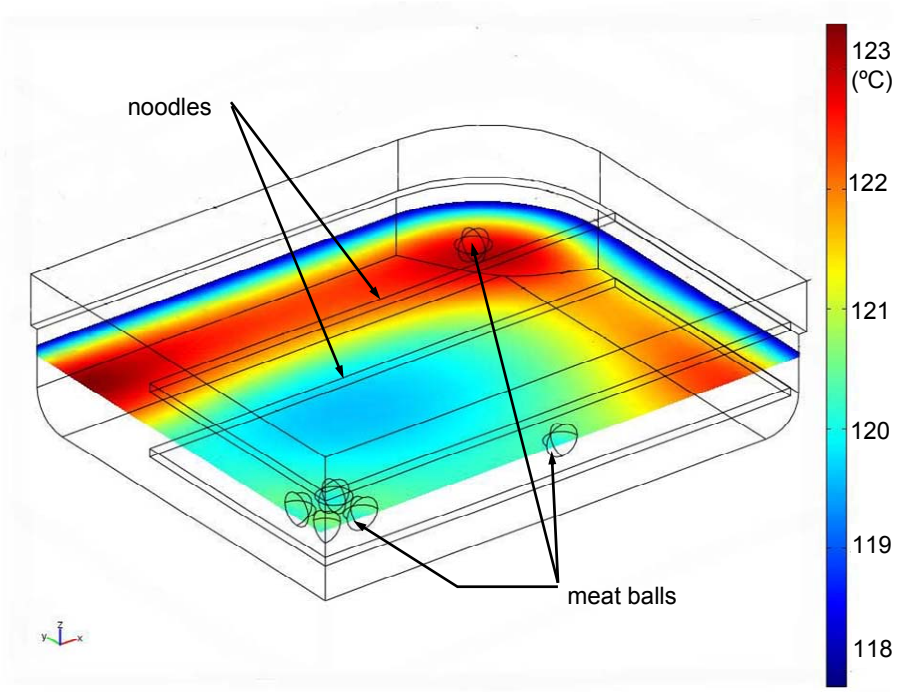

(a)

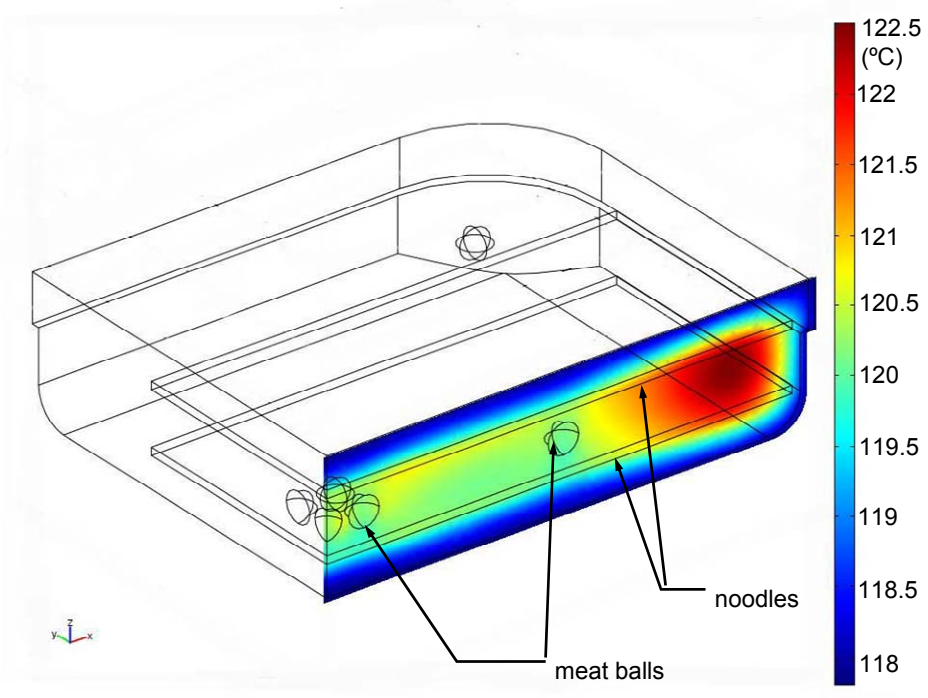

(b)

Figure 5.11: Temperature distribution at a) plane 1 and b) plane 2 (Figure 5.8)

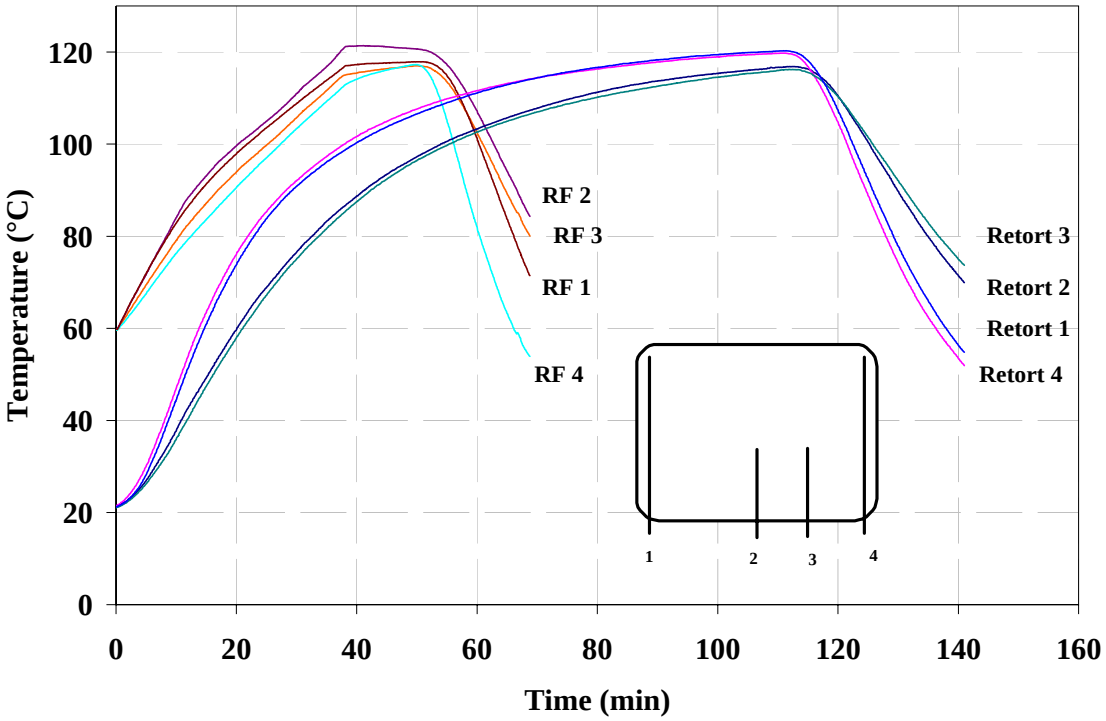

Figure 5.12: Comparison of the temperature-time profile of beef meatballs at different locations inside a polymeric tray thermally processed by RF and retort heating. The sensors positions are shown in Figure 5.1b.

Appendices

Appendix 5.1: Dielectric properties of beef meatballs (mean ± standard deviation of triplicate) (Luechapattanaporn, 2005b)

T (°C)		27 MHz	40 MHz	915 MHz	1800 MHz
20	ε_r'	68.75±3.59	56.57±2.73	41.94±0.48	40.14±0.66
	ε_r''	474.44±9.52	323.89±6.02	20.46±0.68	14.29±0.27
30	ε_r'	70.63±3.37	57.61±1.88	40.93±0.19	39.31±0.49
	ε_r''	561.65±40.58	382.92±27.05	22.71±1.05	14.92±0.39
40	ε_r'	72.13±4.97	63.97±5.45	38.65±2.85	36.25±3.70
	ε_r''	639.50±4.28	434.68±4.81	24.47±0.81	16.1±0.01
50	ε_r'	76.57±1.30	67.52±2.89	39.78±2.35	36.98±3.50
	ε_r''	800.89±11.22	544.06±8.48	29.82±0.88	18.48±0.04
60	ε_r'	79.06±0.68	69.06±1.36	39.36±1.59	36.41±2.81
	ε_r''	921.97±10.41	625.39±5.84	33.62±0.19	20.23±0.33
70	ε_r'	83.88±5.44	72.55±2.59	39.93±0.65	36.78±0.63
	ε_r''	1096.57±119.9	743.64±79.87	39.19±3.24	22.98±2.16
80	ε_r'	88.82±9.76	75.48±5.36	39.89±1.88	36.62±0.64
	ε_r''	1269.39±229.82	860.10±153.54	44.47±6.30	25.52±3.64
90	ε_r'	91.54±11.79	76.79±6.40	39.22±1.95	35.78±0.66
	ε_r''	1394.81±262.62	944.46±175.23	48.38±7.24	27.45±4.08
100	ε_r'	95.77±14.87	78.97±7.83	39.06±2.06	35.42±0.83
	ε_r''	1557.51±296.33	1054.09±197.73	53.55±7.92	30.15±4.26
110	ε_r'	93.42±8.30	76.84±3.25	36.92±0.65	33.08±1.86
	ε_r''	1553.88±82.04	1051.76±53.65	53.72±1.44	30.16±0.97
121	ε_r'	92.9±3.41	75.66±0.78	35.34±2.59	31.39±3.72
	ε_r''	1604.5±57.27	1086.19±40.14	55.43±2.74	30.98±1.24

Appendix 5.2: Dielectric properties of mozzarella cheese (mean ± standard deviation of triplicate) (Luechapattanaporn, 2005b)

T (°C)		27 MHz	40 MHz	915 MHz	1800 MHz
20	ε_r'	55.57±8.8	49.38±8.99	28.16±6.36	25.57±5.43
	ε_r''	358.53±56.89	245.52±39.07	17.18±2.95	11.87±2.01
30	ε_r'	60.46±8.22	53.01±8.89	29.18±6.16	26.54±5.42
	ε_r''	482.79±57.79	329.63±39.70	21.17±2.74	13.80±1.82
40	ε_r'	66.22±6.87	57.10±7.91	29.07±6.82	27.29±4.86
	ε_r''	621.43±35.22	423.28±24.75	25.59±1.89	15.95±1.35
50	ε_r'	70.80±6.88	60.31±8.17	30.23±5.42	27.37±4.75
	ε_r''	740.50±32.19	503.85±22.69	29.43±1.72	17.82±1.24
60	ε_r'	74.60±6.78	62.95±8.61	30.32±5.37	27.23±4.66
	ε_r''	853.59±25.48	579.93±18.35	30.23±5.29	22.13±2.31
70	ε_r'	77.45±6.75	64.46±8.48	29.96±4.90	26.99±4.55
	ε_r''	956.35±19.24	649.95±14.40	36.37±1.30	21.48±1.31
80	ε_r'	78.68±9.10	64.91±10.22	29.60±4.87	26.55±4.55
	ε_r''	1050.62±58.70	713.31±40.90	39.21±2.65	22.93±2.01
90	ε_r'	81.23±8.03	66.06±9.68	29.35±4.87	26.17±4.48
	ε_r''	1168.79±40.97	792.74±29.02	42.75±2.02	24.78±1.77
100	ε_r'	82.21±6.87	66.08±9.04	29.09±4.82	25.80±4.23
	ε_r''	1266.94±28.04	858.88±20.2	45.59±1.53	26.30±1.55
110	ε_r'	83.08±5.55	65.87±8.20	28.79±4.53	25.80±4.09
	ε_r''	1368.88±32.60	927.33±23.04	48.50±1.56	27.84±1.53
121	ε_r'	84.22±2.37	65.84±5.83	28.61±3.99	25.28±3.63
	ε_r''	1525.13±25.23	1032.20±15.74	53.03±0.44	30.31±0.45

Appendix 5.3: Dielectric properties of noodles (mean ± standard deviation of triplicate) (Luechapattanaporn, 2005b)

T (°C)		27 MHz	40 MHz	915 MHz	1800 MHz
20	ε_r'	92.52±0.87	84.32±0.83	54.74±0.08	50.85±0.05
	ε_r''	516.82±15.33	353.33±10.08	25.46±0.05	19.64±0.06
30	ε_r'	92.10±1.29	83.87±1.14	54.35±0.31	50.75±0.31
	ε_r''	617.19±18.91	420.41±12.49	27.84±0.17	19.86±0.37
40	ε_r'	87.83±1.53	79.91±1.24	53.93±0.47	50.53±0.48
	ε_r''	708.48±20.70	480.57±13.56	29.73±0.29	20.53±0.01
50	ε_r'	85.57±1.84	77.26±1.60	53.46±0.27	50.26±0.27
	ε_r''	812.46±25.99	549.97±17.21	31.90±0.43	21.22±0.13
60	ε_r'	85.16±1.61	76.15±1.68	52.67±0.08	49.61±0.18
	ε_r''	943.27±39.31	637.68±26.49	35.24±0.84	22.51±0.36
70	ε_r'	84.95±1.46	74.87±1.58	51.76±0.02	48.77±0.03
	ε_r''	1084.04±53.19	732.35±35.55	38.95±1.24	24.09±0.56
80	ε_r'	84.57±1.60	73.73±1.36	50.79±0.24	47.91±0.08
	ε_r''	1228.08±68.33	828.87±45.65	42.74±1.72	25.74±0.85
90	ε_r'	84.46±0.74	72.26±1.14	49.75±0.34	46.88±0.25
	ε_r''	1367.72±91.82	922.58±61.28	46.45±2.35	27.42±1.19
100	ε_r'	85.09±0.12	71.74±0.64	48.73±0.46	45.93±0.35
	ε_r''	1496.56±108.89	1009.18±72.45	49.84±2.88	28.94±1.41
110	ε_r'	85.52±0.40	70.69±0.35	47.73±0.52	45.03±0.44
	ε_r''	1638.48±125.61	1104.25±83.87	53.68±3.32	30.76±1.70
121	ε_r'	85.85±0.83	69.73±0.11	46.53±0.55	43.93±0.50
	ε_r''	1811.70±138.63	1220.18±92.56	58.39±3.66	32.99±1.83

Appendix 5.4: Dielectric properties of sauce (mean ± standard deviation of triplicate) (Luechapattanaporn, 2005b)

T (°C)		27 MHz	40 MHz	915 MHz	1800 MHz
20	ε_r'	86.22±2.47	82.02±3.20	79.16±5.24	76.42±4.20
	ε_r''	1045.34±6.83	703.23±4.53	38.83±6.57	27.57±4.59
30	ε_r'	84.86±2.65	79.49±3.58	76.36±4.89	74.13±4.11
	ε_r''	1243.78±10.44	836.35±6.55	43.42±6.66	28.95±4.87
40	ε_r'	81.46±0.67	75.33±1.96	71.85±2.41	69.72±1.59
	ε_r''	1461.76±53.94	965.65±12.96	48.09±6.14	30.42±4.31
50	ε_r'	79.05±0.64	71.91±1.09	67.79±0.70	66.15±0.12
	ε_r''	1652.37±56.86	1110.48±38.65	53.27±4.95	32.09±3.16
60	ε_r'	77.71±2.62	68.98±0.23	64.43±0.81	63.11±1.22
	ε_r''	1862.10±109.73	1250.82±74.00	58.43±3.32	34.36±2.40
70	ε_r'	78.99±2.28	68.56±0.19	62.55±1.19	61.69±1.15
	ε_r''	2150.73±156.01	1446.54±108.48	65.69±2.21	37.62±1.36
80	ε_r'	81.73±0.67	69.02±3.22	61.40±0.39	61.03±0.86
	ε_r''	2448.59±80.38	1648.99±54.91	73.96±4.49	41.48±2.37
90	ε_r'	83.32±3.28	68.65±5.20	59.54±1.17	59.51±1.94
	ε_r''	2743.22±44.95	1848.30±31.59	82.14±5.83	45.39±3.09
100	ε_r'	85.64±4.78	69.02±7.37	58.25±3.03	57.79±2.79
	ε_r''	3043.76±21.30	2051.15±16.23	91.05±7.67	50.43±4.80
110	ε_r'	87.10±5.76	68.43±8.86	55.79±2.84	56.25±3.77
	ε_r''	3333.53±2.88	2247.21±3.71	98.85±8.29	53.77±4.39
121	ε_r'	88.29±7.20	67.62±9.63	52.22±0.91	53.04±2.16
	ε_r''	3599.88±34.46	2428.12±18.82	105.96±8.64	56.57±3.53

CHAPTER SIX

RECOMMENDATIONS FOR FUTURE STUDIES

This study demonstrates that RF heating can process high quality shelf-stable heterogonous foods in 6-pound capacity trays. The RF heating process can overcome the inherent shortage of slow heat conduction that obstructs conventional retorting to provide high quality food in a short time. However, future research is needed in the following areas before RF sterilization can be implemented on an industrial scale.

1. Optimization of electric conductivity of circulating water and dielectric properties of food

In this study both experiments and computer simulations demonstrated that an increase of conductivity in circulating water improves the heating uniformity of food but reduces heating rates. The dielectric properties of foods can introduce pronounced influences on heating patterns and rates. Although the introduction of circulating water was shown to reduce the fringing electric field and edge-heating effects, a large amount of energy was dissipated in the circulating water instead of the food, raising concerns about energy inefficiency. Further investigation on the influence of the relationship between water electric conductivity and food dielectric properties on heating patterns and rates to optimize the heating process would therefore be beneficial.

2. Computer simulation

Although the simulation model based on a 6 kW pilot-scale RF heating system in this study provided relatively accurate results that conformed to the experimental results, it only considered the heating cavity part of the total RF heating system. RF heating systems with conventional power oscillator design is mostly adopted in the US market,

for the conventional power oscillator design, the RF applicators and foods are part of the power generator circuit. The variations in applicator separation, food product dielectric properties, and other factors may change the capacitance and quality factor of the applicator in the circuit. Further studies are thus needed to include the whole circuit of the RF heating system when modeling to obtain more accurate simulation results.

3. RF heating system efficiency improvement

The current 6 kW pilot-scale RF heating system did not provide very high efficiency. No more than 40% of total energy was used to heat the food. With an improved numerical model, further studies should explore possible reasons that cause the waste of energy, and provide useful information for future design of RF heating equipment.

4. Continuous multiple-trays system

To achieve successful commercial RF sterilization, continuous multiple-tray processing systems are needed. Based on the experimental and simulation results of the current pilot-scale RF heating system, electrical and mechanical design of continuous multiple-tray systems are possible.

5. Economics study

Economic studies should be conducted on future continuous multiple-tray systems for energy efficiency, processing time and throughput. It is necessary to compare the prevailing conventional industrial heating technologies to verify the possibility of commercial success before filing for Food and Drug Administration approval and mass production.